

**Modeling and Simulation Approach to Characterize the Magnitude and
Consistency of Drug Exposure using Sparse Concentration Sampling**

by

Yan Feng

B.S. in Pharmacy, China Pharmaceutical University, 1998

M.S., in Pharmaceutical Analysis, China Pharmaceutical University, 2001

Submitted to the Graduate Faculty of
University of Pittsburgh in partial fulfillment
of the requirements for the degree of
Doctor of Philosophy

University of Pittsburgh

2006

UNIVERSITY OF PITTSBURGH
SCHOOL OF PHARMACY

This dissertation was presented

by

Yan Feng

It was defended on

[March 3rd, 2006]

and approved by

Robert R. Bies, Assistant Professor, Pharmaceutical Sciences Department

Bruce G. Pollock, Professor, Psychiatry Department

Randall B. Smith, Associate Dean, Pharmaceutical Sciences Department

Robert S. Parker, Assistant Professor, Chemical and Petroleum Engineering Department

Mark Sale, Director, Clinical Pharmacology and Discovery Medicine, GlaxoSmithKline

Robert E Ferrell, Professor, Human Genetics Department

Dissertation Advisor: Robert R. Bies, Assistant Professor, Pharmaceutical Sciences
Department

Copyright © by Yan Feng

2006

Modeling and Simulation Approach to Characterize the Magnitude and Consistency of Drug Exposure using Sparse Concentration Sampling

Yan Feng, PhD

University of Pittsburgh, 2006

Population pharmacokinetic (PK) and pharmacodynamic (PD) modeling using a mixed effect modeling (MEM) approach has been widely used for various drug classes during development. The MEM approach provides a significant advantage when analyzing large scale clinical trials and special population where only a few samples are available per subject.

The aims of this thesis are to explore the applications and advantages of MEM approach in the analysis of target populations (e.g., late-life depression, intensive care unit patients) from various aspects.

1): To characterize the sources of variability and evaluate the impact of patients' specific characteristics on SSRIs disposition using hyper-sparse concentration data. This study demonstrated that age and weight are significant covariates on citalopram clearance and volume of distribution. The age effect persists across the entire age range (22 to 93 years). Thus elderly subjects may need to receive different dose of citalopram based on their age. The other late-life depression study shows that weight and CYP2D6 polymorphisms significantly impact on maximal velocity (V_m) of paroxetine elimination. Thus, female and male subjects with different CYP2D6 genotypes may receive different dose based on their metabolizer genotype.

2): To optimize a dosing strategy for general medical and intensive care unit (ICU) patients receiving enoxaparin by continuous intravenous infusion. The study suggests that dose should be individualized based on patients' renal function and weight. It is also found that patients in the ICU tend to have higher exposure, thus should receive lower dose than those in the general medical unit.

3): To evaluate the consistency of exposure using the deviation between model-predicted and observed concentrations (C_{pred}/C_{obs} ratio) and assess the stability and robustness of using

the ratio in reflecting erratic adherence patterns. The simulations demonstrate that ratio could be used as the indicator of the extreme adherence conditions for both long and short-half life drug.

The knowledge gained in the thesis will contribute to the understanding the sources of variability in target population, including subjects specific characteristics, enzyme genetics and adherence, under conditions of highly sparse concentration sampling. This provides a basis whereby the magnitude and consistency of exposure can be examined in conjunction with the maintenance response of subjects in a future study as response data become available.

TABLE OF CONTENTS

<u>PREFACE.....</u>	<u>XIII</u>
<u>CHAPTER 1 INTRODUCTION.....</u>	<u>1</u>
1.1 Overview.....	2
1.2 Population analysis approaches.....	5
1.2.1 Two-stage approach.....	5
1.2.2 The mixed effect modeling approach.....	6
1.2.3 Estimation method and software.....	14
1.2.4 Model building criteria.....	16
1.2.5 Model evaluation.....	17
1.3 Model based simulation.....	18
1.4 Objectives of the thesis.....	19
<u>CHAPTER 2 OPTIMIZATION OF DOSE SELECTION USING BIOMARKER RESPONSE WITH SPARSE DATA.....</u>	<u>21</u>
2.1 Abstract.....	22
2.2 Introduction.....	23
2.3 Subjects and Method	24
2.3.1 Subject.....	24
2.3.2 Population Pharmacokinetic analysis.....	25
2.3.3 Simulation of steady state anti-Xa concentration.....	26
2.4 Result.....	28
2.5 Discussion.....	32
2.6 Conclusion.....	35
2.6 Acknowledgements.....	35

<u>CHAPTER 3 DETERMINATION COVARIATE EFFECTS ON EXPOSURE OF A</u>	
<u>DRUG WITH LINEAR PHARMACOKINETIC CHARACTERISTICS</u>	
<u>GIVEN HIGHLY SPARSE DATA.....46</u>	
3.1	<u>Abstract.....47</u>
3.2	<u>Introduction.....48</u>
3.3	<u>Methods49</u>
3.4	<u>Results.....52</u>
3.5	<u>Discussion.....53</u>
3.6	<u>Acknowledgements.....55</u>
3.7	<u>Supplemental results.....55</u>
<u>CHAPTER 4 DETERMINATION OF COVARIATES (INCLUDING CYP2D6</u>	
<u>GENOTYPE) EFFECTS ON EXPOSURE OF A DRUG WITH</u>	
<u>NONLINEAR PHARMACOKINETIC CHARACTERISTICS USING</u>	
<u>HIGHLY SPARSE DATA.....67</u>	
4.1	<u>Abstract.....68</u>
4.2	<u>Introduction.....69</u>
4.3	<u>Subjects and Method70</u>
4.3.1	<u>Subject.....70</u>
4.3.2	<u>Analytical Procedures.....71</u>
4.3.3	<u>CYP2D6 Genotyping.....72</u>
4.3.4	<u>Population Pharmacokinetic Analysis.....72</u>
4.4	<u>Result.....76</u>
4.5	<u>Discussion.....78</u>
4.6	<u>Conclusion.....81</u>
4.7	<u>Acknowledgements.....81</u>
<u>CHAPTER 5 ASSESSMENT OF THE CONSISTENCY OF DRUG EXPOSURE USING</u>	
<u>SPARSE DATA MEASUREMENT BY MODELING AND SIMULATION</u>	
<u>APPROACH.....92</u>	
5.1	<u>Abstract.....93</u>
5.2	<u>Introduction.....95</u>

5.3	Methods.....	97
5.4	Results.....	104
5.5	Discussion.....	109
5.6	Conclusion.....	112
CHAPTER 6 OVERALL SUMMARY AND FUTURE DIRECTION.....		125
APPENDIX A. LIST OF ABBREVIATION& NOMENCLATURE.....		130
APPENDIX B. MODELING AND EXPERIMENT METHODS		131
	Prediction of creatinine clearance from serum creatinine.....	134
	Relevant part of the NONMEM code for enoxaparin covariate model.....	135
	Relevant part of the NONMEM code for citalopram covariate model (1-compartment model using FOCEI method).....	138
	CYP2D6 genotyping protocol.....	140
	Relevant part of the NONMEM code for paroxetine covariate model.....	143
	Relevant S script for adherence rate calculation	146
BIBLIOGRAPHY.....		147

LIST OF TABLES

Chapter 2 Optimization of dose selection using biomarker response with sparse data

Table 1	Patient characteristics for the two studies.....	36
Table 2	Pharmacokinetic parameter estimates for two-compartment model.....	37
Table 3	Percent of predicted anti-Xa C _{ss} higher than 1.2 IU/ml or Percent of predicted anti-Xa C _{ss} lower than 0.5 IU/ml when general medical unit and ICU patient receiving enoxaparin at different infusion rates of 8.3, 5.8, 5.0 and 4.2 IU/kg/h..	38
Table 4	Percent of predicted anti-Xa C _{ss} higher than 1.2 IU/ml or Percent of predicted anti-Xa C _{ss} lower than 0.5 IU/ml when general medical unit and ICU patient receiving enoxaparin at different infusion rates of 8.3, 5.8, 5.0 and 4.2 IU/kg/h for subjects at each renal function group (1: CrCL < 30 ml/min; 2: CrCL 30-50 ml/min; 3: CrCL > 50 ml/min).....	39

Chapter 3 Determination covariate effects on exposure of drug with linear pharmacokinetic characteristics given highly sparse data

Table 1	Patient characteristics and data available from the Bipolar Depression and the Elderly Depression studies.....	62
Table 2	Population model development (FOCE method).....	63
Table 3	Pharmacokinetic parameter estimates for the 1-compartment model.....	64
Table 4	Population model development (FOCEI method).....	65
Table 5	Pharmacokinetic parameter estimates (FOCEI method) for the 1-compartment model and bootstrap analysis.....	66

Chapter 4 Determination of covariates (including CYP2D6 genotype) effects on exposure of a drug with nonlinear pharmacokinetic characteristics using highly sparse data

Table 1	<u>Conditions of CYP2D6 genotyping study: including the specific primers, restriction enzyme, restriction pattern, and agarose gel.....</u>	<u>82</u>
Table 2	<u>Genotype/Phenotype frequencies in Caucasian (CA) and African - American (AA) subjects in the MTL D-2 trial.....</u>	<u>83</u>
Table 3	<u>Patient characteristics for the MTL D-2 study.....</u>	<u>84</u>
Table 4	<u>CYP2D6 allele frequency in Caucasian and African - American patients.....</u>	<u>85</u>
Table 5	<u>Pharmacokinetic parameter estimates for the two-compartment model.....</u>	<u>86</u>
Table 6	<u>Population Pharmacokinetic Model Development (2-compartment with nonlinear elimination).....</u>	<u>87</u>

Chapter 5 Assessment of the consistency of drug exposure using sparse data measurement by simulation approach

Table 1	<u>The detailed description of simulation scenarios for long half-life drug and short half-life drug</u>	<u>113</u>
Table 2	<u>Correctly classified rate at weekly adherence rate condition for long half-life drug and short half-life drug.....</u>	<u>114</u>
Table 3	<u>Correctly classified rate at 2 days adherence rate condition for or long half-life drug and short half-life drug.....</u>	<u>115</u>
Table 4	<u>The overall bias and precision of parameter estimates under positive and negative control for long half-life drug.....</u>	<u>116</u>
Table 5	<u>The overall bias and precision of parameter estimates under positive and negative control for short half-life drug.....</u>	<u>117</u>

Appendix

Table B4.1	<u>PCR mix (25µl) for CYP2D6 allele amplifications.....</u>	<u>141</u>
Table B4.2	<u>Digestion Buffers for CYP2D6 alleles</u>	<u>142</u>

LIST OF FIGURES

Chapter 1 Introduction

Figure 1	Sources of variability.....	3
Figure 2	General form of two-compartment model	8

Chapter 2 Optimization of dose selection using biomarker response with sparse data

Figure 1	Population predicted anti-Xa concentrations versus Observed for the two-compartment model with CrCL and weight covariates in the model.....	40
Figure 2	Three-D surface showing the relationship between CrCL, weight and predicted C _{ss}	41
Figure 3	The percentage of predicted C _{ss} falling out of therapeutic range at different infusion rate (8.3, 5.8, 5.0, 4.2 IU/kg/h) for ICU patients with different renal function.....	42
Figure 4	The percentage of predicted C _{ss} falling out of therapeutic range at different infusion rate (8.3, 5.8, 5.0, 4.20 IU/kg/h) for general medical unit patients with different renal function.....	44

Chapter 3 Determination covariate effects on exposure of drug with linear pharmacokinetic characteristics given highly sparse data

Figure 1	Frequency histogram showing the sampling distribution for citalopram plasma concentration measurements.....	57
Figure 2	Observed (DV) versus population predicted (PRED) citalopram concentration values for the one-compartment model used with weight and age covariates in the model.....	58

Figure 3	<u>Three-dimensional surface showing the relationship between age, weight and predicted clearance.....</u>	<u>59</u>
Figure 4	<u>Dose normalized AUC in ng/mL*hr versus age in years.....</u>	<u>60</u>
Figure 5	<u>Observed versus population predicted citalopram concentration values for the one-compartment model used FOCE interaction method.....</u>	<u>61</u>
Chapter 4	<u>Determination of covariates (including CYP2D6 genotype) effects on exposure of a drug with nonlinear pharmacokinetic characteristics using highly sparse data</u>	
Figure 1	<u>Frequency histogram showing the sampling distribution for paroxetine sampling measurements.....</u>	<u>88</u>
Figure 2	<u>Diagnostic plots of final PK model.....</u>	<u>89</u>
Figure 3	<u>Boxplot of Vm estimates for each CYP2D6 phenotype group.....</u>	<u>91</u>
Chapter 5	<u>Assessment of the consistency of drug exposure using sparse data measurement by simulation approach</u>	
Figure 1	<u>Boxplot of the overall all ratio distribution at each adherence rate condition for long half-life drug (escitalopram).....</u>	<u>118</u>
Figure 2	<u>Boxplot of the overall all ratio distribution at each adherence rate condition for short half-life drug (risperidone).....</u>	<u>120</u>
Figure 3	<u>The association between Cipred/Cobs ratio and adherence rate in long half-life drug and in short half-life drug</u>	<u>122</u>
Figure 4	<u>Bias and precision of parameter estimates under negative and positive control.....</u>	<u>123</u>

PREFACE

First and foremost I would like to extend my deep appreciation and gratitude to the people who make this work possible, have encouraged, and helped me over the years.

I would like to sincerely thank my advisor, Dr. Robert Bies, for his patience and guidance, his supporting and enhancing my knowledge and interest in the geriatric pharmacokinetics research. His door is always open and he is always willing to share his brilliant ideas. He is an excellent mentor and friend throughout my stay here in Pittsburgh.

Many thanks to my committee members, Dr. Bruce Pollock, Dr. Randy Smith, Dr. Robert Ferrell, Dr. Mark Sale, and Dr. Robert Parker, for their guidance and advice towards my dissertation work and thanks for their valuable suggestions, advice and encouragement. Especially, I would like to thank Dr. Pollock, Dr. Ferrell and Mark Kimak for helping me on the CYP2D6 genotyping work, the continuous financial support in the project, assistance with the paroxetine paper and bearing with a digest-enzyme scavenger like me.

Thank you, Dr. Bruce Green and Dr. Stephen Duffull, Dr. Sandra Kane-Gill, Dr. Charles F. Reynolds III and Dr. Marc Gastonguay, my co-authors – for all the contributions to my thesis projects. Thanks Bruce and Steve for their generosity of sharing their data and ideas with us. A special thanks to Bruce for his tremendous time in guiding and advising on the enoxaparin project. And thanks Sandy for reading through the manuscript and providing valuable comments. I would like to thank Dr. Curtis E Haas for sharing his paper and Dr. Alan Forrest for the helpful advice on the enoxaparin manuscript. Thanks, Charles F. Reynolds III, for your suggestions on the paroxetine paper. I would like to thank Dr. Marc Gastonguay for all the valuable comments and suggestions on the pred-ratio project.

Thank you, Dr. Marc Pfister for offering me a great internship opportunity and thank you, Bristol-Myers Squibbs modeling & simulation group, for providing me an amazing learning environment.

I would like to thank Dr. Merrill Egorin, Dr. Raman Venkataramanan, and Dr. Wen Xie, my rotation mentors, for your help and guidance. Thanks PK lunch for many laughs and for the wonderful learning environment.

I would like to extend a special thanks to my family, who always believe me, support me and serves as my grounding force. Thank you, my Mom and Dad, for teaching me patience and fairness. Thanks to my sister, for believing in and encourage me all those times I questioned myself. I would like to thank my husband Haitao, for his love, understanding, sacrifices and continuing support through the entire study period.

I would like to thank all the faculties, staffs and graduate students in School of Pharmacy for making my years in Pittsburgh an exceptional experience for me.

CHAPTER 1 INTRODUCTION

1.1 OVERVIEW

Pharmacokinetic (PK) studies aim to study the time course of absorption, distribution, metabolism and elimination of a drug, which is considered as ‘what the body does to the drug’.¹⁻³ Pharmacodynamic (PD) studies aim to study the time course of the drug concentration and link this to the time course of pharmacologic effects, which is considered as ‘what the drug does to the body’.⁴ An integration of the determined relationship of concentration-time (PK) and concentration-effect (PD) is generally used to predict the temporal pattern of drug’s pharmacologic effect and thus to optimize an effective dosage. It is commonly observed in the clinical studies that subjects receiving the same dose of a drug can respond differently, where some patients have ineffective therapy whereas some patients experience toxicity. The population approach is the analysis which attempts to understand PK/PD difference among population subgroups and attempt to determine and classify sources and hierarchies of variability.

Population approach has been widely used in various drug classes during drug development, such as anticoagulants⁵⁻⁸, anti-cancer drugs⁹, CNS drugs^{10, 11} and antibacterial drugs¹². The ultimate objective of a population analysis is to provide information that can be applied to develop guidelines for individualizing drug dosage regimens. Thus understanding the sources of variability and its impact on drug disposition is very important for rational drug pharmacotherapy in the target population. Moreover, increasing the magnitude of random variability may possibly cause decreased efficacy and safety of a drug.

The sources of variability which influence the observed data can be categorized as measurable (fixed effect or attributable) and unobservable variability (random effect or non-attributable) (Figure 1). Traditional PK approaches (e.g., Naïve pooled data (NPD) and standard two-stage (TS) analysis) used in population analysis, usually involves intensive sampling in small homogenous population (e.g., 6-12 healthy volunteers). NPD approach pools the data from all individuals neglecting the differences between individuals and fits an individual’s model for it.

The estimation of variability from NPD approach is typically overestimated since all sources of random variability (inter- and intra-individual variability) are pooled together.¹³⁻¹⁵ Thus NPD analysis is unable to provide information that allows an adequate characterization of the sources of variability and its implication for drug therapy. Standard TS method is able to work fairly well in the situations where there is intensive data per individual. The random inter-individual variability from TS approach can be overestimated, which is related to both true biological variability and the uncertainty of the individual parameter estimate.^{13, 14} However, this problem is unlikely to be important for the traditional well-defined PK study with intensive sampling measurements and a simple model structure. The other approach for population analysis is the mixed effect modeling (MEM) approach, which is ideally suited for analyzing data from large clinical trials (e.g., phase II and phase III study) and data from special populations (e.g., geriatrics, pediatrics and critical care unit patients), where only a few samples are available for each subject due to the ethical and/or medical concerns.¹⁰ The MEM approach can also be applied in combined data analysis, which can be used to stabilize the population analysis with prior information.¹⁶

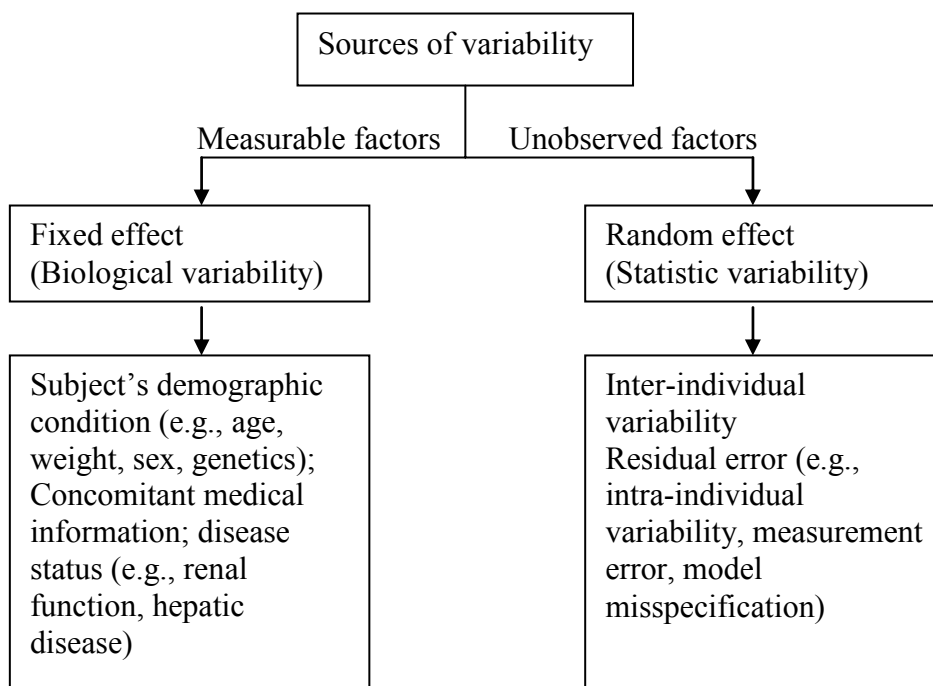


Figure 1: Sources of variability

Population PK analysis (mixed effect modeling approach) has many advantages over traditional PK approach.¹⁰ Unfortunately, the drug dosing history is often poorly recorded and the extent of non-adherence is usually underestimated, which leads to biased parameter estimates.¹⁷⁻²³ In clinical trials, it is reported that the average adherence rate is only 43-78% among subjects receiving chronic treatment.^{24,25} There are many other similar terminologies used in the literature to describe adherence, such as compliance, concordance and alliance.^{26,27} In this thesis, adherence is defined in two ways: the percentage of prescribed doses taken and the percentage of days of therapy when the medication was taken appropriately. Thus we focus on the continuous middle “execution” phase of drug intake that concerns the pattern that occurs before the discontinuation phase.²⁸ Adherence, a major concern for many chronic disease therapies (e.g., hypertension, diabetes and depression), is a widespread phenomenon causing decreased efficacy, relapse and recurrence during treatment.^{29, 30} Many studies have suggested that adherence is related to the clinical outcomes.²⁹⁻³³ It is a challenging area of investigation for the clinical settings. A 100% reliable indirect measure for adherence doesn't exist to date. Medication Event Monitoring System (MEMS)³⁴ is a microprocessor-based method for continuous monitoring of adherence, which provides more accurate information than simple adherence measurement (e.g., self-report, direct interrogations, tablet estimates or prescription count). Adherence can also be measured by evaluating the stability of plasma level / dose (L/D) ratios.^{30, 35} However, L/D ratio requires exquisitely precise timing of the last dose as well as the sample measurement. In the population PK analysis, the poorly recorded dosing history can cause biased estimation, which can mislead the decision making in clinical trials and drug pharmacotherapy.¹⁷⁻²³ Utilization of a prior established PK model may allow one to utilize these biases by evaluating the deviation between the prior model predicted and the observed drug concentrations. The deviation may be used to infer consistency of drug exposure and the erratic consistency of exposure can be used to reflect the adherence patterns.

The work discussed in the thesis explores the advantages of MEM approach in the analysis of sparse data sampling situation from several perspectives, including 1): the evaluation of the covariate effect on selective serotonin reuptake inhibitor (SSRI) disposition in late-life depression using highly sparse sampling measurement (Chapter 3 and 4); 2): the evaluation of the consistency of the exposure using the ratio of predicted versus observed concentrations,

which was then applied to reflect the erratic adherence pattern (Chapter 5); and 3): the dosage optimization using modeling and simulation approach for an anticoagulant drug (Chapter 2).

In the following sections, the traditional PK analysis (Standard TS approach) and MEM approaches are discussed first, and then the advantages and disadvantages of the two methods are compared. After that, the base model development is discussed which shows how to select a base model and what constitutes the inter-individual variability. The covariate model development is discussed after the base model section, which include the criteria for covariate selection and formulation of covariate model. Different model validation and evaluation methods are then discussed. Finally, the model-based simulation is addressed.

1.2 POPULATION ANALYSIS APPROACH

Population PK analysis is able to obtain typical PK parameter estimates, and identify sources of and correlations of variability in plasma concentrations between individuals for a specific dose across a number of individuals.³⁶ Population PKs is widely used in drug safety and efficacy evaluation. Population PK modeling can be done using different approaches, such as NPD, standard TS method, and a MEM approach.^{37, 38} In the section below, we are focusing on the standard TS approach and parametric MEM approach.

1.2.1 Standard Two-Stage approach

In the 1st stage, the individual PK parameters are calculated separately from a dense data set, using classical fitting procedures (e.g., Weighted Least Squares) as shown below.

$$OBJ(P_i) = \sum_{j=1}^n (C_{obs,j} - C_{pred,j})^2 \times W_{ij} \quad (1)$$

Where P_i is the PK parameters for i^{th} individual, W_{ij} is the weight of j^{th} observation in i^{th} individual. The weighted least squares assume a heteroscedastic error structure, where the random error is assumed to be some function of the observed concentrations, such as $W_{ij}=1/C_{obs,j}$ which assumes the variance is proportional to the concentrations.

In the 2nd stage, the population mean and standard deviation (SD) of the PK parameters are calculated for the study population. The relationship between the covariates and the PK parameters across subjects can be evaluated using regression analysis. The population parameters (mean and variance) across the subjects can be calculated as below:

Arithmetic mean and variance:

$$\text{Mean} = \sum_{i=1}^n P_j / N \quad (2)$$

$$\text{Variance} = \sum_{i=1}^n (P_j - \text{mean})^2 / N \quad (3)$$

The TS approach is simple and usually generates unbiased mean parameter estimates. However, the random inter-individual variability from TS approach can be overestimated, which is associated with both true biological variability and the uncertainty of the individual parameter estimate.^{13, 14} The traditional two-stage method requires intensive sampling measurements at appropriate time to obtain accurate parameter estimate in stage 1, and it is generally not applicable in the highly sparse data sampling situation (e.g., 1-2 sample per subject), since estimating the individual parameters is out of the question.

1.2.2 The mixed effect modeling approach

The MEM approach is a one stage analysis approach, which considers the population study sample, rather than the individual, as a unit of analysis for the estimation of the distribution of parameters and their relationship with covariates within the population. The word “mixed” refers that the method evaluates both fixed and random effects.

The MEM approach is ideally suited for analyzing data from large clinical trials, where only a few samples are available for each subject.¹⁰ This technique identifies individual-specific characteristics that impact the disposition of a drug. In addition, the results are more generalizable than those of the traditional methodology because a greater number of subjects are evaluated.³⁹ MEM can identify both individual specific and overall population PK parameters based on sparse data sampling, and use each data point to inform the entire analysis.^{10, 38, 40}

In the population analysis, it is natural to fit the data into a hierarchical modeling structure, which allows the variability in concentrations to be separated into inter- and intra-

individual variability. In the 1st stage, the data of a particular individual is modeled conditioned on individual parameters, and the relationships between individuals are modeled in the 2nd stage. The hierarchical structure in the two stages is described below:

1st Hierarchy:

Each subject has a set of drug concentrations, and the predicted concentration ($h_1(\theta_i, t_{ij}, d_i)$) is defined as below:

$$Y_{ij} = H_1(\theta_i, t_{ij}, d_i) + \varepsilon_{ij} \quad (4)$$

With ε_{ij} independent and identically distributed as $\varepsilon \sim N(0, \sigma^2)$. Y_{ij} is the j^{th} observed concentration in the i^{th} individual; h_1 is the functional form of PK model, $h_1(\theta_i, t_{ij}, d_i)$ is the j^{th} predicted concentrations in i^{th} individual; d_i is the dosing history, including amount of dose and the time of administration for i^{th} individual; θ_i is the value of the i^{th} individual's PK parameter.

2nd Hierarchy:

The model used in second stage is defined as below:

$$\theta_i = H_2(\mu, \text{Cov}_i) + \eta_i \quad (5)$$

With η_i independent and identically distributed as $\eta \sim N(0, \omega^2)$. Cov_i represent the covariates for the i^{th} individual and μ is the population parameter. The predicted values of PK parameters for the i^{th} individual at time t_{ij} are defined by H_1 in equation 4. H_2 is a function, which describes the relationship between i^{th} individual's covariates and i^{th} individuals' PK parameters.

Stages 1 and 2 of the hierarchy explicitly partition the variability in the observed data into two variance components. These are called intra- (sometimes also called residual unknown variability) and inter-individual variability. The objective of population modeling is to identify covariates which are responsible for between-individual variability and to quantify the remaining variability.

1.2.2.1 Model definition

The population PK model is a combination of three basic components:

- The structural PK model component, which defines the PK parameters and describes the plasma concentration-time profile

- The statistical PK model component, which comprises both intra- and inter-individual variability. The residual error model component describes the underlying distribution of the error in the measured PK variable and the inter-individual error model component describes the inter-individual variation in PK parameters after correction for fixed effects
- The covariate model component, which describes the influence of fixed effects (i.e., demographic factors) on PK parameters

The description for each model component is presented below.

1.2.2.1.1 Base model development

Structure of the PK model

The structure of the PK model represents the best description of the data without considering the effect of subject's specific covariates. Structural PK models usually are expressed by using primary PK parameters such as clearance (CL) and volume of distribution (V) rather than rate constants, which can generate primary PK parameters in combination forms. Using primary PK parameters allows us to assess the impact of covariate on these parameters e.g., age, weight, sex, race or genotypes which may alter plasma concentration. The two-compartment linear model with oral administration is shown below:

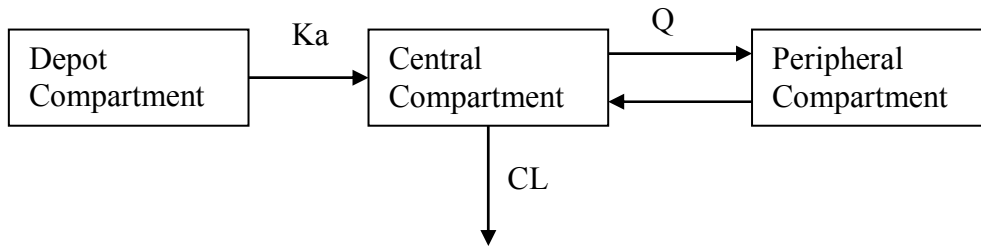


Figure 2 General form of the two-compartment model

In the diagram above, K_a is the absorption rate constant, Q is the inter-compartment clearance, and CL is the oral clearance. The mass balance equations are given by:

$$\frac{dA_1}{dt} = -K_a \times A_1 \quad (6)$$

$$\frac{dA_2}{dt} = Ka \times A_1 - (CL + Q) \times \frac{A_2}{V_2} + Q \times \frac{A_3}{V_3} \quad (7)$$

$$\frac{dA_3}{dt} = Q \times \frac{A_2}{V_2} - Q \times \frac{A_3}{V_3} \quad (8)$$

Where V_2 is the volume of the central compartment, V_3 is the volume of the peripheral compartment, A_2 is the amount of drug in central compartment and A_3 is the amount of drug in peripheral compartment. Equation and model above describes a linear PK drug, where AUC is proportional to dose and clearance is a constant regardless of drug concentrations.

If AUC of a drug is non-linear by dose group e.g., paroxetine, clearance changes with concentration. The structural model should be reflected by a non-linear model, where the typical values such as V_{max} and K_m should be evaluated. The Michaelis - Menten equation is applied for clearance estimation in a non-linear model as shown below:

$$CL = \frac{V_{max}}{K_m + \frac{A_2}{V_2}} \quad (9)$$

Where V_{max} is the maximum rate, K_m is the Michaelis - Menten constant, which is equal to substrate concentration at half of the maximal velocity.

Inter-individual variability

In this model component, the individual parameter estimates are modeled as a function of typical value for the population and individual random deviations. The inter-individual variability of the PK parameters can be described as below:

$$\text{Exponential: } CL = TVCL \times \text{EXP}(ETA_{CL}) \quad (10)$$

$$\text{Additive: } CL = TVCL + ETA_{CL} \quad (11)$$

$$\text{Proportional: } CL = TVCL \times (1 + ETA_{CL}) \quad (12)$$

Where, $TVCL$ is the typical value of clearance for the population; CL is the individual parameter estimate; ETA_{CL} is the inter-individual variability term on CL , representing the difference between the individual parameter estimate and the population mean. The random effects of inter-individual variability are assumed normally distributed, with a mean of zero and

variance of ω^2 . In the exponential form, the distribution of parameter is skewed to the right which is commonly observed for the PK parameter distribution.

Intra-individual variability

The difference between the predicted concentration and observed concentrations is defined as residual variability, which is comprised of but not limited to intra-individual variability, experimental errors, and process noise and / or model misspecifications. It can be modeled using additive, proportional and combined error structure as described below:

$$\text{Additive error: } y_{ij} = \hat{y}_{ij} + \varepsilon_{ij} \quad (13)$$

$$\text{Proportional error: } y_{ij} = \hat{y}_{ij} \times (1 + \varepsilon_{ij}) \quad (14)$$

$$\text{Combined additive and proportional error: } y_{ij} = \hat{y}_{ij} \times (1 + \varepsilon_{ij}) + \varepsilon_{ij}' \quad (15)$$

Where y_{ij} is the j^{th} observation in the i^{th} individual, \hat{y}_{ij} is the corresponding model prediction, and ε_{ij} (or ε_{ij}') is a normally distributed random error with a mean of zero and a variance of σ^2 .

The additive error (constant absolute error) model is applied when the variance is assumed to have a constant absolute magnitude and independent for all measurements. The proportional error (constant coefficient of variation error) model is applied when the measurements to be modeled have heteroscedastic property and the error represents a constant proportion of the observed data. In the case of PK concentrations, where wide range of concentrations is measured, the error in measurement based on the analytical method is usually a combination of additive and proportional error. Use of a combined error model would improve predictions at lower limit of assay precision where variance may be assumed a constant and a proportional error model at higher concentration range.

1.2.2.1.2 Covariate model development

An important objective of a population PK analysis is to identify the sources of variability from observable covariates and their correlation with the individual PK parameters, which can

explain part of the inter-individual variability besides the part which has been explained by random effect in the base model. As mentioned in the overview section, many factors in the biological system can potentially contribute to variability such as age, sex, weight, renal function, polymorphic enzymes and concomitant medication. Quantitative assessment of the relationship between covariates and PK parameters is important for drug development because it provides information on whether the special dosage is necessary for a subgroup of patients.

Covariate identification and its selection criteria - The effect of subjects' specific covariates e.g., age, weight, and gender is tested on PK parameter during the final model development. The covariate models can be developed by a forward inclusion / backward elimination using the likelihood ratio test. Covariates that are significant at the 0.05 level are retained in the model (χ^2 , $\Delta\text{OFV}=-3.84$, $\text{df}=1$). Once all the covariates that are significant at the 0.05 level have been included in the model, a backward elimination process is conducted. A significant level of 0.01 is used for the backward elimination ($\Delta\text{OFV}=-6.63$, $\text{df}=1$). The backward elimination process is repeated until all remaining covariates are significant ($p<0.01$). Covariate influence on inter-individual variability and goodness of fit is also examined. Covariate factors should also have clinical or physiological relevance. Thus, if the magnitude of covariate effects is less than 20% of the parameter estimates for the typical subjects, the covariates may not be considered clinically relevant and may not be included into final model despite reductions in the objective function value (OFV).⁶

Incorporation of covariate - The covariates can usually be classified as continuous covariate like age, weight, height and discrete covariates include: sex, race, and enzyme genotypes.

These two types of covariates can be incorporated into the model as described below:

Example for continuous covariate

The incorporation of a continuous covariate for the parameter CL:

$$TVCL = \theta_{CL} + (Cov / Med_{Cov})^{\theta_{Cov}} \quad (16)$$

$$TVCL = \theta_{CL} \times (Cov / Med_{Cov})^{\theta_{Cov}} \quad (17)$$

$$TVCL = \theta_{CL} \times (1 + \theta_{Cov} \times (Med_{Cov} - Cov)) \quad (18)$$

$$CL = TVCL \times EXP(ETA_{CL}) \quad (19)$$

where TVCL is the population estimate of CL for individuals having a specific covariate; θ_{CL} is the population estimate for CL without a covariate effect; Cov is the continuous covariate that is affecting CL; θ_{Cov} is constant describing association between covariate and typical value of parameter estimates; and Med_{Cov} is the median value of Cov; CL is the individual estimate of clearance, which is the population estimate for clearance incorporating the covariate and inter-individual variability; ETA_{CL} is the inter-individual variability term for CL.

Example for discrete covariate

The incorporation of a discrete covariate involves assigning a numeric value to the covariate (e.g., sex, male = 0, female = 1). The equations below show sex as a discrete covariate in an exponential, a proportional, and an additive form respectively on the parameter CL.

$$TVCL = \theta_{CL} + Sex \times EXP(\theta_{Sex}) \quad (20)$$

$$TVCL = \theta_{CL} \times (1 + Sex \times \theta_{Sex}) \quad (21)$$

$$TVCL = \theta_{CL} + Sex \times \theta_{Sex} \quad (22)$$

$$CL = TVCL \times EXP(ETA_{CL}) \quad (23)$$

When sex is male, TVCL equals θ_{CL} since numeric value for male = 0 causing a zero multiplier for the covariate effect. For female, the θ_{Sex} term is added to the population estimate of CL to modify it.

If discrete covariate had more than two groups, for example the categorical variables are assigned to each of the three CYP2D6 phenotype groups (i.e, Poor metabolizers (PMs) = 1, Intermediate metabolizers (IMs) =2, Extensive metabolizers (EMs) = 3), the incorporation of this covariate is shown below:

$$\text{IF (PHENOTYPE.EQ.1) } TVCL = \theta_{PMs} \quad (24)$$

$$\text{IF (PHENOTYPE.EQ.2) } TVCL = \theta_{IMs} \quad (25)$$

$$\text{IF (PHENOTYPE.EQ.3) } TVCL = \theta_{EMs} \quad (26)$$

Missing covariate value - In subjects without a recorded covariate value, it is better to impute the missing covariate values for these subjects than to exclude them from analysis which will decrease the sample size and lose information. The simple imputation approach can be applied, including mean estimation and predicting missing values from regression. Mean estimation method is to replace missing data with the median or mean covariate value calculated from non-missing subjects in the population dataset. To predict missing values from regression is to impute each independent variable on the basis of other independent variables in model using regression analysis. Simple imputation does not reflect the uncertainty about the predictions of the missing data, thus the standard deviation and standard errors are underestimated since there is no variation in the imputed values.⁴¹ The other attractive method is multiple imputation (MI) approach proposed by Rubin, which replaced each missing data with a set of plausible values with representation of the uncertainty about the right value to impute.^{42, 43} MI requires the assumption of independency and missing at random, meaning that the probability that some data are missing does not depend on the actual values of the missing data, or missing completely at random, meaning the probability of an observation being missing does not depend on observed or unobserved measurements. The basic process of MI include: 1): impute missing values using an appropriate model that incorporates random variation; 2): do this m times, which produce m complete data sets; 3): analyse the m complete data sets using standard methods, e.g., Expectation Maximization method and Markov Chain Monte Carlo method; 4): combine the results from the m complete data sets and the point estimates from the MI and the standard errors can be calculated as below:

Point estimate:

$$\bar{Q} = \frac{1}{m} \sum_{i=1}^m Q_i \quad (27)$$

The variance estimate: (Total variance = within variance + between variance)

$$v = \frac{1}{m} \sum_{i=1}^m v_i + \frac{m+1}{m} \left[\frac{1}{m-1} \sum_{i=1}^m (Q_i - \bar{Q})^2 \right] \quad (28)$$

Where m is the number of sets imputed and analyzed, Q_i is the estimate from analyzing the i^{th} data set, and v_i is the variance estimate from analyzing the i^{th} data set. The advantages of MI are that it introduces random error into the imputation process which reduces the probability of introducing biased estimate of all parameters than that in simple imputation method (deterministic imputation), it also allows one to obtain good estimates of the standard errors. However, there are often strong reasons to suspect that the data are not missing at random, where even accounting for all the available observed information, the reason for observations being missing still depends on the unseen observations themselves.

In summary, the intra-subject model and the inter-subject model specifications together complete the model formulation for the population analysis with the non-linear mixed effects modeling approach.

1.2.3. Estimation method and software

Objective function and likelihood - The best model should provide the best model fit across all subjects through fitting. These ‘best’ parameter estimates in the model are typically obtained by minimizing or maximizing some objective function (OBJ), such as ordinary least squares, weighted least squares and extended least squares. The objective functions are shown below:

$$\text{Ordinary Least Squares: } OBJ = \sum_{i=1}^n (Y_{Obs_i} - Y_{Pred_i})^2 \quad (29)$$

$$\text{Weighted Least Squares: } OBJ = \sum_{i=1}^n [(Y_{Obs_i} - Y_{Pred_i})^2 \times W_i] \quad (30)$$

$$\text{Extended Least Squares: } OBJ = \sum_{i=1}^n \left[\frac{(Y_{Obs_i} - Y_{Pred_i})^2}{\text{var}_i} + \ln \text{var}_i \right] \quad (31)$$

Where var_i models the variance of the observation, $Y_{\text{obs } i}$ are the observed concentrations and $Y_{\text{pred } i}$ are the predicted concentrations. W is the weight which reflects the relative uncertainty attached to the individual estimate. The extended least square is designated as a maximum likelihood if the random effects assume to be normally distributed.

The objective function quantifies the difference between observed and predicted data for a given parameter set. The estimation method commonly used in nonlinear mixed effect modeling is the maximum likelihood approach, which is an alternative of the least square objective function (extended least squares). In the nonlinear mixed effect modeling, all the parameters are estimated simultaneously. The likelihood for the population parameters are shown below:

$$L = F(Y, Model) = \prod_{i=1}^N \{p[y_i, Model Parameter (x_i)]\} \quad (32)$$

Where L is likelihood, F represents some function of the observations and the model, and p is the probability of observation occurs at a given parameter set.

The likelihood is the product of probabilities for each individual observation (i) to occur, given the respective model and parameters. Since the parameters are selected to maximize the probability, the greater the likelihood of the model means the large the probability of the dependent variable to occur, therefore, the better the model describes the data.

Software - All software alternatives and approaches are based on the hierarchical nonlinear mixed effect modeling methods described above. The programs can be categorized into three groups: parametric maximum likelihood, nonparametric maximum likelihood and Bayesian. The programs using parametric methods are NONMEM, NLME in S-plus, WinNonMix, Kinetica 2000, MCPM in S-ADAPT (a version of ADAPT II) and NLINMIX in SAS. The programs using nonparametric methods are NPML, NPEM and NLMIX. The difference between non-parametric and parametric method is that parametric approach has the assumption of specific distribution of the random effect. The programs using Bayesian approaches include BUGS/WinBUGS, and JAGS (Just Another Gibbs Sampler), which require the specification prior and hyper-prior information of the parameter in the estimation. The computer program NONMEM[®] developed by Beal and Sheiner in 1980 at UCSF is the first computer program available for sparse data analysis in a PK setting and has been widely used in population analysis. The NONMEM software is used as the analysis platform in all population PK analyses in the thesis projects and is also the focus in the following sections.

Estimation in NONMEM – In the compartment model, the flow between compartments can be defined by a series of linear differential equations, which yields a concentration time model as described in stage 1 of H_1 (equation 4), a nonlinear function with unknown parameter. Due to the nonlinear dependency of the observations on the random variability of the η and ε , the integrals in likelihood cannot be evaluated analytically. Therefore, some form of approximation is needed.

In NONMEM, the first order (FO) method estimates the typical value for each parameter, ω^2 and σ^2 . FO method linearizes nonlinear model via a first order Taylor series expansion and is evaluated at the expected value of the random effects at 0. The detailed description about the approximation for FO method has been reported.⁴⁴ The FO method provides the population parameter estimates. The individual parameter estimates can be obtained using the POSTHOC option in NONMEM program using empirical Bayes methods to estimate η values for each individual. The first-order conditional method (FOCE) method is more time consuming than using FO method, because the individual estimate are determined for every iteration of the regression. The FOCE method also linearizes the nonlinear model via a first order Taylor series expansion about the value of individual η (with the assumption that the eta is not very different from zero but is potentially non-zero) instead of 0.^{45, 46} The FOCE with interaction (FOCEI) option in NONMEM assumes the interaction between η and ε . FOCEI differs from FOCE without interaction, which assumes the homoscedastic intra-individual variability across individuals. Applying FOCE and FOCEI methods are more time consuming for computation than that of FO method, but these methods have a more accurate approximation to the likelihood than the FO method. The Laplacian method uses a second-order Taylor series expansion about the η values. In the higher nonlinear model e.g., Emax model, logistic model, using Laplacian method can obtain more accurate parameter estimates than that of FOCE method.⁴⁵

1.2.4. Model building criteria

The adequacy of the developed structure models is evaluated using both statistical and graphical methods. The likelihood ratio test is used to discriminate between alternative (nested) models. The likelihood ratio test is based on the property that the ratio of the NONMEM objective function values (-2 log-likelihood) is asymptotically χ^2 distributed. A reduction of the

objective function by 3.84 units is considered significant (χ^2 $P < 0.05$ $df = 1$). For comparison between non-nested models, the Akaike Information Criterion (AIC) can be applied,⁴⁷ which is AIC equals to objective function value plus 2 times the number of parameters.

1.2.5. Model evaluation

Model validation/evaluation aims to determine whether the model is a good description of the validation data set. The model validation approach can be different based on the objective of the population analysis and the question that needs to be addressed. Not all population models need to be validated. Model validation can be classified as internal (e.g., bootstrap, data splitting and cross validation) and external (e.g., data from new studies) validation based on the sources of the data applied for validation.

External validation is the most stringent type of validation. However, it needs external data from the new study, which is usually not available in most situations. Internal validation methods are commonly used, which rely on the analysis of the subsets from the total data with the majority of data used in model building. Data splitting method involves randomly dividing data into an index data set and a test data set, where the index data set (e.g., 2/3 of the original data set) is used to develop the model and the test data set (e.g., 1/3 of the original data set) is used to evaluate the model performance. Cross over validation method is a ‘leave-one-out’ or ‘leave-some-out’ validation approach. Data is divided into m subsets. Fit the models from $m-1$ data set and each of the $m-1$ estimation subsets is used to predict the unused subset. The mean prediction error ($Y_{pred} - Y_{obs}$) calculated for each of these m models is used as measure of accuracy and mean absolute prediction error is used for precision measurement. Bootstrap analysis⁴⁸ is a widely used internal validation approach. It is a re-sampling methodology that provides a nonparametric assessment of the variances and confidence intervals without requiring asymptotic assumption on the distribution of parameters. This is a general technique for estimating sampling distribution. New “virtual” datasets are created by selecting patients at random. The model is re-run or parameters re-estimated for each of these datasets (e.g., 1000 times). The results provide a good measure of model stability, confidence intervals, variances and parameter distributions. The characteristics of the confidence intervals reflect how well or how poorly the model captured the parameters given the available dataset. The other model evaluation method is predictive performance check. It is based on comparing meaningful

statistics of observed data, with corresponding statistics calculated from data simulated under a model. Statistics of the data which are meaningful depend on the objectives of the modeling analysis and are specified as a prior. Briefly, empirical distributions of these statistics under a model are constructed from data generated by Monte Carlo simulation. The validity of a model is assessed by determining the probability of obtaining the value of a statistic calculated from observed data given the simulated empirical distribution of the statistic.⁴⁹

1.3 MODEL-BASED SIMULATION

Simulation has been widely used in various areas, such as engineering, economics, marketing and statistics. In the field of drug development, model-based simulation approach has been shown to be a very useful tool to facilitate dose selection by evaluating and understanding the consequences of different study designs.^{6,7 50} Simulation reveals the effect of input variables and assumptions on the results of a planned population analysis. Monte Carlo simulation is a widely used simulation approach.⁵¹⁻⁵³ The ultimate objective for a simulation study is to determine the factors affected the virtual subjects' response and thus provide the related information to the new clinical trial design. The beauty of a clinical trial simulation is to test various assumptions and hypotheses based on the prior information obtained from the previous studies, before conducting a real study. For example, simulation can be used to address the question on what would the 'best dose' for target population if the random variability is reduced by 50% after formulation modification, what is the efficacy/safety outcome would possibly look like if subjects receive half of the recommended dose, or if they receive two times the recommended dose. Except for the advantages discussed above, simulated data lacks the complexity of real data generated by clinical trials. Covariate data is hard to mimic through simulation, especially for time-varying covariates.

1.4 OBJECTIVES OF THE THESIS

The thesis explores the usefulness of MEM approach in several aspects for the clinical studies under sparse data sampling situation, including 1): the evaluation of the covariate effects on SSRIs disposition in the late-life depression using highly sparse sampling measurement (Chapter 3 and 4); 2): the assessment of the deviation between the model-predicted and observed concentrations (C_{pred}/C_{obs} and C_{ipred}/C_{obs}) in reflecting the erratic adherence patterns (Chapter 5); and 3): the dosage optimization using modeling and simulation approach in anticoagulant drug where a dynamic marker is measured (Chapter 2). The aims for each study are described below:

Chapter 2: To determine an appropriate dosage for patients receiving continuous intravenous infusion of enoxaparin

- To describe the PK for subjects administrated enoxaparin by continuous intravenous infusion using population analysis
- To optimize a dosage strategy for subjects receiving CII enoxaparin using model-based simulation approach

Chapter 3: To assess covariate affecting exposure to drug with linear PK characteristics given highly sparse sampling measurements

- To describe PK parameters of selective serotonin reuptake inhibitor (citalopram) with linear PK characteristics using highly sparse sampling measurements in a depressed population
- To evaluate the impact of covariates, including age, weight, race, and sex on citalopram PK parameters in late-life depression

Chapter 4: To assess CYP2D6 genotype effects on PK of a drug with nonlinear pharmacokinetic characteristics

- To describe PK parameters of selective serotonin reuptake inhibitor (paroxetine) with nonlinear PK characteristics using limited sampling measurements in late-life depression
- To evaluate the impact of covariates, including CYP2D6 genotypes, race, age, sex, weight, on paroxetine PK parameters in late-life depression

Chapter 5: To identify erratic adherence pattern by evaluating the consistency of drug exposure using a simulation approach

- To evaluate the overall distribution of the deviation between model predicted and observed concentrations (C_{pred}/C_{obs} and C_{ipred}/C_{obs} ratio) across the adherence patterns (high adherence rates to extremely low adherence rates) for both long and short half-life drugs under the situation when the subjects' correct dosing history (negative control) and when the incorrect dosing history (positive control) is applied in population analysis

- To evaluate the association between ratio and the rate under positive control

- To evaluate the bias and precision of parameter estimates under negative and positive controls

CHAPTER 2 OPTIMIZATION OF DOSE SELECTION USING BIOMARKER RESPONSE WITH SPARSE DATA

This chapter is based on the following paper:

Yan Feng, Bruce Green, Stephen B. Duffull, Sandra L. Kane, Mary B. Bobek, Robert. R. Bies. Development of a dosage strategy in patients receiving enoxaparin by Continuous Intravenous Infusion using modeling and simulation. *British Journal of Clinical Pharmacology*. 2006

Copyright is to be assigned to Journals Rights & Permissions Controller (Blackwell Publishing). The permission of using the full article in the thesis had been granted from the copyright owner (Blackwell Publishing).

Abstract

Objective: To develop an appropriate dosing strategy for continuous intravenous infusions (CII) of enoxaparin by minimizing the percentage of steady state anti-Xa concentration (C_{ss}) outside the therapeutic range of 0.5 -1.2 IU/ml.

Methods: A nonlinear mixed effects model was developed with NONMEM[®] for 48 adult patients who received CII of enoxaparin with infusion durations that ranged from 8 to 894 h at rates between 100 and 1600 IU/h. Three hundred and sixty three anti-Xa concentration measurements were available from patients who received CII. These were combined with 309 anti-Xa concentrations from 35 patients who received subcutaneous enoxaparin. The effect of age, body size, height, sex, creatinine clearance (CrCL) and patient location (Intensive Care Unit (ICU) or general medical unit) on pharmacokinetic (PK) parameters were evaluated. Monte Carlo simulations were used to 1) evaluate covariate effects on C_{ss}; and 2) compare the impact of different infusion rates on predicted C_{ss}. The best dose was selected based on the highest probability that the C_{ss} achieved would lie within the therapeutic range.

Results: A two-compartment linear model with additive and proportional residual error for general medical unit patients and only a proportional error for patients in ICU provided the best description of the data. Both CrCL and weight were found to significantly affect clearance and volume of distribution of the central compartment, respectively. Simulations suggested that the best doses for patients in the ICU setting were 50 IU/kg/12h (4.2 IU/kg/h) if CrCL < 30 ml/min; 60 IU/kg/12h (5.0 IU/kg/h) if CrCL was 30-50 ml/min; and 70 IU/kg/12h (5.8 IU/kg/h) if CrCL > 50 ml/min. The best doses for patients in the general medical unit were 60 IU/kg/12h (5.0 IU/kg/h) if CrCL < 30 ml/min; 70 IU/kg/12h (5.8 IU/kg/h) if CrCL was 30-50 ml/min; and 100 IU/kg/12h (8.3 IU/kg/h) if CrCL > 50 ml/min. These best doses were selected based on providing the lowest equal probability of either being above or below the therapeutic range and the highest probability that the C_{ss} achieved would lie within the therapeutic range.

Conclusions: The dose of enoxaparin should be individualized to the patients' renal function and weight. There is some evidence to support slightly lower doses of CII enoxaparin in patients in the ICU setting.

Introduction

Venous thromboembolism is a common cause of morbidity and mortality. Low molecular weight heparins (LMWHs) are as effective and safe as unfractionated heparin (UFH) for the treatment of deep vein thrombosis (DVT) and pulmonary embolus (PE).⁵⁴⁻⁵⁷ LMWHs are also superior to and as safe as unfractionated heparin for acute coronary syndromes.⁵⁸⁻⁶⁰ When compared to UFH, LMWHs have superior bioavailability,⁶¹ a more predictable anticoagulation response, and a lower incidence of heparin-induced thrombocytopenia and osteoporosis with long term treatment.⁶²

Enoxaparin is one of the most widely used LMWHs in Europe and the US,^{63, 64} with anti-Xa activity widely used as a marker of enoxaparin concentration.^{5, 6, 65} It is predominantly eliminated by the kidney.⁶⁶ Studies suggest that renal dysfunction leads to increased anti-Xa concentrations,^{5, 67, 68} which in turn is associated with bleeding complications. Therefore, dosage adjustment based on renal function is suggested to decrease the risk of adverse bleeding events.^{7, 69, 70}

Compared with general medical unit patients, critically ill patients have more medical complications due to pre-morbid and surgical conditions, invasive treatments, and prolonged immobility.⁷¹ Cook et al.⁷² found that Intensive Care Unit (ICU) patients with multiple predisposing factors have a high risk of venous thromboembolism and PE, which may result in a higher risk of mortality. Moreover, a range of organ dysfunction in ICU patients may result in more variable exposure to drugs and thus response.⁷³ Investigators at the University of Buffalo⁷⁴ have observed substantial variability in anti-Xa concentrations measured in multiple trauma critically ill patients. Unreliable and extensive variable anti-Xa concentrations were found in these trauma critically ill patients when the standard recommended dose and route of administration (subcutaneous (SC)) of enoxaparin for the prevention of venous thromboembolism was applied. This has led the group to examine alternate means of administration (intravenous infusion) to attempt to reduce variability in the observed anti-Xa concentrations after enoxaparin administration in trauma critically ill populations. Under the circumstance where patients were reported to have substantial variability⁷⁴ (e.g. intensive care unit patients) in the observed anti-Xa concentrations with SC enoxaparin, intravenous infusion /

CII could be utilized as a possible approach to reducing the variability. Therefore, it is desirable to attempt to understand these factors and attempt to control exposure to drug more closely.

The modeling and simulation work presented here represents a pilot examination of enoxaparin administered via continuous intravenous infusion and provides a first look at the nature of the inter-individual variability (including covariate examination) for this administration method.

Dosing strategy and extensive population pharmacokinetic analysis for patients receiving enoxaparin by continuous intravenous infusion (CII) has not been reported in the literature. The purpose of this study was to describe the pharmacokinetics (PK) for CII enoxaparin by developing a population PK model. This model was then used to guide a dosing strategy for CII enoxaparin.

Subjects and Methods

Subjects

Anti-Xa concentrations were available from two studies. Patient characteristics for the two studies are shown in Table 1. The first study was conducted at the Cleveland Clinic Foundation.⁷⁵ In the CII study, patients who received enoxaparin from January 1997 to December 1998 were identified, and a retrospective chart review was completed subsequent to institutional review board approval. The study provided 48 patients (23 male) with 363 anti-Xa concentrations with an average (Mean±SD) age and weight of 60.3±17.7 years, 73.9±14.6 kg, respectively. Patients were located in both general medical unit (n=29) and the ICU (n=19) and initially received enoxaparin 100 IU/kg/12h (8.3IU/kg/h) by CII. Routine monitoring of anti-Xa concentration was determined by chromogenic assay of LMWHs.⁷⁶

The second study, reported by Green et al., provided detailed subject information for the subcutaneous (SC) use of enoxaparin.⁷ The study included 35 patients with 309 anti-Xa concentrations. The patients' age, weight and CrCL were (Mean±SD): 75.1±10.5 years, 67.7±15.5 kg, 39.2±21.6 ml/min respectively.

The Brater equation⁷⁷ was used to calculate the CrCL for individuals with unstable serum creatinine (SCr) in the CII study when two SCr concentrations measured over 12 hours apart were

different by more than 0.2 mg/dL. CrCL for individuals with stable SCr concentrations was calculated using the Cockcroft and Gault (CG) equation in the CII and SC study, using ideal body weight (IBW) as a body size descriptor.⁷⁸

Population PK analysis

The population PK analysis for the combined data set was performed by using NONMEM® (version V, GloboMax, Hanover, MD)⁷⁹ with the subroutine ADVAN4, TRANS4. The first order conditional estimation with interaction (FOCEI) method was used to estimate parameters.

The likelihood ratio test was used to discriminate between alternative models. An objective function decrease of 3.84 units was considered significant (χ^2 P<0.05 df=1). The covariates age, height, sex, CrCL and body size [total body weight (weight), body surface area (BSA), body mass index (BMI), IBW, lean body weight (LBW), adjusted body weight (ABW), and percent ideal body weight (%IBW)^{6, 80}] were introduced into each parameter one by one. The continuous covariate weight on clearance (CL) was incorporated into the model in several ways. These are shown as below:

$$TVCL = \theta_1 + (\text{weight} / \text{Med}_{\text{weight}})^{\theta_{\text{weight}}}$$

$$TVCL = \theta_1 * (\text{weight} / \text{Med}_{\text{weight}})^{\theta_{\text{weight}}}$$

$$CL = TVCL * \exp(\eta_{\text{CL}})$$

TVCL is the typical value for the population and η_i is the random effect representing the difference of the i^{th} patient from the population mean. The random effects of between subject variability were assumed to be log-normally distributed, with a mean of zero and standard deviation of ω . Weight is the total body weight in kilograms and $\text{Med}_{\text{weight}}$ is the median total body weight. Weight and other body size descriptors were included in the analysis to help examine whether the departure from the normal body size affected disposition.

CrCL (creatinine clearance in L per h) was included in CL as below:

$$TVCL = \theta_1 + (\text{CrCL} / 4.8) * \theta_{\text{CrCL}}$$

$$CL=TVCL*\exp(\eta_{i_{CL}})$$

The non-renal component of clearance (θ_1) was evaluated in this model as a fixed parameter (0.229) reported by Green et al,⁷ as well as being directly estimated by NONMEM. If CrCL was missing, then $TVCL = \theta_{missing}$ was used. A sensitivity analysis was used to evaluate the impact on the other parameter estimates if θ_1 was fixed. The reported parameter estimates for θ_{NR} (non-renal clearance component) and θ_{CrCL} (renal component clearance) were 0.229 and 0.681 respectively in the literature.⁷ To assess how the previously published parameters (see above) would impact on the analysis, θ_{NR} was fixed to the published value of 0.229. The fixed value for θ_{NR} was then changed in 10% increments over a range of $\pm 50\%$ to assess whether or not this affected the other parameter estimates.

Residual variability was modeled using additive, proportional and combined error structures.

Graphical assessment of Bayesian individual parameter estimates versus covariates was evaluated to help identify possible covariate relationships. Covariates were retained in the model if inclusion in the model decreased the objective function value (OFV) by 3.84 ($\chi^2 P < 0.05$ $df = 1$). The model improvement was assessed by the OFV values and parameter estimates. In addition, the significance of the covariates was assessed using a randomization test with Wings for NONMEM.^{81, 82} This approach provided a calibration for the changes in OFV versus p-value for determination of statistical significance. In addition, graphics of goodness of fit were utilized to assess model robustness.⁸³

Simulation of steady state anti-Xa concentration

Two types of simulations were performed; the first was a deterministic simulation which assessed the impact of covariate effects on predicted C_{ss}. Anti-Xa concentrations were simulated using mean model parameters obtained from the final covariate model with random effects fixed to zero. This was done to more clearly evaluate covariate effect on C_{ss}. The calculation of C_{ss} is shown below:

$$C_{SS} = \frac{R_0}{CL} \quad (1)$$

The second simulation set used a Monte Carlo approach⁵¹⁻⁵³ to identify an appropriate dose for CII enoxaparin. The final covariate model was used as the input-output model to predict concentrations. The final model and parameter estimates obtained from the final model were used for the Monte Carlo simulations. The distribution of PK parameters was set to a log-normal distribution. Simulations were conducted to compare the percentage of the predicted C_{ss} values that were outside of the therapeutic range for the general medical unit and ICU patients receiving enoxaparin at infusion rates of 8.3, 5.8, 5.0, 4.2 IU/kg/h. The lowest infusion rate (4.2 IU/kg/h) was selected based on the best dose suggested by Green et al⁷ for renal dysfunction patients receiving SC enoxaparin. The highest infusion rate (8.3 IU/kg/h) is the current dosing strategy of enoxaparin administered by SC administration. A unique covariate distribution model was developed for general medical unit and ICU patients. The model constituted a joint distribution of weight and CrCL based on the ICU and the general medical unit patients in CII study. The correlation of weight and CrCL in the covariate distribution model was 0.33 for general medical unit patients and 0.30 for ICU patients in the CII study.⁷⁵ One thousand general medical unit patients and 1000 ICU patients were simulated from the joint distribution model. Two hundred simulations of 2000 patients were performed for each infusion rate using NONMEM[®]. For twice daily SC administration, the therapeutic range of anti-Xa is 0.5 IU/ml – 1.2 IU/ml.^{76, 84-88} This therapeutic range was applied as the target range for dose selection in simulation study for CII. The percentage of predicted C_{ss} which was higher than 1.2 IU/ml or which was lower than 0.5 IU/ml was calculated for each simulation using code written by the researchers in True-BASIC[®] (developed in 1965 by John Kemeny & Thomas E. Kurtz). The mean, 5th and 95th percentiles (90% predicted interval (PI)) were calculated from 200 simulations for the percent of predicted C_{ss} falling out of therapeutic range at each infusion rate. The patients were classified into 3 categories (CrCL<30ml/min; CrCL: 30-50 ml/min; CrCL>50 ml/min) prior to the simulation study, which was based on the severity of kidney impairment. These probabilities were then calculated for patients with varying degrees of renal function (CrCL<30 ml/min; CrCL: 30-50 ml/min; CrCL>50 ml/min), and the percentile of the mean, 5th and 95th (90% PI) is represented graphically. The best dosing regimens were selected based on the highest probability that the achieved concentrations would fall within the desired therapeutic range.

Results

Patient Characteristics

Eight patients in the CII study had unstable SCr; three of them were general medical unit patients and five were ICU patients. The CrCL for twenty seven patients in the CII study was unavailable. The duration of infusion for the 48 patients ranged from 8 to 894 h (138±158 h) and infusion rates ranged from 100 to 1600 IU/h (500±210 IU/h).

Population PK modeling

A two-compartment linear model with exponential inter-individual variability on clearance (CL) and volume of distribution of central compartment (V_2) adequately described the data. The basic PK parameters of CL, V_2 and volume of distribution of peripheral compartment (V_3), absolute bioavailability (F1) and absorption rate constant Ka (for SC study) are shown in Table 2. The residual error model accounted for differences in the residual error variance between the general medical unit and ICU patients. The residual error model was a combined additive and proportional model for general medical unit patients and proportional only for ICU patients. Allowing the residual error variance to partition based on location of the patient improved the OFV by 62.6 units (P<0.005).

The best residual error was described by the equation:

For general medical unit patients: $Y_{ij} = IPRED_{ij} * (1 + \epsilon_{ij1}) + \epsilon_{ij2}$

For ICU patients: $Y_{ij} = IPRED_{ij} * (1 + \epsilon_{ij3})$

where $IPRED_{ij}$ represents the j th predicted concentration for the i th individual, Y_{ij} is the observed anti-Xa concentration, and ϵ are the i.i.d. normally distributed random effects with normal distribution with a mean zero and standard deviation σ . ϵ_1 and ϵ_3 are the proportional component, and ϵ_2 is the additive component.

Visual inspection of individual empirical Bayes estimates of clearance showed a systematic change with CrCL. Thus CrCL was chosen for inclusion in the model as below:

$$CL = \theta_{NR} + (CrCL/4.8) * \theta_{CrCL} * \exp(\eta_{i\ CL})$$

The θ_{NR} and θ_{CrCL} are non-renal and renal clearance components, respectively.⁷ The reported parameter estimates for θ_{NR} and θ_{CrCL} were 0.229 and 0.681 respectively in the literature.⁷ From the sensitivity analysis, the CV% of all other parameter estimates, including mean parameter estimates (CV%: 0.4%-2.5%), inter-individual (CV%: 3.4% (ω_{cl}); 3.0% (ω_{v2})) and intra-individual variability (CV%: 0.1% (σ_1); 0.2% (σ_2); 1.2% (σ_3)), was less than 10% as a result of changing the value of θ_{NR} with one exception. θ_{CrCL} , which is correlated with the θ_{NR} value, had a larger change in value (CV%: 19%) than all the other parameters in the analysis. However CV% of total CL estimates were less than 10%, which may explain the compensatory change of θ_{CrCL} with θ_{NR} value. Therefore, fixing θ_{NR} to 0.229 did not affect the estimation of other parameters (mean parameter estimates, inter- and intra-individual variability), based on the sensitivity analysis. We left this value fixed at 0.229 as it was estimated under a much more robust experimental design and thus more likely to be an accurate reflection of non-renal clearance.⁷

CrCL was the most significant covariate on CL ($\Delta OFV = -10.1$; $P < 0.005$). Weight was the most significant covariate on V_2 ($\Delta OFV = -11.8$; $P < 0.005$). After incorporating the effect of CrCL on CL, weight was the most significant covariate on V_2 ($\Delta OFV = -21.56$; $P < 0.005$). The final model included CrCL on CL and weight on V_2 . The critical values of the delta OFV, according to the randomization test, to accept CrCL and weight were 2.6 and 2.3 respectively. The final model for CL and V_2 was therefore:

$$CL = 0.229 + (CrCL/4.8) * \theta_{CrCL} * \exp(\eta_{iCL})$$

$$V_2 = \theta_2 * (weight/70) * \exp(\eta_{iV_2})$$

where θ denotes the fixed effects, η denotes random effects with log normal distribution with zero mean and standard deviation ω , 0.229 (L/h) is the fixed value for non-renal clearance component, 80 ml/min (4.8 L/h) is considered as the cut-off value for normal renal clearance.^{89, 90}

The final PK parameter estimates are shown in Table 2. Population predicted anti-Xa concentrations versus observed anti-Xa concentrations are shown in Figure 1. ICU patients had an approximately 2 fold higher proportional residual variability than those general medical unit

patients. Inter-individual variability of CL and V_2 decreased by 38% and 53% respectively in the covariate model compared to the base model.

Upon inspection, the 48 patients in the CII study, ICU patients had a lower CL (0.79 ± 0.40 L/h) than general medical unit patients (0.99 ± 0.39 L/h), which is consistent with our previous results.^{75, 91} The individual dosage adjustment was calculated using individual estimates from NONMEM[®]. To achieve a target concentration of 0.5 IU/ml anti-Xa concentration, the infusion rates for typical ICU and general medical unit patients with weight of 70 kg were 5.6 ± 2.7 IU/kg/h and 7.0 ± 2.7 IU/kg/h, respectively.

Simulation of steady state anti-Xa concentrations

Assessing significant covariates that affect anti-Xa concentrations: Since weight and CrCL were significant covariates for PK parameters, simulations were applied to evaluate their impact on target anti-Xa concentration at steady state with weight varying from 30 to 120 kg and CrCL varying from 10 to 120 ml/min. Steady state anti-Xa concentrations were simulated using a 2-compartment model with parameters fixed to the final parameters under the covariate model and all random effects set to zero.

Anti-Xa concentration at steady state was calculated by equation 1. The effect of weight and CrCL on C_{ss} when administering enoxaparin at a rate of 100 IU/kg/12h by CII, is shown in figure 2. Clearance increased from 0.6 to 0.9 L/h when CrCL increased from 30 to 80 ml/min. As CrCL decreased and weight increased, predicted C_{ss} increased. This was particularly pronounced, when CrCL was below 30 ml/min.

Comparing the percent of predicted C_{ss} outside of therapeutic range at infusion rates of 8.3, 5.8, 5.0 and 4.2 IU/kg/h: CrCL was simulated using the covariate distribution model. The distribution of the covariates in patients with simulated values was comparable to that of general medical unit and ICU patients in the CII study. The final PK model with covariates was used as the input-output model. The percent for a predicted C_{ss} higher than 1.2 IU/ml or lower than 0.5 IU/ml was calculated for each simulation when general medical unit and ICU patients received infusion rate at 8.3, 5.8, 5.0 and 4.2 IU/kg/h respectively.

The percentage of predicted C_{ss} outside of therapeutic range (mean, 5th and 95th percentiles) at each infusion rate for general medical unit and ICU patients was shown in Table 3. The percentage of predicted C_{ss} outside of therapeutic range at each infusion rate for these subjects with different renal function was shown in Table 4. For both general medical unit and ICU patients, when the infusion rate decreased, the percentages of the predicted C_{ss} that were higher than 1.2 IU/ml decreased and the percentages of the predicted C_{ss} that were lower than 0.5 IU/ml increased (Figure 3a, 3b, 4a, 4b). General medical unit patients achieved the lowest total percentage (with an equal probability of either being above or below the therapeutic range) of the predicted C_{ss} falling outside of therapeutic range at an infusion rate of 8.3 IU/kg/h, while ICU patients achieved the lowest total percentage at 4.2 IU/kg/h.

Figure 3, Figure 4 and Table 4 illustrate the percentage of patients' predicted C_{ss} falling out of therapeutic range for ICU and general medical unit patients. These figures reflect that, given an optimization of dosage to result in an equal probability of being either above or below the therapeutic range, general ward unit subjects achieved the lowest total percentage of C_{ss} falling outside of therapeutic range at infusion rate of 5.0 IU/kg/h if CrCL<30 ml/min, 5.8 IU/kg/h if CrCL was 30-50 ml/min and 8.3 IU/kg/h if CrCL>80 ml/min, while ICU subjects achieved the lowest total percentage of C_{ss} falling outside of therapeutic range at infusion rate of 4.2 IU/kg/h if CrCL<30 ml/min, 5.0 IU/kg/h if CrCL was 30-50 ml/min and 5.8 IU/kg/h if CrCL>80 ml/min. The difference between different dosing strategies is shown graphically in Figure 3a, b and Figure 4a, b. If the current dosing guideline (100 IU/kg/twice a day) of enoxaparin administered SC were used for patients with CrCL<30 ml/min receiving CII, 64.6-68.1% of ICU patients and 52.1-60.9% of general medical unit patients would have anti-Xa concentration > 1.2 IU/ml (Figure 3b, 4b). This can be reduced to 24.1-29.2% for ICU patients when dosing is decreased to 4.2 IU/kg/h and to 21.4-28.3% for general medical unit patients when the dosing decreased to 5.0 IU/kg/h. When using the revised dosing strategy, simulated ICU and general medical unit patients with a CrCL<30 ml/min experienced a 28% and 22% (Table 4) decrease in the percentage of the total predicted C_{ss} falling out of therapeutic range respectively, when compared with the patients receiving 8.3 IU/kg/h of enoxaparin.

In some situations, the best dose selected based on the total percentage of C_{ss} outside of the therapeutic range was found to be indistinguishable from other doses (change of total % C_{ss} outside of the therapeutic range less than 10%). For example, if ICU patients, with CrCL<30

ml/min that received enoxaparin at infusion rate of 5.0 IU/kg/h, the total percent C_{ss} outside of therapeutic range was reduced by 3% compared to the situation when the best dose of 4.2 IU/kg/h was applied. This is also true for general medical unit patients with CrCL < 30 ml/min, the total percentage of C_{ss} falling outside of therapeutic range at infusion rate of 5.0 IU/kg/h was 48% and became 49% at the rate of 5.8 IU/kg/h. However, in the “best dose” situations, patients have a similar probability of being either above or below the therapeutic range (Figure 3c, 4c). If the change of the total % C_{ss} outside of the therapeutic range was less than 10% when dose other than best dose was applied, the dose was considered to be indistinguishable from the best doses suggested above. Thus the range of dosage at each of the patient types were indicated, where the total probability of being outside the therapeutic range was indistinguishable: for general medical patients 4.2-5.8 IU/kg/h if CrCL < 30 ml/min, 5.0 – 8.33 IU/kg/h if CrCL was 30-50 ml/min and 5.8-8.33 IU/kg/h if CrCL > 50 ml/min; for ICU patients, 4.2-5.0 IU/kg/h if CrCL < 30 ml/min, 4.2 – 5.8 IU/kg/h if CrCL was 30-50 ml/min and 5.0-5.8 IU/kg/h if CrCL > 50 ml/min. However, the clinician will have to consider the risks to a particular patients associated with the relative probability of that patients being either above or below the range when tailoring the actual dose administered to the patient.

Discussion

Dosing strategies developed by many SC enoxaparin studies were based on weight and renal function, which may help to reduce bleeding complications,^{65, 67, 68, 84} and these changes are amplified in complicated patient populations that are present in critically ill multiple trauma patients⁷⁴. Highly variable and unreliable anti-Xa concentrations were observed when the standard dose of enoxaparin for prevention of venous thromboembolism was applied. In this study, the bioavailability estimation for general medical unit patients in SC study was 0.94. Whether the extensive variability of anti-Xa concentrations in critically ill patients from Dr. Haas⁷⁴ study is due to the variable bioavailability for SC enoxaparin is unknown. Applying CII enoxaparin is one approach to evaluate this issue and may reduce the variability observed after SC administration in critically ill patients. This has led some investigators to begin examining the continuous IV administration of enoxaparin to examine this issue. Despite this, no extensive population pharmacokinetic analysis or dosing adjustment suggestions have been reported for

enoxaparin given by CII. This is the first study to evaluate factors affecting anti-Xa concentrations following CII administration of enoxaparin. This information is used to develop a dosing guideline based on the percentage of the predicted steady state anti-Xa concentrations falling out of the therapeutic range with CII using Monte Carlo simulations.

In previous population data analyses, combined data sets were used to help stabilize estimations.¹⁶ In our study, combining additional data from the SC study with the CII data allowed us to better describe and characterize the PK parameters for CII. Compared with the CII data analysis alone, there was a 50% decrease of standard error of estimation for CL and V_2 in the combined data analysis. Moreover, the inter-individual variability of CL and V_2 decreased 37% and 47% respectively, compared with the CII data analysis alone.⁷⁵

Approximately half of the subjects in CII study were from ICU. This may contribute to additive PK complexity as those patients were prone to have fluid shifts, organ dysfunction, and drug binding alteration.^{71, 92} Different PK parameters (CL) were found in ICU and general medical unit patients in this study and our previous report.⁷⁵ The different clearance between ICU and general medical unit patients was also found by Priglinger et al.,⁷³ where they demonstrated that SC administration of LMWH may not work well in critically ill patients due to different PK behavior as compared with general medical unit patients. Simulations suggest that an infusion rate of 5.6 ± 2.7 IU/kg/h for ICU patients and 7.0 ± 2.7 IU/kg/h for general medical unit patients were needed to achieve lower limit of therapeutic range of 0.5 IU/ml anti-Xa concentration. The model for ICU patients showed a higher proportional residual error than that from general medical unit patients. This may be a function of model misspecification in the highly dynamic ICU population compared to the more stable general medical unit patients

Similar to previous reports of SC administration of enoxaparin,^{7, 68} this study showed that enoxaparin CL increased with increasing CrCL. One study in 96 obese patients reported by Green et al.⁶ demonstrated that LBW is a significant covariate on CL and weight on V_2 . After including CrCL on CL and weight on V_2 , no body size descriptor other than weight was found as a significant covariate on PK parameters. Green et al.⁷ reported a series recommended dosing regimens based on the glomerular filtration rate (GFR) estimated using CG equation, where dose of 0.4 mg/kg/12h was suggested to subjects with GFR less than 30ml/min. A simulation study for CII administration found that CrCL had a higher impact on C_{ss} in patients with renal

dysfunction (CrCL<30 ml/min) than in patients with moderate renal impairment and normal renal function patients. Results from 200 simulations at each infusion rate (8.3, 5.8, 5.0, 4.2 IU/kg/h) demonstrated that general medical unit patients achieved the lowest total percent of predicted C_{ss} outside of the therapeutic range at 8.3 IU/kg/h (90% PI: 48.0%-56.8%), while ICU patients achieved the lowest total percent at 4.2 IU/kg/h (90% PI: 47.7%-54.2%) (Table 3). Furthermore, if CrCL was less than 30 ml/min (renal dysfunction), the best doses for patients in the ICU and general medical unit were 4.2 IU/kg/h and 5.0 IU/kg/h, respectively; 5.0 IU/kg/h and 5.8 IU/kg/h, respectively, if CrCL is between 30 and 50 ml/min (moderate renal impairment). For ICU and general medical unit patients with CrCL greater than 50 ml/min, the best dose was 5.8 IU/kg/h and 8.3 IU/kg/h respectively (Table 4). Based on these results, most patients will achieve expected steady state anti-Xa concentrations between 0.5 IU/ml and 1.2 IU/ml, if a): ICU patients with CrCL > 50 ml/min receive enoxaparin at 5.8 IU/kg/h, and general medical unit with CrCL > 50 ml/min receive enoxaparin at 8.3 IU/kg/h infusion rate; 2): ICU patients with CrCL between 30 to 50 ml/min receive enoxaparin at 5.0 IU/kg/h, and general medical unit patients with CrCL between 30 to 50 ml/min receive 5.8 IU/kg/h; and 3): ICU patients with CrCL< 30 ml/min receive enoxaparin at 4.2 IU/kg/h and medical unit patients with CrCL< 30 ml/min receive enoxaparin at 5.0 IU/kg/h. These best doses also represented the optimal solution where the probability of being above the therapeutic range is not different from being below the range (Figure 3c, 4c). Given different therapeutic risks in the clinic, it was felt that this would provide a starting point. The additional information on the total risk of being outside the therapeutic range can then be considered in concert with this information tailoring to the patient with respect to whether or not it is worse for that patient to be above or below the range. Given the equal total probabilities of being outside the range for multiple dosage levels, we have provided a range of dosages where that total probability is indistinguishable across groups can be determined from Table 4. However, the clinician will have to consider the relative probability of above or below the range when tailoring the actual dose administered to the patient.

CII administration of enoxaparin had been used in the treatment of acute pulmonary embolism.^{93, 94} Patients with acute pulmonary embolism received an i.v bolus of 0.5 mg/kg enoxaparin and followed by an initial dosage of 2-3 mg/kg/day CII enoxaparin. Anti-Xa concentrations were measured daily. The dosage was adjusted to maintain anti-Xa concentration between 0.2 – 0.6 IU/ml.^{93, 94} No deleterious hemorrhagic side effects were found during the

treatment of acute pulmonary embolism.⁹⁴ This might be due to the dosage adjustment by daily measurements of anti-Xa and anti-IIa concentrations, which lead to more constant level of anticoagulation. The dosing adjustment recommended in this paper can be applied when CII is used in clinical practice to patients with varying renal function, which is not available in literature yet.

Unfortunately, the limitations of a retrospective study are the availability of documented data in a medical unit record review. Even with the electronic laboratory information, SCr concentrations were unavailable in twenty seven patients in the CII study. The need to evaluate SCr was at the discretion of the physician since this was an observational evaluation. We acknowledge the small sample size of patients with available SCr in the CII study and accounted for this by combining data in the PK analysis with additional patients from a second study. This approach has been discussed previously.¹⁶ Combining datasets assisted in identifying CrCL as a significant covariate of CL.⁷⁵

Conclusion

This study evaluated the pharmacokinetic profile and defined a dosage strategy for administering enoxaparin by continuous intravenous infusion in patients with varying renal function. CrCL was identified as a significant covariate on CL and total body weight on V_2 .

Acknowledgements

Financial Support: This work was financially supported by National Institute for Biomedical Imaging and Bioengineering Grant # P41 EB001975-06 (For Dr.Bies); and Supported in part by a grant from Aventis Pharma Australia Pty Ltd.

The authors would like to acknowledge Dr. Curtis E Haas for sharing his paper and Dr. Alan Forrest for helpful advice on the manuscript.

Table 1: Patient characteristics for the two studies

Demographics	SC	CII		Combined
	General medical unit	General medical unit	ICU	
Sample size	35	29	19	83
Age (years)	75.1 (44-86)	60.9 (16-90)	59.3 (23-77)	66.6 (16-90)
Weight (kg)	67.7 (32-95)	74.1 (46.5-108)	73.3 (46.5-97.5)	71.0 (32-108)
Height (cm)	164.0 (147-184)	168.7 (152-182)	166.2 (151-177)	166.0 (147-184)
Gender (Male/Female)	17/18	16/13	7/12	40/43
CrCL (ml/min)	39.2 (14.9-95.7)	63.5 (31.1-128.3)	26.8 (7.6-49.6)	45.0 (7.6-128.3)

Abbreviations: SC: subcutaneous, CII: continuous intravenous infusion, CrCL= Creatinine Clearance.

* Twenty seven patients in the CII study did not have a serum creatinine (SCr) concentrations.

Table 2: PK parameter estimates for two compartment model

Parameters	Base model	SE%	Parameters	Final model	SE%
CL (L/h)	0.693	9.5	CLmissing (L/h)	0.972	10.5
θ_{NR}	N/A	N/A	θ_{NR} (L/h)	0.229	N/A
θ_{CrCL}	N/A	N/A	θ_{CrCL} (1 /4.8 CrCL)	0.744	18.7
V_2 (L)	7.07	22.5	V_2 (L/ 70 kg weight)	6.78	19.2
V_3 (L)	5.99	25.4	V_3 (L)	6.19	24.9
Q (L/h)	0.494	27.9	Q (L/h)	0.429	24.7
Ka (/h)	0.428	29.0	Ka (/h)	0.476	27.3
F1	1	1.1	F1	0.94	9.7
$\omega_{cl}\%$	65.5	44.1	$\omega_{cl}\%$	40.7	23.8
$\omega_{v2}\%$	61.9	31.3	$\omega_{v2}\%$	29.4	82.2
$\sigma 1\%$	22.6	28.4	$\sigma 1\%$	12.1	100
$\sigma 2$ (IU/L)	75.4	36.6	$\sigma 2$ (IU/L)	132	44.7
$\sigma 3\%$	43.1	26.0	$\sigma 3\%$	44.0	26.3

Abbreviations: CL=clearance, CrCL=creatinine clearance, IU=international units, SE=standard error, weight=total body weight, V_2 =volume of distribution of central compartment, V_3 =volume of distribution of peripheral compartment, ω =coefficient of variation of inter-individual variability, $\sigma 1$ =proportional coefficient of variation of residual error for general medical unit patients, $\sigma 2$ =additive coefficient of variation of residual error for general medical unit patients, $\sigma 3$ = proportional coefficient of variation of residual error for ICU patients; N/A: not available, $\theta_{NR} = 0.229$ (fixed), Unit of weight=kg, Unit of CrCL=L/h, F1: absolute bioavailability

Table 3: Percent of predicted anti-Xa C_{ss} higher than 1.2 IU/ml or Percent of predicted anti-Xa C_{ss} lower than 0.5 IU/ml when general medical unit and ICU patient receiving enoxaparin at different infusion rates of 8.3, 5.8, 5.0 and 4.2 IU/kg/h

Infusion rate (IU/kg/12h)	General medical unit Patients				ICU Patients			
	Percent of C _{ss} <0.5IU/ml		Percent of C _{ss} >1.2IU/ml		Percent of C _{ss} <0.5IU/ml		Percent of C _{ss} >1.2IU/ml	
	Mean	90%PI	Mean	90%PI	Mean	90%PI	Mean	90%PI
8.3	18.1	16.7-20.7	33.9	31.3-36.1	5.8	4.5-6.8	61.1	59.4-63.9
5.8	35.8	33.8-38.2	17.0	15.0- 19.0	13.8	12.5-15.1	41.4	40.4-43.5
5.0	44.9	42.5-47.1	11.9	10.3-13.5	20.5	19.2-22.2	31.0	30.3-33.3
4.2	55.2	52.5-57.5	7.50	6.40-8.70	28.3	26.5-29.8	22.7	21.2-24.4

Abbreviations: ICU = intensive care unit, C_{ss} = steady state anti-Xa concentration, h= hour, PI=predicted interval

Table 4: Percent of predicted anti-Xa C_{ss} higher than 1.2 IU/ml or Percent of predicted anti-Xa C_{ss} lower than 0.5 IU/ml when general medical unit and ICU patient receiving enoxaparin at different infusion rates of 8.3, 5.8, 5.0 and 4.2 IU/kg/h for subjects at each renal function group (1: CrCL < 30 ml/min; 2: CrCL 30-50 ml/min; 3: CrCL > 50 ml/min).

Infusion rate (IU/kg/12h)	CrCL (ml/min)	General medical unit Patients		ICU Patients	
		Mean percent of C _{ss} <0.5IU/ml	Mean percent of C _{ss} >1.2IU/ml	Mean percent of C _{ss} <0.5IU/ml	Mean percent of C _{ss} >1.2IU/ml
8.3	<30	6.74	54.4	4.1	65.8
	30-50	11.9	42.7	7.4	55.5
	>50	22.4	28	13.3	44
5.8	<30	16.6	32.3	10.97	46.1
	30-50	28.2	21.6	16.8	36.2
	>50	43.8	11.6	25.8	22.9
5.0	<30	23.7	24.3	16.8	35.1
	30-50	36.8	15.3	24.2	26.4
	>50	53.3	7.59	36.8	14.5
4.2	<30	32.8	16.3	24.1	26.4
	30-50	47.4	9.93	32.4	18.4
	>50	63.8	4.47	48.0	9.13

Abbreviations: ICU = intensive care unit, C_{ss} = steady state anti-Xa concentration, h= hour

Figure 1: population predicted anti-Xa concentrations versus Observed for the two-compartment model with CrCL and weight covariates in the model. Individual data points were shown as dots and the unity was shown as a solid line.

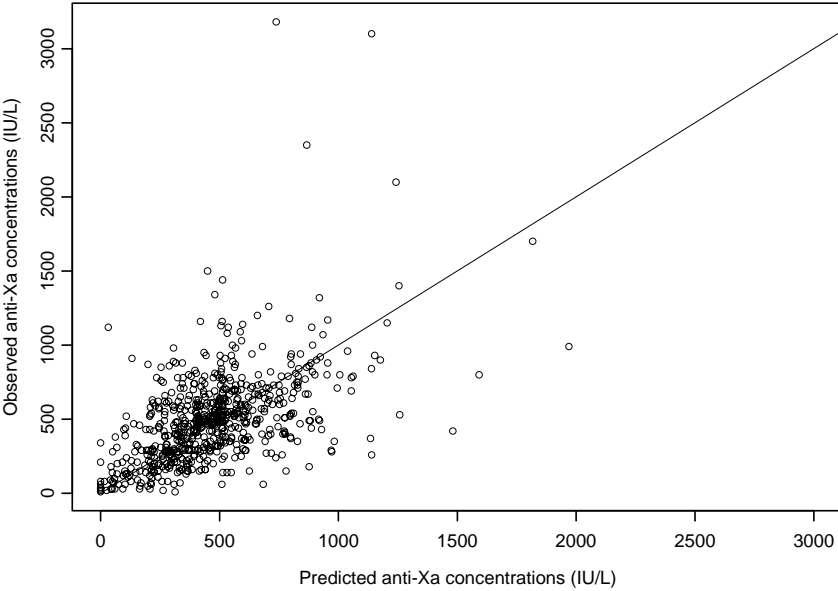


Figure 2: Three-D surface showing the relationship between CrCL, weight and predicted C_{ss}. The surface shows how the C_{ss} changes with both weight and CrCL simultaneously.

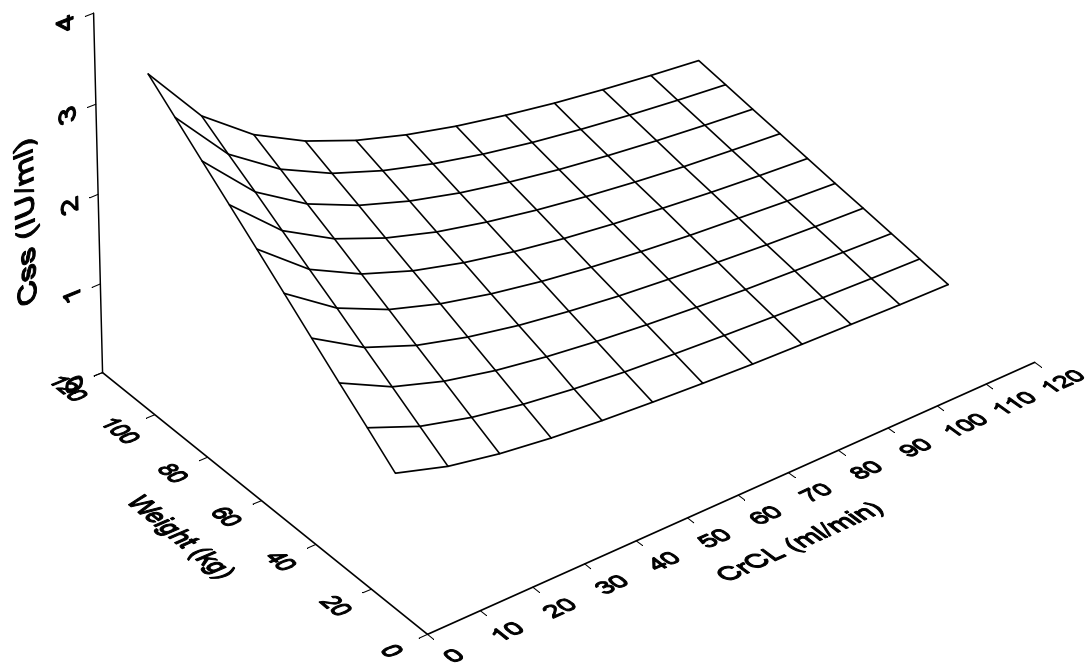


Figure 3: The percentage of predicted C_{ss} falling out of therapeutic range at different infusion rate (8.3, 5.8, 5.0, 4.2 IU/kg/h) for ICU patients with different renal function (1: CrCL < 30 ml/min; 2: CrCL 30-50 ml/min; 3: CrCL > 50 ml/min). Dash lines represent the 5th and 95th percentiles (90% PI).

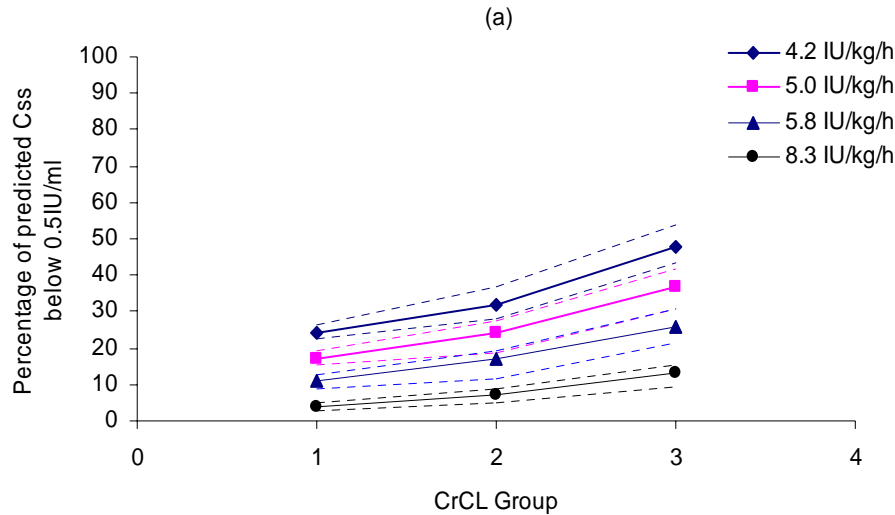
a): Percentage of predicted C_{ss} which is lower than 0.5 IU/ml

b): Percentage of predicted C_{ss} which is higher than 1.2 IU/ml

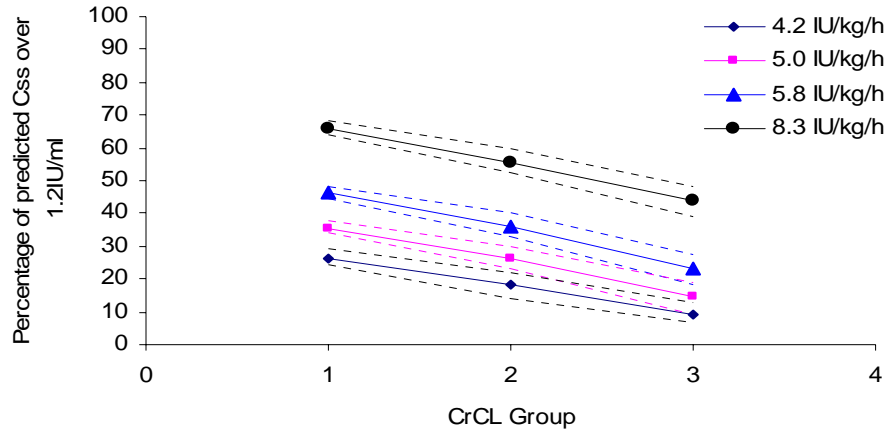
(Rhombus ◆: 4.2 IU/kg/h; Square ■: 5.0 IU/kg/h; Triangle ▲: 5.8 IU/kg/h; Dot ●: 8.3 IU/kg/h)

c): Percentage of predicted C_{ss} falling out of therapeutic range (0.5-1.2 IU/ml) when patients with CrCL < 30 ml/min received enoxaparin at 4.2 IU/kg/h infusion rate and CrCL between 30 and 50 ml/min received enoxaparin at 5.0 IU/kg/h infusion rate and CrCL > 50 ml/min received enoxaparin at 5.8 IU/kg/h infusion rate.

(Square ■: > 1.2 IU/ml; Dot ●: < 0.5 IU/ml)



(b)



(c)

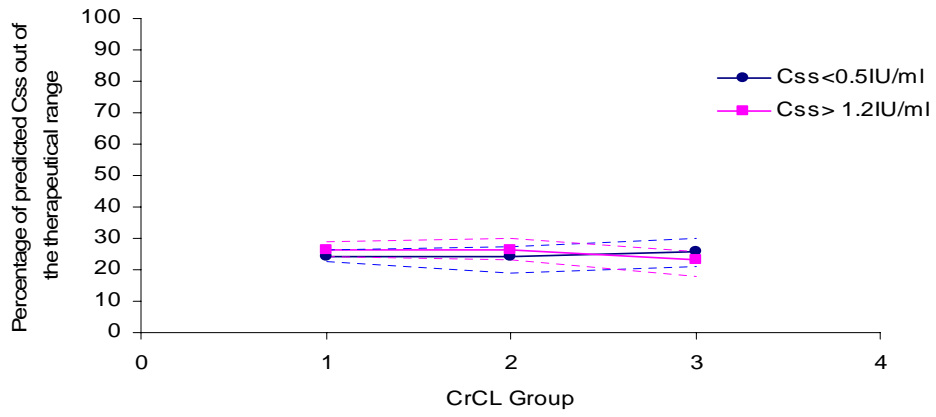


Figure 4: The percentage of predicted C_{ss} falling out of therapeutic range at different infusion rate (8.3, 5.8, 5.0, 4.20 IU/kg/h) for general medical unit patients with different renal function (1: CrCL < 30 ml/min; 2: CrCL 30-50 ml/min; 3: CrCL > 50 ml/min).

Dash lines represent the 5th and 95th percentiles (90%PI).

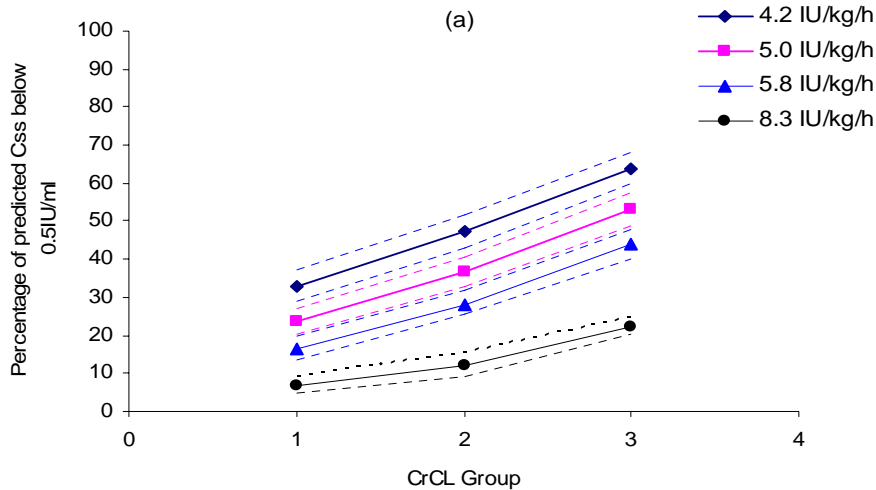
a): Percentage of predicted C_{ss} which is lower than 0.5 IU/ml

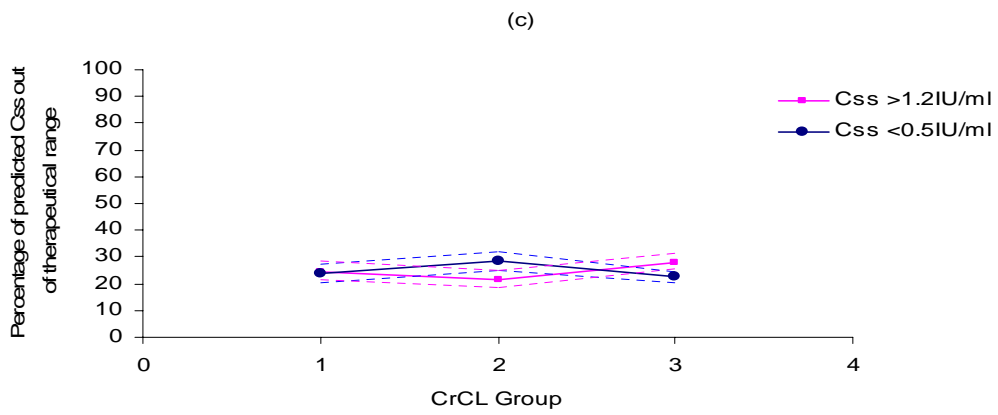
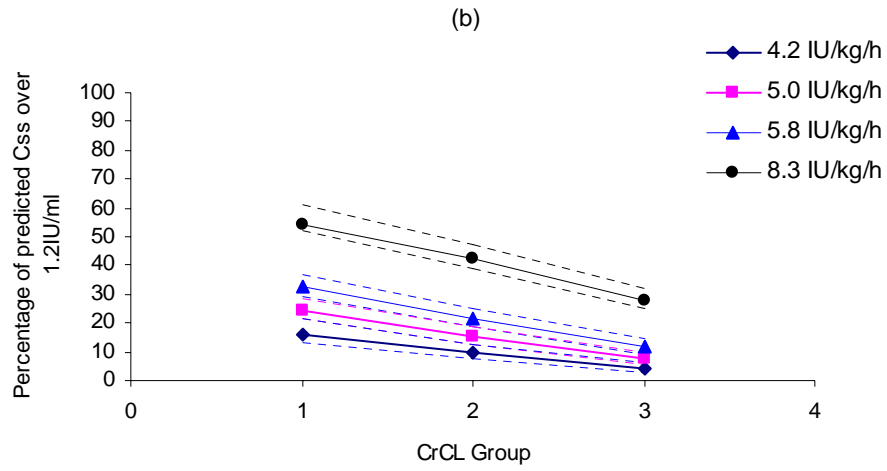
b): Percentage of predicted C_{ss} which is higher than 1.2 IU/ml

(Rhombus ◆: 4.2 IU/kg/h; Square ■: 5.0 IU/kg/h; Triangle ▲: 5.8 IU/kg/h; Dot ●: 8.3 IU/kg/h)

c): Percentage of predicted C_{ss} falling out of therapeutic range (0.5-1.2 IU/ml) when patients with CrCL < 30 ml/min received enoxaparin at 5.0 IU/kg/h infusion rate and CrCL between 30 and 50 ml/min received enoxaparin at 5.8 IU/kg/h infusion rate and CrCL > 50 ml/min received enoxaparin at 8.3 IU/kg/h infusion rate.

(Square ■: > 1.2 IU/ml; Dot ●: < 0.5 IU/ml)





**CHAPTER 3 DETERMINATION COVARIATE EFFECTS ON EXPOSURE OF
DRUG WITH LINEAR PHARMACOKINETIC CHARACTERISTICS GIVEN HIGHLY
SPARSE DATA**

This chapter is based on the following paper:

Bies, Robert R, **Feng, Yan**, Lotrich, Francis E, Kirshner, Margaret A, Roose, Steven P, Kupfer, David J, Pollock, Bruce G. Utility of sparse concentration sampling for citalopram in elderly clinical trial subjects. *Journal of Clinical Pharmacology*, 2004, 44(12):1352-1359.

The supplemented results from the further study after publication were also presented.

Copyright has been assigned to Sage Publications. The permission of using the full article in the thesis had been granted from the copyright owner (Sage Publications).

ABSTRACT

Objective: To evaluate whether the disposition of the selective serotonin reuptake inhibitor, citalopram, could be robustly captured using 1 to 2 concentration samples per subject in 106 patients participating in two clinical trials.

Methods: Nonlinear mixed effects modeling was used to evaluate the pharmacokinetic parameters describing citalopram's disposition. Both a prior established 2-compartment and a de-novo 1-compartment pharmacokinetic model were used. Covariates assessed were concomitant medications, race, sex, age (22-93 years) and weight. Covariates affecting disposition were assessed separately and then combined in a stepwise manner.

Results: Pharmacokinetic characteristics of citalopram were well captured using this sparse sampling design. Two covariates (age and weight) had a significant effect on the clearance and volume of distribution in both the one and two compartment pharmacokinetic models. Clearance decreased 0.23 L/hr for every year of age and increased 0.14 L/hr per kg body weight.

Conclusions: Hyper-sparse sampling designs are adequate to support population pharmacokinetic analysis in clinically treated populations. This is particularly valuable for populations such as the elderly, who are not typically available for pharmacokinetic studies.

INTRODUCTION:

Selective serotonin reuptake inhibitors (SSRIs) such as citalopram are commonly used to treat depression in geriatric patients.⁹⁵ There are limited data on the variability and exposure characteristics of these compounds once in general clinical use. Elderly patients are not easily studied using the intensive concentration sampling required for classical pharmacokinetic (PK) analysis approaches. These data are potentially available using a sparse-sampling approach to measuring concentration exposure.

The limitation of traditional PK studies with small numbers of healthy volunteers is in the ability to extrapolate the results to clinical populations. For certain drugs, such as citalopram, large differences in PK/PD profiles may be found across individuals. Mixed effects population PK methods are better suited for evaluating inter-individual and intra-individual random effects in large-scale clinical trials, and only require a few samples per patient in a large number of patients.⁹⁶ Moreover, covariate effects, when evaluated using this methodology, are supported by all data in the analysis. Thus, systematic error is reduced when compared to classical PK approaches.⁹⁷

Despite this, there have been no studies evaluating in a continuous manner, the nature of PK changes for citalopram in clinically treated populations, particularly with regard to age. Age-related differences in citalopram pharmacokinetics have been reported as general differences between groups of young and elderly individuals.^{98,99} For example, Frederiscon Overo et al⁹⁸ measured citalopram PK in 11 elderly patients aged 73 to 90 years, and Gutierrez and Abramowitz⁹⁹ similarly examined citalopram disposition in 24 healthy elderly volunteers aged 65 to 77 years. Both of these studies found a reduction in clearance in the elderly group, with Frederiscon Overo et al showing a range of clearance from 4.8 to 18 L/hr in the elderly and approximately 24 L/hr in the young.⁹⁸ In 2 other studies utilizing data from therapeutic drug monitoring, age was correlated with drug concentrations¹⁰⁰ or with dose/concentration ratios,¹⁰¹ although specific pharmacokinetic parameters were not assessed. However, there is a need to quantitatively evaluate differences in PK for drugs used in the elderly across a range of ages and to account for the role of other individual specific characteristics that may impact exposure to drug.

This study evaluated the performance of nonlinear mixed effects modeling in capturing exposure to citalopram as well as individual specific characteristics affecting that exposure with very limited sampling in a large number of psychiatric patients from two clinical trials. We quantitatively explored, using nonlinear mixed effects modeling, the relationships between clearance, weight, age sex, race and concomitant medications as well as the degree of inter-individual variability in drug exposure.

METHODS:

General Design

Two clinical trials (see below) provided a total of 199 plasma concentration samples for citalopram from 106 subjects (Table 1). The subjects were started at a dose of 20 mg citalopram daily. The subjects received an average daily citalopram dose of 30 ± 15 mg in study A and 15 ± 5 mg in study B. Population PK analyses were performed using de-identified data. De-identified data does not allow a link to be made between patients and their individual personal and psychiatric information. Both studies were approved by the appropriate institutional review boards and all subjects gave informed consent to participate.

Subject selection

Study A was a multi-site (5 academic medical centers in the U.S, with University of Pittsburgh as the coordinating center) open label study to assess citalopram as treatment for depression in patients with bipolar disorder.¹⁰² The subjects had a diagnosis of DSM-IV bipolar I or II depression. Patients were excluded for mania, rapid cycling, mixed or psychotic forms of depression, any other axis I diagnosis, history of alcohol or substance abuse in the last three months, unstable or untreated medical disorder, and women who were pregnant or breastfeeding or of childbearing potential not on contraception.

Subjects were treated with citalopram in 2 phases, an initial 8-week response phase followed by a 16-week continuation phase for responders. Citalopram was started at 20 mg daily, and could be increased by 20 mg every 2 weeks based on response to a maximum of 60 mg or reduced to a minimum dose of 10 mg based on the appearance of adverse drug reactions. A detailed history of dosage changes was available for the purposes of modeling citalopram pharmacokinetics. Plasma samples were obtained at baseline, week 1, week 8 and the end of study. A histogram showing the distribution of sampling times (time after dose) is shown in Figure 1. The concentration measurements were not scheduled for any particular time as the mixed-effects modeling approach could account for this as long as the last dosage time and the sampling time were known. The dosage times were noted for inpatient subjects and were supplied as self-report from outpatients. Concomitant medications were noted at each of the clinic visits. A total of 45 patients entered this study with 40 of these patients providing 85 citalopram concentration samples.

Study B was a multi-site (10 academic medical centers in the U.S. with Columbia University as the coordinating center) randomized, double-blind study of the treatment of depression with citalopram or

placebo in subjects at least 75 years of age.^{103, 104} Subjects had a DSM-IV diagnosis of major depressive disorder with duration of the episode of greater than four weeks at baseline. Subjects were excluded if they had other axis I disorders, dementia, acute severe or unstable medical illness or if they had a minimal status examination score of less than 18.

Citalopram was given at an initial dose of 20mg daily with the option to increase to 40mg daily for weeks five through eight. Dosages could be reduced to 10 mg daily if there were significant side effects. Plasma samples for citalopram were obtained at baseline, week 4, and week 8 or upon termination, if early termination occurred. No specific timing was scheduled for the citalopram concentration sampling. The distribution of sampling times is shown in Figure 1. The time of last dosage was noted by self-report and the dosage history was available for PK modeling. The clinical trial site recorded the timing of the plasma sample collection for citalopram. A total of 66 patients provided 114 concentration samples.

Citalopram Analysis

Citalopram and metabolites were measured by HPLC with UV detection using a method developed in our laboratory.¹⁰⁵ This assay has been validated with a lower limit of detection of 3ng/mL and coefficients of variation ranging from 3.1% (220ng/mL) to 9.4% (15ng/mL). All concentration measurements were analyzed in the Geriatric Psychopharmacology Laboratory at the University of Pittsburgh using the same analytical protocol.

Pharmacokinetic modeling

A prior nonlinear mixed effects model describing citalopram pharmacokinetics was used to evaluate the data from the two studies described above.^{106, 107} In addition, a new model search was performed evaluating 1 and 2-compartment models. The focus of the modeling was to examine the impact of the covariates weight, age, race, sex and concomitant medications on the oral clearance (CL/F) and volume of distribution (V/F) of citalopram. NONMEM (Globomax Corporation, Hanover MD) was used for the analysis using both ADVAN2 TRANS2 and ADVAN4 TRANS4. An exponential error model for inter-individual variability (equation 1) on the pharmacokinetic parameters was used along with an additive and proportional residual error model (equation 2). In equation 1, CL/F_i is an individual patient's oral clearance value, TVCL/F is the population average oral clearance for an individual of particular age and weight and η is the inter-individual variability shown in exponential form. In equation 2, Y is the

observed concentration value and G is the individually predicted concentration value. ERR(1) and ERR(2) are the residual error terms. Model building and assessment were done initially using the first order estimation method and confirmed using the first order conditional estimation method.

$$CL/F_i = TVCL/F * \exp(\eta_{CL/F}) \quad (1)$$

$$Y = G * (1 + ERR(1)) + ERR(2) \quad (2)$$

Initially, covariate relationships were evaluated using XPOSE,¹⁰⁸ comparing the individual deviations for the parameters to the covariates of interest. Four covariates (weight, age, sex, and race) were evaluated in this way. For Study A, concomitant medication was assessed as an additional covariate.

Covariates were evaluated in the mixed effects PK model in a stepwise fashion. Initially, each covariate was assessed individually and then incorporated into the model in a stepwise fashion. Both a stepwise addition with backward removal and a backward removal with forward addition method were utilized for covariate identification. The difference in objective functions (Δ -2 times the log likelihood (-2LL)) was used to compare alternative models. As the log likelihood difference approximates a χ^2 distribution, the incorporation of a covariate resulting in an objective function decrease of 7.88 units (χ^2 , $P < 0.005$, $df = 1$) was considered significant. Weight was incorporated as:

$$TVCL1/F = \theta_1 * (WT / MedWT)^{\theta_2} \quad (3)$$

where TVCL1/F is the population clearance, θ_1 and θ_2 are the coefficient and exponent surrounding the centered weight term, WT is weight in kilograms and MedWT is the median weight.¹⁰⁹
¹¹⁰ The importance of each covariate was compared based on decreasing of objective functions (Δ -2LL) when the model including a covariate and increase of Δ -2LL when the model excluding a covariate. The most important covariate was retained in the model and then the second included after correction of the first. Age was incorporated in model after inclusion of the weight covariate as shown below where TVCL/F is the population clearance including the age covariate, TVCL1/F is the weight normalized population oral clearance value and the age covariate is centered about the median age in the study (60 years):

$$TVCL/F = TVCL1/F * \exp((age - 60) * \theta_3) \quad (4)$$

In each run, the 95% confidence intervals (CI) of point estimates were determined from the standard errors of estimates (SE) as follows: CI point estimate $\pm 1.96 \times SE$. If the covariate step was unsuccessful,

the 95% CI was determined by bootstrapping (sampling with replacement) method.¹¹¹ This method consisted of repeatedly fitting the model to 200 bootstrap replicates of the data. The 95% CI of bootstrap parameters were calculated by taking as the 2.5th to 97.5th inter-percentile range of the 200 replicates.

RESULTS:

Although the prior 2-compartment model was used as an initial test model for this analysis,^{106, 107} the population PK model that was supported robustly by these data was the 1-compartment linear PK model. The 1-compartment PK model with exponential interindividual variability on both oral clearance and volume of distribution was determined to be the most robust based on both the Akaike information criterion (AIC)⁴⁷ and the confidence intervals around the estimates (AIC = 1562, 1-compartment; AIC = 1569, 2-compartment).

The estimates of oral clearance averaged 6.34 L/h in the older patients (aged 75-93 years) and 16.49 L/h in the younger patients (aged 22-65 years). The oral clearance values ranged from 2 L/h for the eldest patient (aged 93 years) in the study to approximately 19.5 L/h in the youngest subjects (aged 22-29 years). This is consistent with studies using intensive PK sampling in limited numbers of subjects, in which oral clearance was approximately 4 L/h in the elderly group and 24 L/h in the young.¹¹²

Details of the model-building process with the first-order (FO) and first-order conditional estimation (FOCE) methods are discussed below and also shown in Table 2. The incorporation of weight and age as covariates on CL/F and V/F resulted in significant changes in the objective function. The final models for CL/F and V/F were as follows:

$$TVCL1/F = \theta1 * (WT/80)^{\theta2}$$

$$TVCL/F = TVCL1/F * \exp((AGE-60) * \theta3)$$

$$CL/F = TVCL/F * \exp(\eta1)$$

$$TVV1/F = \theta4 * (WT/80)^{\theta5}$$

$$TVV/F = TVV1/F * \exp((AGE-60) * \theta6)$$

$$V/F = TVV/F * \exp(\eta2)$$

Beginning with a basic model not incorporating age or weight, a series of four additional models were tested using both FO and FOCE methods. The best model for both FOCE method and FO method,

showed that weight and age were statistically significant covariates on both CL/F and V/F (Base Model OFV=1680, Best model with Covariates OFV=1567, FOCE). After incorporation of weight as a covariate on CL/F and V/F, the incorporation of age as a covariate on CL/F and V/F further improved model fitness (FO: $\Delta=-102.3$; FOCE: $\Delta=-36.93$, $P<0.005$). Observed versus model population predicted plots for the one-compartment model with both covariates using FOCE are shown in Figure 2. This latter model effectively described twice the inter-individual variability on CL/F and V/F than the model without covariates. A 2-compartment model was also evaluated. Although the 1-compartment model had more robust parameter estimates, both models showed an age and weight effect on CL/F and V/F (see above for AIC values). The parameters for the 1-compartment model are listed in Table 3. Figure 3 shows the relationship between the post-hoc predicted oral clearance versus weight and age as a 3-dimensional response surface. In the covariate free model, oral clearance increases while weight increases. A similar relationship (although in the opposite direction) was seen in comparing the post-hoc predicted oral clearance to age (Figure 3). Notably the oral clearance decreased as age increased across the entire weight range. Covariate plots generated by XPOSE of oral clearance versus age given weight and oral clearance versus weight given age also illustrated these inter-relationships (data not shown).

In determining the individual specific PK parameters, we also calculated the dose-normalized AUC_{0-24} to compare the relative exposure per milligram of drug dosed across age. As age increased the average exposure increased. The average dose-normalized AUC (+/-SD) values were 69.7(+/-28.9) ng/mL*hr and 189.9(+/-78.4) ng/mL*hr for the 22-65 year and the 75-93 year old groups respectively (Figure 4). The standard deviation in the old elderly group (75-93years) was more than two times greater than that in the younger group (aged 22-65, although the %CV is similar). Consistent with the higher dose-normalized AUC observed in elderly subjects, the averaged dose was less than half than that used in younger adults (13+/-5 mg vs. 29+/-14 mg daily, respectively). Subjects ultimately receiving less than 20mg (i.e., less than the initial dose both protocols) had lower CL/F values.

DISCUSSION:

In this study, we successfully implemented a population PK analysis in the spirit of Krecic-Shepard et al¹¹³ and Kang et al¹¹⁴ using a small number of samples per subject in a large number of subjects to determine the oral clearance and volume of distribution in patients ranging in age from 22 to 93 years. Specifically, our estimates of oral clearance averaged 6.34 L/hr in the older patients (75-93 years of age)

and 16.49 L/hr in the younger patients (aged 22-65 years of age). The oral clearance values ranged from 2L/hr for the eldest patient in the study to approximately 27 L/hr in the younger subjects. This is consistent with studies using intensive PK sampling in limited numbers of subjects, where oral clearance was approximately 4 L/hr in the elderly group and 24 L/hr in the young.^{98, 115}

The two metabolites of citalopram measured are typically present at lower concentrations than the parent compound and do not readily cross the blood brain barrier. In our case, the concentrations for the demethyl-citalopram metabolite were less than or equal to those of the parent and the concentrations of the didemethyl-citalopram were less than 50% of the citalopram level. This, in combination with EC50 values that are three (demethyl-citalopram) to 15 times (didemethyl-citalopram) lower than that for citalopram, lead us to assume the metabolites do not significantly contribute to response.¹¹⁶ However, we did evaluate the metabolite concentrations versus the predicted clearance for citalopram. This showed no relationship between observed concentration and citalopram or its metabolites (data not shown). This arises from the fact that samples were taken at random across the dose-concentration time profile.⁹⁵

This study allowed us to evaluate the covariate (body weight, age, race, sex, concomitant medications) effects on the PK parameters. When weight was included in the description the CL/F and V/F parameters, the model fit improved greatly both in the numeric indicator (objective function) and visually. This was anticipated as the volume of distribution is dependent on body weight due to the direct relationship between total body water and body size^{109, 110}. Also, the clearance (if solely a flow dependent process) is also related to the body weight with a hyperbolic function (usually $BW^{0.75}$).^{109, 110, 117} Age was also a highly significant covariate in this analysis. In our study, using the covariate free model, oral clearance decreased from 19.50 L/h (age range: 22 to 29 years) to 2.05 L/h (age: 93 years). This decrease was consistent across the entire age range. Thus, age was included as a covariate affecting oral clearance (after weight), greatly decreasing the objective function by 70.53 (FO) units ($P < 0.005$) and 57.10 (FOCE) units ($P < 0.005$). Other covariates tested were not significantly associated with the PK parameters.

Although minimal samples were acquired for each patient (1 - 2 samples per patient), the results are consistent with findings from analyses from intense and therapeutic drug monitoring datasets.⁹⁸⁻¹⁰¹ Our study was able to extend these findings by demonstrating a continuous relationship between age and clearance of citalopram, as well as simultaneously account for the effect of weight on the pharmacokinetics of citalopram. Clearance decreased 0.23 L/hr for every year of age and increased 0.14

L/hr for every kg of body weight. We were also able to assess for additional potential covariate effects, however, none showed a significant association with the PK parameters.

Both dose-normalized magnitude of exposure and the absolute variability of that exposure increased dramatically as age increased. The largest magnitudes and variabilities per milligram of drug exposure occurred in the 75-93 year old subjects. Interestingly, there may have been a natural adjustment based on tolerability of the medications. Despite the fact that the dose titration protocols were similar across all ages, the final average dose in the older group was lower. In particular, the average dose was lower in individuals with lower clearance.

In conclusion, our findings may have implications for how nonlinear mixed effects modeling approaches can glean useful information from sparsely sampled populations (ie, elderly, children, adolescents) not typically accessible in clinical trials. This information would be important in understanding both the magnitude and the variability of the exposure, as well as the specific factors that contribute to inter-individual differences in this exposure.

ACKNOWLEDGEMENTS:

We are very grateful to the investigators of the Old-Old Study Group and the Multicenter Bipolar Depression Study, Denise Sorisio BS, for measurement of drug concentrations and Deborah Stapf BA, for assistance with data analysis.

SUPPLEMENTAL RESULTS:

Rationale for the supplemental study

In the published article, the final model was developed using FOCE method. Age and weight were significant covariates on PK parameters (CL and V). The covariate selection criteria were based on significant reduction of OFV value, reduction of inter-individual variability and improvement of goodness of fit in diagnostic plots. The diagnostic plot in the previous study suggested that the model can adequately describe the data. However, the parameter estimate (V/F) didn't agree with the PK parameter reported from the previous PK studies^{112, 118, 119}, where V/F of citalopram was typically greater than 1000 L, due to its highly lipophilic property. In order to obtain physiological meaningful PK parameter estimates, further model development was performed.

Supplemental Results

The further model development was performed using FOCE with interaction (FOCEI) method. The variance of the inter-individual variability of K_a was fixed to 1, which helped to stabilize the NONMEM model run. Nonparametric bootstrap methods were applied as an internal model validation approach. The detailed covariates selection during model development was shown in Table 4. The parameter estimate and the 90% CI from bootstrap (n=1000) analysis were showed in Table 5. The observed citalopram concentrations versus population predicted citalopram concentrations diagnostic plot are shown in Figure 5.

One of the major aims of this study was to assess covariate effect on PK parameters. Age was the most significant covariate on CL, with reduction of OFV by 62.7 units ($p < 0.005$) and reduction of inter-individual variability on CL by 30%. After incorporation of age on CL, the incorporation of weight on CL further improved model fitness. Comparing to the model with age on CL, OFV reduced by 15.8 units ($p < 0.005$) and inter-individual variability on CL reduced by 10% after incorporation both age and weight on CL. The OFV values were further reduced when including sex or race on CL (M10 and M11), weight on V (M12) in the model with age on CL, and when including age on V (M13), sex or race on CL (M14 and M15) in the model with age and weight on CL. However, none of them reduced the inter-individual variability. The improvement of goodness of fit was not noticeable in the diagnostic plot as well. Thus none of the covariates were included in the final model (M9).

Figure 1: Frequency histogram showing the sampling distribution for citalopram plasma concentration measurements. The x-axis is broken into two-hour bins. Several individuals were sampled past 30 hours (n=18 samples, <10% of all measurements, sampling times 31-178 hours after dose). The y-axis shows the proportion of samples taken in each interval.

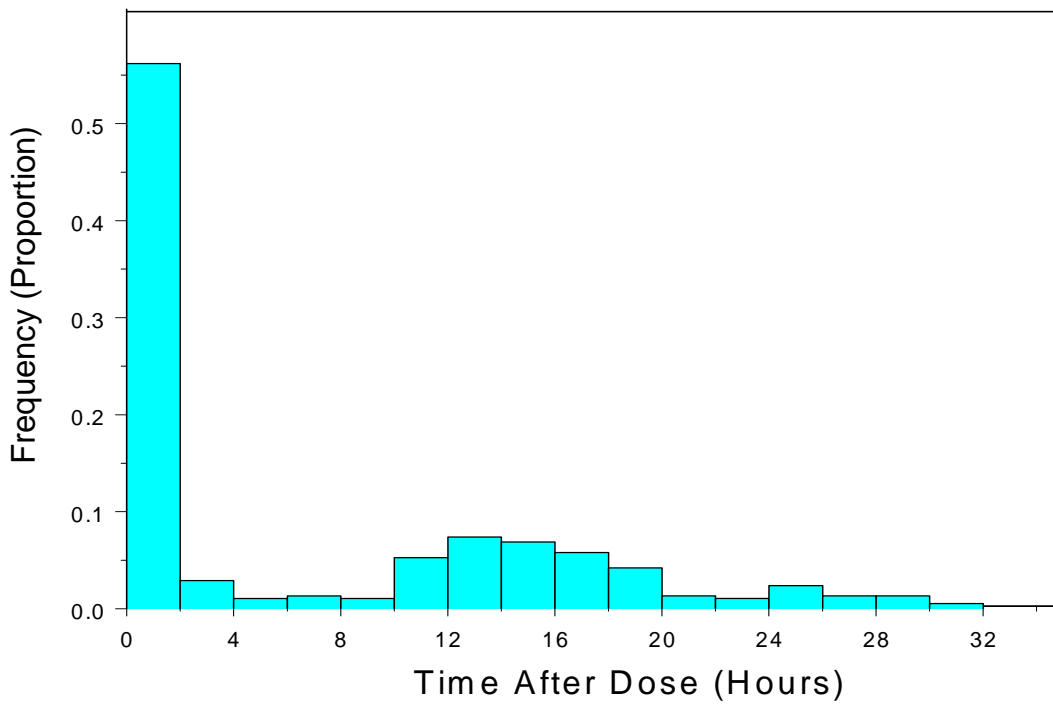


Figure 2: Population predicted (PRED) versus observed (DV) citalopram concentration values for the one-compartment model used with weight and age covariates in the model. Individual data points are shown as diamonds and the unity is shown as a solid line.

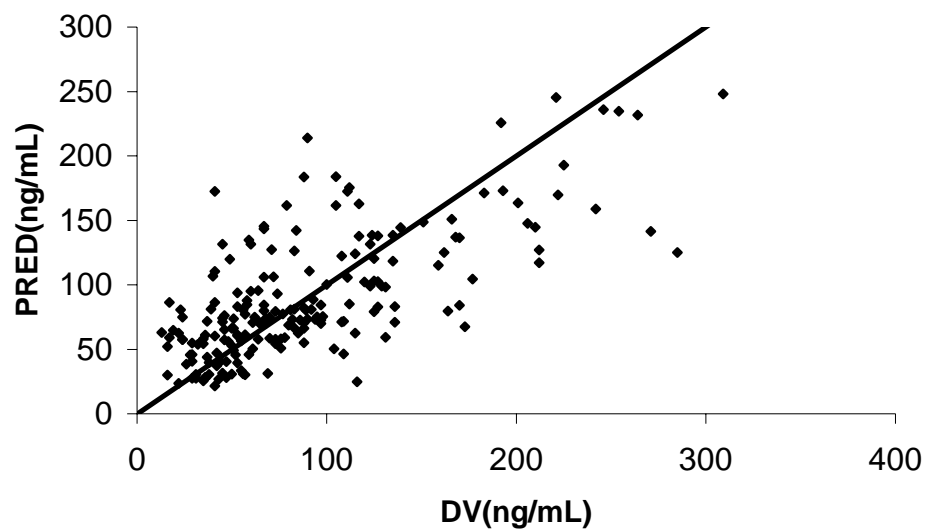


Figure 3: Three-dimensional surface showing the relationship between age, weight and predicted clearance. The shading shows the exponentiated relationship for both weight and age across the entire range of these covariates. The surface shows how the clearance changes with both weight and age simultaneously.

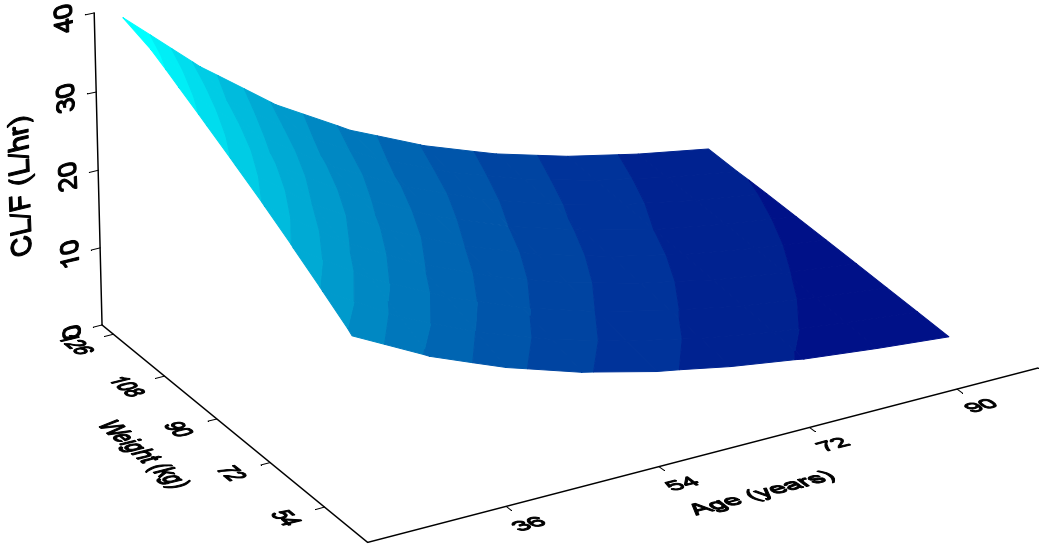


Figure 4: Dose normalized AUC in ng/mL*hr versus age in years. The AUC was calculated from the individual specific post-hoc predicted pharmacokinetic parameters.

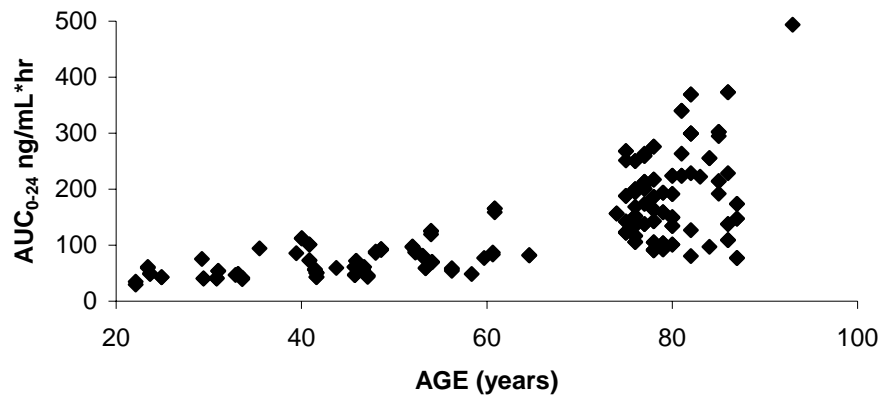


Figure 5: Observed citalopram concentrations versus population predicted citalopram concentrations plot of citalopram with 1-compartment model using FOCE interaction method. The solid line was the unity line.

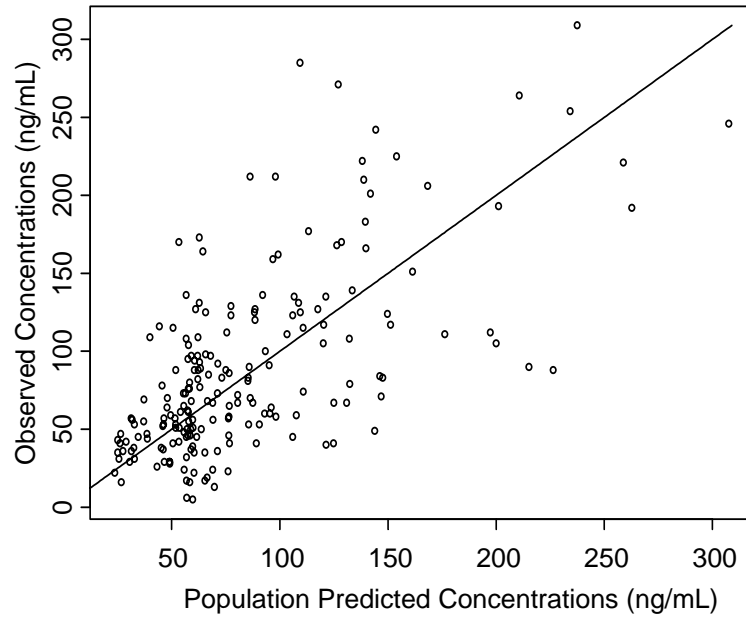


Table 1: Patient characteristics and data available from the Bipolar Depression and the Elderly Depression studies.

Patient data	Study A	Study B
N	40	66
# of observations	85	114
Sex	Male:36; Female: 4	Male:33; Female: 33
Race	White:26; Black:14	White:62; Black:4
Age range (years)	22-70	75-93
MEAN±SD Age (years)	43.32±11.43	79.80±4.09
MEAN±SD Weight (kg)	86.79±8.34	72.28±14.45
MEAN±SD Dose (mg)	29.18±14.41	13.33±4.90

Table 2: Population model development (FOCE method)

Covariate	Model	-2LL	Δ -2LL	P value
1	Base model	1693.136		
2-1				
CL(WT)	M1	1650.527	-42.609	6.685e-11
CL(AGE)	M2	1601.486	-91.65	0
CL(RACE)	M3	1669.3	-23.836	1.047e-06
CL(SEX)	M4	1661.315	-31.821	1.691e-08
2-2				
V(WT)	M5	1680.49	-12.646	.00047027
V(AGE)	M6	1678.371	-14.765	.00012177
V(RACE)	M7	1686.147	-6.989	.00820122
V(SEX)	M8	1678.769	-14.367	.00015042
3-1				
CL(AGE, WT)	M9	1589.255	-12.23	.00047027
CL(AGE, SEX)	M10	1607.927	6.44	1
CL(AGE, RACE)	M11	1610.617	9.131	1
3-2				
CL(AGE),V(WT)	M12	1603.299	1.813	1
CL(AGE),V(RACE)	M13	1610.547	9.061	1
CL(AGE),V(SEX)	M14	1596.939	-4.547	.03297648
4-1				
CL(WT, AGE), V(AGE)	M15	1578.504	-10.75	.00104279
CL(WT, AGE), V(SEX)	M16	1593.99	4.735	1
CL(WT, AGE), V(WT)	M17	1581.881	-7.374	.00661736
4-2				
CL(WT, AGE), V(AGE, WT)	M18	1567.299	-11.2	.00081797

Δ -2LL was the objective function value from the covariate model minus the covariate-free model. -2LL values in 2-1 and 2-2 were compared with base model; -2LL values in 3-1 and 3-2 were compared with M2; -2LL values in 4-1 were compared with M9 and values in 4-2 was compared with M15. LL, log likelihood; WT, weight, Age (60 years) and WT (80 kg) were median values.

Models: base model: $TVCL/F = \theta_1$, $TVV/F = \theta_2$; M1: $TVCL/F = \theta_1 * (WT/80) * \theta_4$, $TVV/F = \theta_2$; M2: $TVCL/F = \theta_1 * \exp((AGE-60)) * \theta_4$, $TVV/F = \theta_2$; M3: $TVCL/F = \theta_1 + (1-Race) * \theta_4$, $TVV/F = \theta_2$; M4: $TVCL/F = \theta_1 + (1-Sex) * \theta_4$, $TVV/F = \theta_2$; M5: $TVCL/F = \theta_1$, $TVV/F = \theta_2 * (WT/80) * \theta_4$; M6 $TVCL/F = \theta_1$, $TVV/F = \theta_2 * \exp((AGE-60)) * \theta_4$; M7: $TVCL/F = \theta_1$, $TVV/F = \theta_2 + (1-Race) * \theta_4$; M8: $TVCL/F = \theta_1$, $TVV/F = \theta_2 + (1-Sex) * \theta_4$; M9: $TVCL/F = (\theta_1 * \exp((AGE-60)) * \theta_4) * (WT/80) * \theta_5$, $TVV/F = \theta_2$; M10 $TVCL/F = (\theta_1 * \exp((AGE-60)) * \theta_4) + (1-Sex) * \theta_5$, $TVV/F = \theta_2$; M11: $TVCL/F = (\theta_1 * \exp((AGE-60)) * \theta_4) + (1-Race) * \theta_5$, $TVV/F = \theta_2$; M12: $TVCL/F = (\theta_1 * \exp((AGE-60)) * \theta_4)$, $TVV/F = \theta_2 * (WT/80) * \theta_5$; M13: $TVCL/F = (\theta_1 * \exp((AGE-60)) * \theta_4)$, $TVV/F = \theta_2 + (1-Sex) * \theta_5$; M14: $TVCL/F = (\theta_1 * \exp((AGE-60)) * \theta_4)$, $TVV/F = \theta_2 + (1-Race) * \theta_5$; M15: $TVCL/F = (\theta_1 * \exp((AGE-60)) * \theta_4) * (WT/80) * \theta_5$, $TVV/F = \theta_2 * \exp((AGE-60)) * \theta_6$; M16: $TVCL/F = (\theta_1 * \exp((AGE-60)) * \theta_4) * (WT/80) * \theta_5$, $TVV/F = \theta_2 + (1-Sex) * \theta_6$; M17: $TVCL/F = (\theta_1 * \exp((AGE-60)) * \theta_4) * (WT/80) * \theta_5$, $TVV/F = \theta_2 * (WT/80) * \theta_6$; M18: $TVCL/F = (\theta_1 * \exp((AGE-60)) * \theta_4) * (WT/80) * \theta_5$, $TVV/F = \theta_2 * \exp((AGE-60)) * \theta_6 * (WT/80) * \theta_7$.

Table 3: PK parameter estimates for one compartment model.

Parameters	Cov-free model	95%CI	Final model	95%CI
Oral Clearance (L/h)	7.09	6.95-7.23	10.2	5.41-75.1
V/F (L)	1.23	0.995-1.47	157	0.00306-2000
Ka	0.00574	-0.851-0.862	0.0088	0.00156-5
WT (θ_{wt-CL})	N/A	N/A	0.663	0.0659-1.7
AGE (θ_{age-CL})	N/A	N/A	-0.0285	-0.0416-0.0368
WT (θ_{wt-V_d})	N/A	N/A	3.61	0.0005-94.9
AGE (θ_{wt-V_d})	N/A	N/A	-0.131	-0.946-1.25
$\omega_{cl}\%$	80.4	80.15-80.65	57.7	19.3-229.7
$\omega_{v2}\%$	450.5	448.6-452.5	279	0.0006-4582
$\omega_{ka}\%$	94.9	93.1-96.7	45.1	0.00009-8700
$\sigma_1\%$	17.37	-2.57-37.31	40.5	N/A
σ_2 (ng/mL)	4.39	3.49-5.29	3.46	N/A

CI=confidence interval, WT=weight, V/F=volume of distribution, ω =coefficient of variation of inter-individual variability, σ =coefficient of variation of residual error, N/A: not available

Table 4: Population Pharmacokinetic Model Development (1-compartment using FOCEI method)

Covariate	Model	-2LL	Δ -2LL	P value
1	Base model	1664.743		
2-1				
CL				
WT	M1	1636.694	-28.049	< 0.005
AGE	M2	1602.017	-62.726	< 0.005
RACE	M3	1658.054	-6.689	< 0.05
SEX	M4	1648.254	-16.489	< 0.005
2-2				
V				
WT	M5	1663.543	-1.2	> 0.05
AGE	M6	1658.25	-6.493	< 0.05
RACE	M7	1663.205	-1.538	> 0.05
SEX	M8	1664.702	-0.041	> 0.05
3-1				
CL, V				
CL(AGE,WT)	M9	1586.19	-15.827	< 0.005
CL(AGE, SEX)	M10	1591.258	-10.759	< 0.05
CL(AGE, RACE)	M11	1597.967	-4.05	< 0.05
CL(AGE),V(WT)	M12	1599.33	-2.687	> 0.05
3-2				
CL and V				
CL(WT, AGE), V(AGE)	M13	1577.613	-8.577	< 0.05
CL(WT, AGE, SEX)	M14	1578.305	-7.885	< 0.05
CL(WT, AGE, RACE)	M15	1581.042	-5.148	< 0.05

* WT=weight; CL=clearance, V=volume of distribution of central compartment; Δ -2LL was objective function value (OFV) from the covariate model minus the base model; -2LL values in 2-1 and 2-2 were compared with base model; -2LL values in 3-1 were compared with model M2; while values in 3-2 were compared with 3-1 M9.

Table 5: PK parameter estimates from one-compartment model (FOCEI method) and bootstrap analysis

Parameters	Final model result		Bootstrap results	
	Parameter estimate	SE%	Median	95% CI
CL/F (L/h)	10.1	5.0	10.0	9.1-11
V/F (L)	4520	47.6	3525	63.6-9673
Ka (/h)	1.55	81.3	1.74	0.003-19445
Age (θ_{Age-CL})	-1.1	12.5	-1.1	-1.36-0.89
WT- (θ_{WT-CL})	0.829	25.6	0.85	0.471.22
$\omega_{cl}\%$	41.0	16.2	40.3	34.2-46.2
$\omega_{v2}\%$	89.5	30.5	79.4	0.0004-254
$\sigma 1\%$	20.5	35.5	20.4	12.8-25.9
$\sigma 2$ (ng/mL)	10.4	44.9	9.9	4.1-14.1

* Abbreviations: CL=clearance, SE=standard error, weight=total body weight, V=volume of distribution of central compartment, ω =coefficient of variation of inter-individual variability, σ =coefficient of variation of residual error, WT=weight, Unit of weight=kg, Unit of age=year, 95% CI: 95% confidence interval.

**CHAPTER 4 DETERMINATION COVARIATE EFFECTS ON
EXPOSURE OF DRUG WITH NON-LINEAR PHARMACOKINETIC
CHARACTERISTICS GIVEN HYPER SPARSE DATA**

This chapter is based on the following paper:

Yan Feng, Bruce G. Pollock, Robert E Ferrell, Mark A Kimak, Charles F. Reynolds III , Robert. R. Bies. Paroxetine: Population Pharmacokinetics Analysis in Late-life Depression using Sparse Concentration Sampling. *British Journal of Clinical Pharmacology*. 2006 (In press)

Copyright is to be assigned to Journals Rights & Permissions Controller (Blackwell Publishing). The permission of using the full article in the thesis had been granted from the copyright owner (Blackwell Publishing).

Abstract

Objective: To develop a population pharmacokinetic (PK) model using sparse sampling of long-term treatment with paroxetine in elderly depressed subjects, incorporating CYP 2D6 genotype as well as other covariates.

Methods: Elderly subjects (age ≥ 70) with non-psychotic, non-bipolar major depressive disorder from the inpatient and outpatient clinic were treated with paroxetine in a five-year clinical trial investigating “Maintenance Therapies in Late-Life Depression” (MTLD-2). Plasma concentrations were collected during regular visits. CYP 2D6 genotype was determined using polymerase chain reaction (PCR) for each individual. A nonlinear mixed-effects model was developed with NONMEM[®] for those subjects who received 10 to 40 mg/day of paroxetine during treatment. One and two compartment models with linear and nonlinear elimination (Michaelis- Menten) were evaluated. Pharmacokinetic parameters as well as inter-individual and residual variability were estimated. The effect of age, weight, sex, race and CYP2D6 genotypes on the pharmacokinetics of paroxetine was evaluated.

Results: One hundred and seventy one subjects with a mean age of 77 years (range 69-95) and a mean weight of 72.0 kg (range 32.9-137.0), were enrolled in the MTLD-2 clinical trial. A total of 1970 paroxetine concentrations were available for population PK analyses. Approximately ten samples were taken per subject. A two-compartment nonlinear PK model with additive and proportional error provided the best base model for description of the data. Weight and CYP2D6 polymorphisms were found to have a significant effect on maximal velocity (V_m), where as sex had an effect on volume of distribution of the central compartment. The V_m estimates in each of the CYP2D6 phenotypic groups were: 125 $\mu\text{g/h}$ in poor metabolizer (PM) (n=1), 182 $\mu\text{g/h}$ in intermediate metabolizers (IMs) (n=28), 454 $\mu\text{g/h}$ in extensive metabolizers (EMs) (n=36), and 3670 $\mu\text{g/h}$ in ultra-rapid metabolizers (UMs) (n=5).

Conclusions: The population PK model adequately described paroxetine data in this elderly depressed population. The data indicate that female and male subjects with different CYP2D6 polymorphisms have different elimination rates, and therefore may need to be dosed differently based on metabolizer genotype.

Introduction

Selective serotonin reuptake inhibitors (SSRIs) are the first-line antidepressants used in primary care and psychiatric practices. The response rate after the first drug administration can be as low as 60% in the general adult population and 39% in the geriatric population.¹²⁰ Large inter-individual variability (IIV) has been found in pharmacokinetic (PK) parameters such as clearance (CL), half-life, area under the curve (AUC) and pharmacodynamic (PD) parameters such as time to response, recurrence, and side effects.^{10, 121-125} This represents a significant clinical problem in the treatment of psychiatric illness in geriatric subjects. Some studies have suggested that the PKs of SSRIs were associated with drug effect.^{126, 127} Thus, understanding the IIV in PKs is important for a PD study.

Paroxetine, one of the most potent SSRIs, is widely used in the treatment of depression and anxiety.¹²⁰ A wide range of IIV was observed for the PK parameters of paroxetine.¹²⁸⁻¹³¹ Following single or multiple administration of paroxetine at doses of 20 to 50 mg, the mean elimination half-life for healthy subjects was approximately 24 hours, with a range of 7 to 65 hours having been reported.¹²⁴ Elderly subjects taking paroxetine have higher plasma concentrations and slower elimination than younger subjects.^{124, 131} Although plasma concentrations have not yet been correlated with paroxetine response or adverse events, these results suggested the initial dosage in the elderly subjects should be reduced.

Paroxetine was mainly metabolized by CYP2D6.^{124, 130} More than 80 allelic variants have been identified for the CYP2D6 gene among different ethnic populations.¹³² These polymorphisms result in variable enzymatic activity and drug-metabolizing phenotypes which can be classified as poor (PMs), intermediate (IMs), extensive (EMs) and ultra-rapid (UMs) metabolizers.^{133, 134} A limited number of studies have reported an association between CYP2D6 polymorphism and paroxetine PKs. Two studies investigated the differences in paroxetine PK between EMs and PMs.^{129, 130} A seven-fold difference in the median $AUC_{0-\infty}$ was found for healthy subjects receiving a single dose of 30 mg of paroxetine, and a 2-fold difference in the median AUC at steady state (AUC_{ss}) after multiple 30 mg doses.¹²⁹ The other study found a 3-fold difference in median steady-state concentration (C_{ss}) after multiple 30 mg doses.¹³⁰ Some studies suggest that the distribution of CYP2D6 activity in EMs also displays substantial IIV.

Ozdemir¹³⁵ found a 2-fold higher median C_{ss} in healthy heterozygous EMs when compared to healthy homozygous EMs receiving paroxetine (20 mg/day). No PMs were included in this study.

Factors that contribute to the variability of paroxetine PK parameters in geriatric depressed population have not been reported. The association between CYP2D6 polymorphisms and paroxetine PK in the geriatric population after chronic paroxetine treatment is unknown. To investigate this association, we applied a nonlinear mixed-effect modeling approach to characterize paroxetine pharmacokinetics in a placebo-controlled study (the “MTLD-2 trial) of the efficacy of paroxetine in preventing recurrence of major depressive episodes in people aged 70 and above. Mixed effect population PK approach is the study of the sources and correlates of variability in plasma concentrations between individuals,³⁶ which is currently widely used in evaluation of drug safety and efficacy. Compared with the traditional pharmacokinetic approach, population pharmacokinetics is more suitable for analyzing large scale clinical trials, where only a few samples are available per subject.

The purpose of this study was a): to apply a nonlinear mixed effect modeling approach to describe paroxetine PK parameters using limited sampling in a large number of geriatric subjects from the MTL D-2 clinical trial, and b): to evaluate the impact of covariates including age, weight, sex, race, and CYP2D6 polymorphisms on the PK parameters.

Subjects and Methods

Subject

The Maintenance Therapies in Late-Life Depression (MTLD-2) study¹³⁶ assessed paroxetine as a maintenance treatment for prevention of recurrent episodes of major depression in geriatric subjects. Subjects (aged 70 or older) were included if they met the diagnostic criteria from the Structured Clinical Interview for DSM-IV Axis I disorders (SCID) for a current episode of major depressive disorder, non-bipolar, non-delusional, and not actively suicidal. Subjects also were required to score 15 or above on the 17-item Hamilton Rating Scale for Depression (HAM D-17) and 18 or higher Folstein Mini-Mental State Exam (MMSE). All the study sites were located in Pittsburgh. The study was approved by institutional review committee of the

University of Pittsburgh and the written informed consent to participate in this study was obtained from each subject.

There were three phases of paroxetine treatment. Subjects were treated during an initial acute phase (which could last up to 26 weeks) to assess for response, followed by a 16-week continuation phase for those subjects who responded. Subjects with a continued response (recovered based on the 16 week continuation phase) entered the two-year maintenance phase and were randomly assigned to a placebo group or to paroxetine. A responder was defined by a HAMD-17 score of less than 10 for three consecutive weeks. Recovery was defined as being free of significant depressive symptoms for 16 weeks of continuation treatment. Recurrence in maintenance treatment was defined by a HAMD-17 score over 15 for at least 2 consecutive weeks and meeting SCID criteria for syndromal major depressive episode, confirmed by an independent senior geriatric psychiatrist. The acute and continuation phases were open-label, and the maintenance phase was double-blind. Subjects visited the clinic weekly during acute treatment, twice monthly during continuation treatment, and monthly during maintenance treatment. Plasma paroxetine samples were taken at each visit for concentration measurement. No specific timing was scheduled for the paroxetine sampling. The dosage time was noted for inpatient subjects and was self-reported by outpatients.

Paroxetine was started at 10 mg daily and could be titrated to a higher dose based on response. Subjects received paroxetine doses ranging from 10 mg to 40 mg daily. De-identified data were applied in a population pharmacokinetic analysis, where the identification (ID) number for each subject was changed by replacing the original ID numbers by a randomly generated number.

Analytical Procedures

Paroxetine plasma concentrations were determined by HPLC technique, as previous described.¹³⁷ Briefly, plasma was extracted using ethyl acetate and heptane (1:4, v/v) and back extracted into 0.025 M potassium phosphate, pH 2.4. Separation was achieved using a Beckman Ultrasphere C18 (150 mm×2 mm) column. Detection wavelength was 205 nm and flow rate was 0.35 ml/min. Fluoxetine hydrochloride was used as the internal standard. The limit of

quantitation was 5 ng/ml. The linear range was 5 to 500 ng/ml with inter-assay variability ranging from 3.4% to 5.4% for spiked controls.

CYP2D6 Genotyping

After separating lymphocytes from whole blood using BD Vacutainer CPT™ tubes, DNA was extracted using the standard procedure.^{138, 139} Genomic DNA fractions were stored at -20°C.

A polymerase chain reaction (PCR)-based allele-specific analysis previously described,¹⁴⁰ was used to determine whether individuals were carrying duplicated *CYP2D6* genes (*CYP2D6* ***XN**), and long PCR was used to amplify a fragment spanning the potential crossing-over sites.^{140, 141} An allele-specific long PCR method developed by Steen et al^{141, 142} was used to detect *CYP2D6* *5 (gene deletion). Nested PCR was performed to detect *CYP2D6**2, *4, *10 and *17 by amplifying the entire *CYP2D6* gene (5 kb).^{140, 143-145} After amplification of the entire gene, subsequent internal PCR was performed to identify the presence of the *CYP2D6**2 (C2938T), *4 (G1934A), *10 (G4286C) and *17 (C1111T) allele. When no mutations were found, the allele was defined as *CYP2D6* *1. The specific primers, restriction enzyme, restriction pattern, and agarose gel for these alleles were shown in Table 1.

The allelic frequency was calculated using the equation:

Allelic frequency for the variant allele

$$= (\text{Homozygous alleles} \times 2 + \text{Heterozygous alleles}) / (\text{Total subjects} \times 2)$$

CYP2D6 genotype was classified into one of four phenotype groups (Table 2) based on the phenotype-genotype relationship reported in the literature.^{146, 147} Subjects carrying two nonfunctional alleles (*0/*0) were assigned to the PM group. Subjects carrying one normal or reduced functional allele and one reduced or nonfunctional allele were assigned to the IM group. Subjects carrying two normal functional alleles were assigned to the EM group and subjects carrying one ***XN** allele were assigned to the UM group.

Population Pharmacokinetic Analysis

The population PK analysis includes the base model and final (covariate) model development. The base model defines the PK parameters and describes the plasma concentration-time profile. The final model describes the influence of fixed effects (i.e., demographic factors) on the PK

parameters. Analysis platform, minimization methods, model building criteria and model validation were described below.

Analysis Platform

Non-linear Mixed Effects Modeling was used for the population PK analysis using NONMEM computer program (Version 5, level 1.1, Globomax, Hanover, MD).^{40, 79} The models consisted of a structural model that described the disposition of the drug following oral administration, and a pharmaco-statistical model that described the inter- and intra-individual variability. Diagnostic graphics, exploratory analyses, and post-processing of NONMEM outputs were performed using S-PLUS (Version 6.2, Insightful, Seattle, WA).

Minimization Methods and Model Building Criteria

The first order estimation method (FO) was used for model building. The adequacy of the developed structural models was evaluated using both statistical and graphical methods. The likelihood ratio test was used to discriminate between alternative models. The likelihood ratio test was based on the property that the ratio of the NONMEM objective function values (OFV) (-2 log-likelihood) were asymptotically χ^2 distributed. An objective function decrease of 3.84 units was considered significant ($\chi^2 p < 0.05$ df=1). Standard errors for all parameters were obtained using the covariance option in NONMEM.

Base Model Development

Structural PK Model: The structural PK model represents the best description of the data without considering the effect of subject-specific covariates. The population PK analysis was performed using NONMEM[®]^{40, 79} with the subroutine ADVAN9, ADVAN2 TRANS2 and ADVAN4 TRANS4. Various structure models were tested, including one and two compartment model, model with linear, nonlinear elimination (Michaelis - Menten) and combination nonlinear with linear elimination.

Inter-individual Variability: It was assumed that the IIV of the PK parameters was log-normally distributed. The relationship between a PK parameter (P) and its variance could therefore be expressed as shown below:

$$P_j = P_{TV} \times e^{\eta_P}$$

where, P_j was the value of PK parameter for the individual j , P_{TV} was the typical value of P for the population, and η_P denoted the difference between P_j and P_{TV} , independently, which was identically distributed with a mean of zero and variance of ω_P^2 .

Intra-Individual Variability: The residual variability, which was comprised of, but not limited to, intra-individual variability, experimental errors, process noise and /or model misspecifications, was modeled using additive, proportional and combined error structures as described below:

Additive error: $y_{ij} = \hat{y}_{ij} + \varepsilon_{ij}$

Proportional error: $y_{ij} = \hat{y}_{ij}(1 + \varepsilon_{ij})$

Combined additive and proportional error: $y_{ij} = \hat{y}_{ij}(1 + \varepsilon_{ij}) + \varepsilon_{ij}'$

where y_{ij} was the j^{th} observation in the i^{th} individual, \hat{y}_{ij} was the corresponding model prediction, and ε_{ij} (or ε_{ij}') was a normally distributed random error with a mean of zero and a variance of σ^2 .

Final Model Development

The final model was developed by testing the effect of subject specific covariates, including age, weight, sex, race, and CYP2D6 polymorphisms on PK parameter estimates. The two types of covariates, including continuous covariates (e.g., age and weight) and discrete covariates (e.g., sex, race and CYP2D6 polymorphisms) were introduced into each parameter in a stepwise fashion. The following example showed the effect of a continuous covariate on V_m (maximal rate):

$$TVVm = \theta_{Vm} \times (Cov / Med_{Cov})^{\theta_{Cov}}$$

TVVm was the typical value for the population; The random effects of between-subject variability were assumed to be log-normally distributed, with a mean of zero and standard deviation of ω . Cov was the continuous covariate that was affecting Vm; and Med_{Cov} was the median Cov.

The following example shows the effect of a discrete covariate (sex) on Vm:

$$TVVm = \theta_{Vm} + (1 - Sex) \times \theta_{Sex}$$

When sex was female (male=0, female=1), TVVm equals θ_{Vm} since numeric value for (1-female) = 0 resulting in a zero multiplier for the covariate effect. For male subjects, the θ_{Sex} term was added to the population estimate of Vm to modify it.

Categorical variables were assigned to each of the four CYP2D6 phenotype groups and for the subjects without CYP2D6 phenotype information (i.e, PMs = 1, IMs =2, EMs = 3, UMs=4, Missing=0). The incorporation of this covariate was shown here for the parameter Vm below:

$$\text{IF (PHENOTYPE.EQ.0) TVVM} = \theta_{Vm}$$

$$\text{IF (PHENOTYPE.EQ.1) TVVM} = \theta_{PMs}$$

$$\text{IF (PHENOTYPE.EQ.2) TVVM} = \theta_{IMs}$$

$$\text{IF (PHENOTYPE.EQ.3) TVVM} = \theta_{EMs}$$

$$\text{IF (PHENOTYPE.EQ.4) TVVM} = \theta_{UMs}$$

$$Vm_i = TVVM \times e^{\eta_i}$$

The graphical assessment of POSTHOC parameter estimates versus covariates was evaluated to help identify possible covariate relationships using S-PLUS 6.2. In addition, goodness of fit plots were utilized to assess model robustness.⁸³ The covariate was retained in the model if it decreased the objective function value (OFV) by 3.84 (χ^2 p < 0.05 df = 1). Covariate influence on inter-individual variability and goodness of fit was also examined. In cases where the covariate value was not recorded at any time during the study for the subject, the median value calculated from the population dataset was used.

Results

Patient Characteristics

The MTL D-2 clinical trial included 171 elderly subjects (58 males) who provided 1970 paroxetine concentrations. Subjects had an average (mean±SD) age and weight of 77.1±5.7 years, 72.0±16.4 kg, respectively (Table 3). With the exception of three subjects who were 69 years of age, subjects aged 70 years or older were included in the MTL D-2 study. The majority of the subjects were Caucasian (CA) (n=156) and only fifteen subjects were African - American (AA). The distribution of paroxetine sampling time (time after dose) was shown in Figure 1.

CYP2D6 Genotyping

CYP2D6 genotype was classified into one of four phenotype groups (Table 2) based on phenotype-genotype relationship reported in the literature, as described in methods section.^{146, 147} Among the 171 subjects, whole blood was available from 68 subjects for CYP2D6 genotyping analysis. Of these 68 subjects, 4 were AA and 64 were CA. Five subjects were identified as UMs, 36 subjects were EMs, 26 subjects were IMs, and one subject was a PM.

The frequency of each CYP2D6 alleles was summarized in Table 4. The CYP2D6 *17 allele, an African and African-American specific allele found in previous studies,^{134, 148} was found in only 25% of the AAs in this study. CYP2D6 *2N was only found in CA subjects.

Population PK modeling

Base Model

The population PK analysis was performed by using NONMEM[®] (version V, GloboMax, Hanover, MD)⁴⁰ with the subroutine ADVAN9. A two-compartment nonlinear model with exponential inter-individual variability on V_m, the Michaelis-Menten constant (K_m), and volume of distribution of the central compartment (V₂) adequately described the data. The best residual error model was a combined additive and proportional model. The basic PK parameters of V_m, K_m, V₂, volume of distribution of the peripheral compartment (V₃) and absorption rate constant K_a were shown in Table 5.

A two-compartment model was determined to be the robust, based on the Akaike information criterion (AIC) ⁴⁷ (AIC = 17265.0, one-compartment; AIC = 17149.9, two-compartment). Moreover, the decrease in residual error (50% decreased in additive residual error) and bias of data fitting were also observed. Nonlinear elimination model improved OFV by 114.0 units ($p < 0.001$) compared to the linear elimination model. Combination of linear and nonlinear elimination model did not further improve model fitness or reduce the OFV value ($\Delta\text{OFV} = -3.2$, $p > 0.05$).

Final Model

CYP2D6 phenotype was the covariate on V_m that resulted in the largest reduction in objective function value ($\Delta\text{OFV} = -137.9$; $P < 0.005$). Weight was a significant covariate on V_2 ($\Delta\text{OFV} = -69.64$; $P < 0.005$). After incorporating the CYP2D6 phenotypic effect on V_m , sex was a significant covariate on V_2 ($\Delta\text{OFV} = -107.1$; $P < 0.005$). After incorporating the CYP2D6 phenotype on V_m and sex on V_2 , the incorporation of weight on V_m further improved model fitness by reducing OFV 62.66 units ($P < 0.005$). The detailed covariates selection during model development was shown in Table 6. The final model V_m and V_2 was:

$$\begin{aligned} \text{IF (PHNO.EQ.0)} \quad \text{TVVM} &= \theta_1 \\ \text{IF (PHNO.EQ.1)} \quad \text{TVVM} &= \theta_7 \\ \text{IF (PHNO.EQ.2)} \quad \text{TVVM} &= \theta_8 \\ \text{IF (PHNO.EQ.3)} \quad \text{TVVM} &= \theta_9 \\ \text{IF (PHNO.EQ.4)} \quad \text{TVVM} &= \theta_{10} \\ \text{TVVM1} &= \text{TVVM} * (\text{WT} / 75)^{\theta_{11}} \\ \text{VM} &= \text{TVVM1} * \text{EXP}(\text{ETA}(1)) \\ \text{TVV2} &= \theta_3 + (1 - \text{SEX}) * \theta_{12} \\ \text{V2} &= \text{TVV2} * \text{EXP}(\text{ETA}(3)) \end{aligned}$$

The final PK parameter estimates were shown in Table 5. Diagnostic plots were shown in Figure 2, including observed paroxetine concentrations versus population predicted paroxetine

concentrations (Figure 2a); observed paroxetine concentrations versus individual predicted paroxetine concentrations (Figure 2b); weighted residual error (WRES) versus population predicted concentrations (Figure 2c); and WRES versus time (Figure 2d). Compared to the base model, proportional and additive residual error was reduced by 12.5% and 20.4% respectively, in the final model. The inter-individual variability on V_m and V_2 both decreased by 41.9%. The standard error (SE) of IIV estimation of V_m was reduced by 66.1% and SE of IIV estimation of V_2 was reduced by 92.6%. The SE of V_m , K_m , and V_3 estimates were also decreased in the final model. However, the estimation of IIV on K_m and the SE of IIV of K_m increased.

The order of magnitude for the V_m estimates by CYP2D6 phenotype was: UMs > EMs > IMs > PMs (Figure 3), which corresponded to the functional allele of the CYP2D6 gene. The population mean (%SE) of V_m estimates in the final model for each CYP2D6 phenotype group were: 125 $\mu\text{g/h}$ (48.8%) in PM, 182 $\mu\text{g/h}$ (19.4%) in IMs, 454 $\mu\text{g/h}$ (49.5%) in EMs, and 3670 $\mu\text{g/h}$ (34.6%) in UMs. The 95% confidence intervals (CI) of V_m in each phenotype group were: 64.41-444.09 $\mu\text{g/h}$ in IMs, 191.35-895.96 $\mu\text{g/h}$ in EMs, and 2073.70-7006.30 $\mu\text{g/h}$ in UMs, (95%CI is unavailable for PM group with $n=1$). The estimates of V_2 in male subjects were: 461.30 ± 259.75 L and in female subjects were: 346.41 ± 255.81 L.

Age did not affect paroxetine disposition in this study, although the V_m estimates in subjects aged 80 or older appeared to be lower than subjects younger than 80 years. The median (25th and 75th percentile) of V_m estimates in subjects aged 80 or older was 275 $\mu\text{g/h}$ (198 $\mu\text{g/h}$ and 468 $\mu\text{g/h}$); in subjects with age less than 80 years was 419 $\mu\text{g/h}$ (291 $\mu\text{g/h}$ and 620 $\mu\text{g/h}$).

Race was a significant covariate on paroxetine PK if CYP2D6 phenotype was not included in the PK model (Table 3). However, once the CYP2D6 phenotype was included in the model, race did not significantly impact on paroxetine PK parameters.

Discussion

The molecular basis of the CYP2D6 polymorphism has been intensively studied, and more than 80 allelic variants, including nonfunctional, normal, reduced or increased functional alleles, have been identified for the CYP2D6 gene among different ethnic populations.^{132, 134} These polymorphisms result in variable enzymatic activity and drug-metabolizing phenotypes,

which can be classified as PMs, IMs, EMs and UMs metabolizers.^{133, 134} Paroxetine is mainly metabolized by CYP2D6 enzyme. However, the relationship between CYP2D6 genotype and paroxetine PKs in the geriatric population has not been reported. This is the first study to assess the impact of CYP2D6 genotype as well as other factors (e.g., weight, sex, age, and race) on paroxetine PKs by using a population modeling approach in a geriatric depressed population with small number of samples per subjects. In addition, we have captured the individual specific drug exposure magnitude over time. This provides a basis where the magnitude of exposure can be examined in conjunction with the maintenance response of subjects in this study in a future study as response data become available.

Both one and two-compartment nonlinear PK models demonstrated that CYP2D6 polymorphisms and weight were significantly related to paroxetine V_m and sex significantly impacts V_2 . The two-compartment PK model was a better description of the data than the one-compartment model, based on the significantly reduced OFV value and a better goodness of fit. The V_m estimates in each CYP2D6 phenotype groups showed that UMs had the highest V_m than other CYP2D6 phenotype groups, while PMs had the lowest V_m population estimate. The order of magnitude for V_m estimates by CYP2D6 phenotype was: UMs > EMs > IMs > PMs and the V_m estimates were: 125 $\mu\text{g}/\text{h}$ in PM, 182 $\mu\text{g}/\text{h}$ in IMs, 454 $\mu\text{g}/\text{h}$ in extensive metabolizers (EMs), and 3670 $\mu\text{g}/\text{h}$ in ultra-rapid metabolizers (UMs). The order of magnitude of the V_m estimate was consistent with the CYP2D6 functional alleles, where the UM phenotype could be caused by alleles carrying multiple 2D6 gene copies^{134, 143} and the PM phenotype was the result inheriting of any 2 nonfunctional (null) alleles (genotype *0/*0). The IM phenotype was the result of both heterozygosity for a null allele and homozygous for two alleles with impaired function (e.g *9, *10, *17). Moreover, the model was able to differentiate IMs and PMs groups. Comparing the differences of V_m estimates between CYP2D6 genotype groups, V_m estimates between PMs (125 $\mu\text{g}/\text{h}$) and IMs (182 $\mu\text{g}/\text{h}$) was similar, which agreed with the suggestion from several studies that the IM phenotype was of clinical importance because drug PKs in IMs could be more similar to the PMs than to the normal EMs, especially after chronic treatment.¹⁴⁷ The V_m for subjects without having CYP2D6 genotype information was 474 $\mu\text{g}/\text{h}$, which is similar to the estimation of V_m in the EMs (454 $\mu\text{g}/\text{h}$), since EMs is the most frequent genotype in both the CA and AA populations.

Nonlinear pharmacokinetics of paroxetine was found in EMs in the study of Sindrup et al.^{129, 130} One explanation of this finding was saturation of CYP2D6 metabolic capacity, where CYP2D6 enzyme activity seems readily to saturate as paroxetine dose increase, as demonstrated by Sindrup et al.¹³⁰ and Preskorn.¹⁴⁹ Another possibility relates to the self-inhibition of paroxetine metabolism, since paroxetine itself can inhibit CYP2D6 enzyme activity.^{130, 150} Without considering self-inhibition, the model with nonlinear elimination (Michaelis-Menten) could under-predict paroxetine concentrations. However the result of MTL D-2 data analysis did not support the self-inhibition mechanism, as no bias or under-prediction was found in the diagnostic plots of the weighted residual versus predicted paroxetine concentrations and the weighted residual versus time. Moreover, the model was tested with different elimination mechanisms (e.g., simple noncompetitive inhibition and uncompetitive inhibition^{151, 152}; data not shown). Model fitness was not significantly improved based on OFV values and diagnostic plots.

Previous studies had reported that paroxetine was mainly metabolized by the high affinity enzyme CYP2D6^{124, 130} and the low affinity enzyme e.g., CYP3A4^{124, 129}. Accordingly, models with linear, nonlinear, and combined linear and nonlinear elimination were evaluated. Results showed that the nonlinear elimination model improved the model fitness and significantly decreased the OFV value compared to the linear elimination model. However, the combined model with linear and nonlinear elimination did not provide further improvement in model fitness.

Elderly subjects taking oral paroxetine had higher plasma concentrations than younger subjects.^{124, 131} Age was identified as a significant covariate on the PKs of another SSRI, citalopram.¹⁰ Age was not a significant covariate on paroxetine PK in this study, although the V_m estimates in subjects aged 80 or older appeared to be lower than subjects younger than 80 years. The small sample size in the MTL D-2 study may lead to a decreased ability to detect an age effect in this study.

Race was determined to be a significant covariate in both the one and two-compartment PK models when CYP2D6 genotype information was not incorporated in the model.¹⁵³ One possible explanation was related to the correlation between race and genotypes. The frequency of *4, the most frequent null allele in CAs, was about 3 fold higher than in AAs.^{134, 143} The CYP2D6 *17 allele was an African and African-American specific allele found in previous studies and this study.^{134, 154} CYP2D6 *2N was only found in CA subjects in this study. When

CYP 2D6 genotype was incorporated, this race effect was no longer significant. The frequency of UMs in CA was 8%, which may be more reflective of Pittsburgh Caucasian population, since the frequency of UMs is higher in Southern Europe (10%) than that in North Europe (1-2%).¹³⁴

Conclusion

The population PK model adequately described paroxetine PK parameters in subjects with late-life depression. The results suggest that weight, sex and genotype contribute to the variability in PK parameters, and that therefore, individuals of different sex or with a different genotype may need to be dosed differently from one another.

Acknowledgements

Financial Support: Advanced Center for Interventions and Services Research for the Study of Late Life Mood Disorders: R37 MH43832 (the MTLTD-2 study), P30 MH71944 (the late-life ACISR), P30 MH52247, R01 MH37869, MH65416, MH30915, MH55756, and NIH MH64173; National Institute for Biomedical Imaging and Bioengineering (NIBIB) Grant # P41 EB001975-06.

The authors would like to acknowledge Kristin Bigos for her assistance in preparing this manuscript.

Table 1: Conditions of CYP2D6 genotyping study: including the specific primers, restriction enzyme, restriction pattern, and agarose gel.

Table a. Long PCR for CYP2D6 genotype determination

CYP2D6 Allele	Specific Primers	PCR product (kb)	Agarose gels
2D6	F: 5'-CCAGAAGGCTTTGCAGGCTTCA-3' R: 5'-ACTGAGCCCTGGGAGGTAGGTA-3'	5.0	0.85%
2D6-dup	F: 5'-CCTGGGAAGGCCCA TGGAAAG-3' R: 5'-CAGTTA CGGCAGTGGTCAGCT-3'	3.5	0.85%
*5 (deletion)	F: 5'-ACCAGGCACCTGTACTCCTCA-3' R: 5'-GCATGAGCTAAGGCACCCAGAC-3'	3.5	0.9%

Table b. Re-amplification reactions performed for CYP2D6 genotype determination

CYP2D6 Allele (Mutation)	Specific Primers	Restriction enzyme	Restriction pattern (bp)	Agarose gels
*2 (C2938T)	F: 5'-AGGCCTTCCTGGCAGAGATGGAG-3' R: 5'-CCCCTGCACTGTTCCCAAGA-3'	<i>cfo I</i>	wt:260, 126 mut: 386	2.0%
*4 (G1934A)	F: 5'-TGCCGCCTTCGCCAACCACT-3' R: 5'-CTCGGTCTCTCGCTCCGCAC-3'	<i>Bst NI</i>	wt:292 mut: 111, 181	1.5%
*10 (G4286C)	F: 5'-GAGACAAACCAGGACCTGCCA-3' R: 5'-GCCTCAACGTACCCCTGTCTC-3'	<i>BstEII</i>	wt:860 mut: 240, 620	1.8%
*17 (1111C) (wt)	F: 5'-CCAAGGTTCAAATAGGACTA-3' R:5'-CCCGAAACCCAGGATCTGGG-3'		wt: 237	1.5%
*17 (1111T) (mut)	F: 5'-CCAAGGTTCAAATAGGACTA-3' R: 5'-CCCGAAACCCAGGATCTGGA-3'		mut: 237	1.5%

* wt: wild type; mut: mutant; F: forward primer; R: reverse primer

Table 2: Genotype/Phenotype frequencies in Caucasian (CA) and African - American (AA) subjects in the MTL D-2 trial

Allele status	Assigned phenotype	Genotype	CA		AA	
			Frequency (%)	n	Frequency (%)	n
0	PMs	*0/*0	1.6	1	0	0
1	IMs	IM/*0, IM/IM, EM/*0, EM/IM	39	25	75	3
2	EMs	EM/EM	52	33	25	1
3	UMs	UM/*X	7.8	5	0	0

* 0 = non-functional alleles (e.g *4, *5); 1 = one normal functional (EM: *1, *2) or reduced-functional allele (IM: *10, *17), plus a reduced or non-functional allele; 2 = two functional alleles or *XN allele plus other allele (UM). CA: Caucasian; AA: African - American.

Table 3: Patient characteristics for the MTL D-2 study

Demographics	MEAN±SD (Range)
Sample size	171
# of observations	1970
Age (years)	77.1±5.8 (69-95)
Weight (kg)	72.0±16.4 (32.9-137.0)
Gender	Male: 58 Female: 113
Race	Caucasian: 156 African-American: 15

Table 4: CYP2D6 allele frequency in Caucasian and African - American patients

CYP2D6 allele	N of CA	Allele frequency in CA	N of AA	Allele frequency in AA
*1	48	0.38	1.00	0.13
*2	45	0.35	4.00	0.50
*4	22	0.17	1.00	0.13
*5	4	0.03	0.00	0.00
*17	0	0.00	2.00	0.25
*10	4	0.03	0.00	0.00
*2x2	5	0.04	0.00	0.00

CA: Caucasian; AA: African - American

Table 5: PK parameter estimates for the two-compartment model

Parameters	Base model Estimates	SE%	Parameters	Final model Estimates	SE%
V _m (μg/h)	208	32.5	V _m (μg/h)	474	19.3
K _m (μg/L)	157	83.4	K _m (μg/L)	205	24.67
V ₂ (L)	254	6.70	V ₂ (L/ 75 kg WT)	230	8.60
V ₃ (L)	2350	102.1	V ₃ (L)	900	81.1
Q (L/h)	1.33	12.3	Q (L/h)	1.05	25.3
K _a (/h)	9.24	8.8	K _a (/h)	9.81	28.0
PM (θ _{v_m})	N/A	N/A	PM (θ _{v_m})	125	48.8
IM (θ _{v_m})	N/A	N/A	IM (θ _{v_m})	182	19.4
EM (θ _{v_m})	N/A	N/A	EM (θ _{v_m})	454	49.5
UM (θ _{v_m})	N/A	N/A	UM (θ _{v_m})	3670	34.6
WT(θ _{v₂})	N/A	N/A	WT(θ _{v₂})	1.83	50.1
Sex (θ _{v₂})	N/A	N/A	Sex (θ _{v₂})	99.3	42.9
ω _{v_m} %	155	168.8	ω _{v_m} %	90.0	57.3
ω _{K_m} %	79	19.4	ω _{K_m} %	109	56.1
ω _{v₂} %	134	245.3	ω _{v₂} %	77.8	18.2
σ ₁ %	40	14.0	σ ₁ %	35.1	14.4
σ ₂ (μg/L)	10.8	90.6	σ ₂ (μg/L)	8.60	103

Abbreviations: V_m=maximal rate, K_m=Michaelis-Menten constant (concentration at half V_m), SE=standard error, WT=total body weight, V₂=volume of distribution of central compartment, V₃=volume of distribution of peripheral compartment, ω=coefficient of variation of inter-individual variability, σ=coefficient of variation of residual error, N/A: not available, Unit of weight=kg.

Table 6: Population Pharmacokinetic Model Development (2-compartment with nonlinear elimination)

Covariate	Model	-2LL	Δ -2LL	P value
1	Base model	17137.900		
2-1				
V _m				
CYP2D6	M1	16977.144	-160.76	< 0.005
WT	M2	17079.98	-57.92	< 0.005
AGE	M3	17143.06	5.155	> 0.05
RACE	M4	17133.65	-4.25	< 0.05
SEX	M5	17070.42	-67.48	< 0.005
2-2				
V ₂				
CYP2D6	M6	17071.83	-66.07	< 0.005
WT	M7	17068.262	-69.64	< 0.005
AGE	M8	17134.346	-3.55	> 0.05
RACE	M9	17142.224	4.32	> 0.05
SEX	M10	17080.828	-57.07	< 0.005
3-1				
V _m , V ₂				
V _m (CYP2D6, WT)	M11	16876.32	-100.82	< 0.005
V _m (CYP2D6), V ₂ (WT)	M12	16900.59	-76.55	< 0.005
V _m (CYP2D6), V ₂ (SEX)	M13	16892.90	-84.24	< 0.005
V _m (CYP2D6, RACE)	M14	16977.165	0.021	> 0.05
3-2				
V _m and V ₂				
V _m (CYP2D6), V ₂ (SEX, WT)	M15	16861.53	-31.37	< 0.005
V _m (CYP2D6, WT), V ₂ (SEX)	M16	16830.24	-62.66	< 0.005

* WT=weight; V₂=volume of distribution of central compartment; Δ -2LL was objective function value (OFV) from covariate model minus base model; -2LL values in 2-1 and 2-2 were compared with base model; -2LL values in 3-1 were compared with model M1; while values in 3-2 were compared with 3-1 M13 and M11. The incorporation of covariates was described in the methods section.

Figure 1: Frequency histogram showing the sampling distribution for paroxetine sampling measurements. The x-axis is broken into 1-hour bins. The y-axis is the proportion of samples taken in each interval.

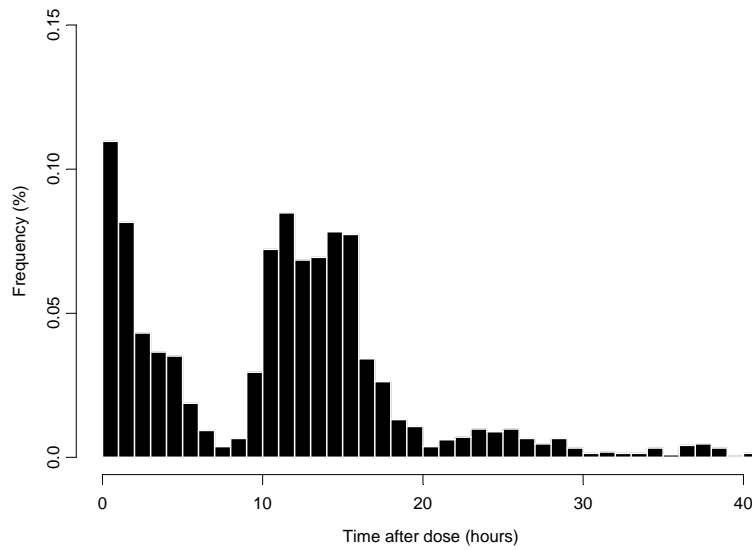


Figure 2: Diagnostic plots of final PK model.

Figure 2a: Plot of population predicted paroxetine concentrations versus observed paroxetine concentrations. Individual data points were shown as dots and the unity line is shown as a solid line.

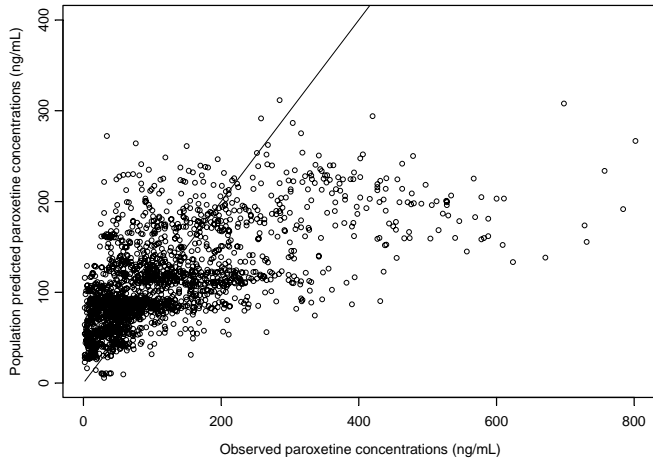


Figure 2b: Plot of individual population predicted paroxetine concentrations versus observed paroxetine concentrations. Individual data points were shown as dots and the unity line is shown as a solid line.

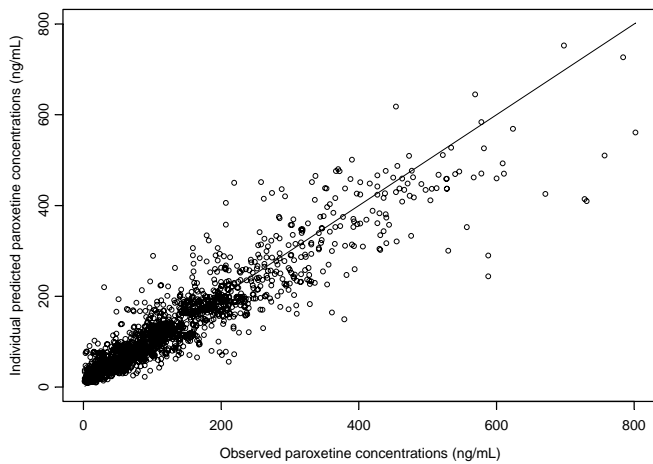


Figure 2c: Plot of weighted residual error (WRES) verse population predicted concentrations

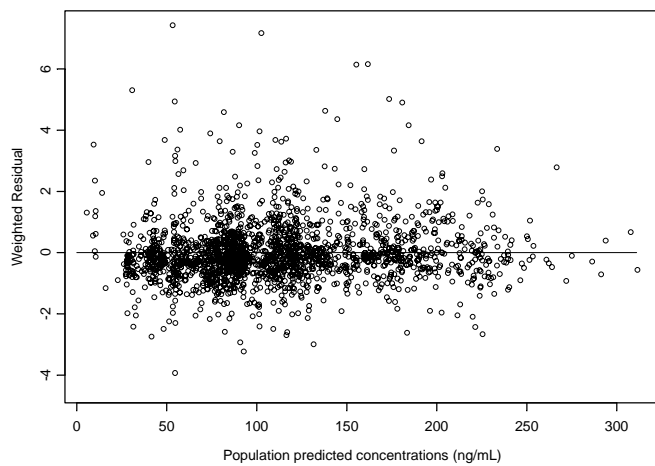


Figure 2d: Plot of WRES verse time.

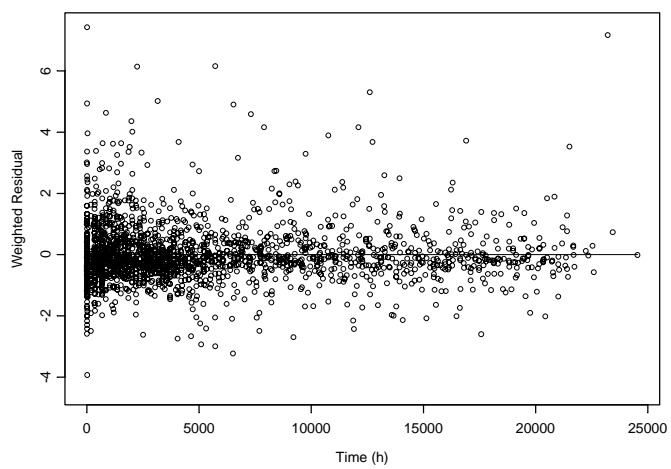
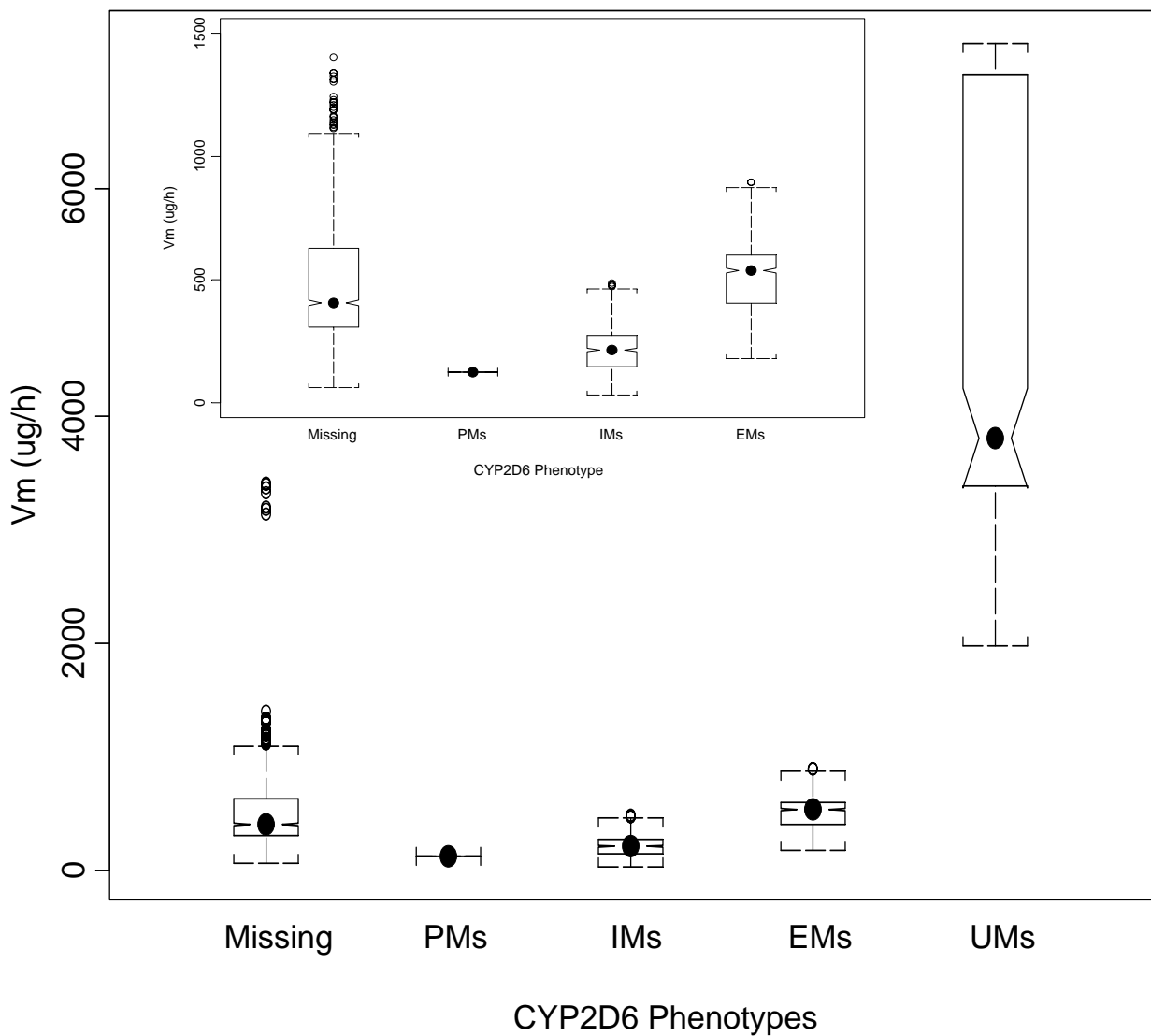


Figure 3: Boxplot of Vm estimates for each CYP2D6 phenotype group. Dots in each group were median values. Notches show approximate 95% confidence limits for the median.

CYP2D6 genotype was classified into one of the four CYP2D6 phenotype groups based on the phenotype-genotype relationship. In this plot, PMs = poor metabolizers, IMs =Intermediate metabolizers, EMs = extensive metabolizers, UMs=ultra-rapid metabolizers. Missing = Subject was missing CYP2D6 phenotype information.



CHAPTER 5 EVALUATION THE CONSISTENCY OF EXPOSURE USING THE PREDICTED/OBSERVED CONCENTRATION RATIO

This chapter is based on the following paper:

Yan Feng, Marc Gastonguay, Robert. R. Bies. Evaluation the consistency of exposure using the predicted/observed concentration ratio. *Journal of Pharmacokinetics and Pharmacodynamics*, 2006 (In preparation)

Copyright is to be assigned to Journals Rights & Permissions Controller (Springer Publishing) if the manuscript is accepted for publication. Once the paper is accept in *Journal of Pharmacokinetics and Pharmacodynamics*, the copyright transfer form will be signed by us, which including the rights of using the full article in the thesis.

Abstract

Purpose: The aim of this study was to evaluate the stability and robustness of using the deviation between Nonlinear Mixed Effects PK model-predicted concentration and observed drug concentration as a measure of erratic drug exposure driven primarily by variable adherence.

Background: Non-adherence is very common among subjects in the schizophrenia and depression treatment. Research has demonstrated that there is a higher probability of re-hospitalization for poorly adherent schizophrenic subjects¹⁵⁵. The relationship between the pattern of fluoxetine dose intake and the probability of positive response among subjects with major depressive disorder showed to be related not to the absolute adherence rate but rather the time to the first drug holiday in the treatment regimen³³. Therefore, measuring an individual's specific adherence characteristics is potentially very important information in clinical trials, since non-response or adverse drug effect may be caused by the inconsistent intake of the drug.

Methods: Population pharmacokinetic (PK) modeling in conjunction with dosage history information comprising the input to the PK model from the Medication Event Monitoring System (MEMS) was used to evaluate the consistency of exposure in the two simulated trials with atypical antipsychotic and antidepressants. Escitalopram (long half-life drug) and risperidone (short half-life drug) were selected as the representative drugs from the clinical trials. The observed adherence rate was calculated based on weekly and 2 days adherence pattern for MEMS data obtained from the clinical trial. The distribution of the deviation between the predicted and observed concentrations (C_{pred}/C_{obs} and C_{ipred}/C_{obs} ratio) was evaluated across all adherence rate patterns under the situations when the subjects' correct (negative control) or incorrect / assumed (positive control) dosing history was applied in population PK analysis. The relationship between this ratio and adherence rate was assessed under the conditions of the positive control. The adherence rate was then assigned based on the relationship described above and the classification error of this approach was calculated under each adherence condition. The bias and precision of the PK parameter estimates was also evaluated under both positive and negative control conditions.

Results: MEMS data showed that the adherence rates varied within subjects during treatment in the real clinical setting. Concentrations tended to be over-predicted in the poorly adherent subjects and under-predicted in the highly adherent subjects. The relationship between rate and ratio was adequately described by exponential functions. The rate was well classified for the clinical events under extreme conditions, e.g., very high and very low adherence rates. The Cipred/Cobs ratio was found to be more differentiable than Cpred/Cobs ratio under positive control, which was suggested by the mean ratio between adherence rate conditions. It was also shown that the percentage of correctly classified adherence rates was higher based on the relationship between Cipred/Cobs ratio and adherence rate than that based on the Cpred/Cobs ratio. For both long and short half-life drugs, the parameters tended to be more biased and less precisely estimated using the incorrect dosing history

Conclusion: This simulation study demonstrated the usefulness of population PK modeling in combination with MEMS information in deriving a Predicted to Observed ratio metric that aimed to reflect the connection to the consistency of exposure. The deviation between the individual model-predicted concentrations and concentration measurements could only adequately reflect the extremes in adherence conditions (i.e., >100% and <5%).

Keywords: adherence, MEMS, dosing history, NONMEM, modeling and simulation

1. Introduction

Mixed effect population pharmacokinetics (PK) is the study of the sources and correlates of variability in plasma concentrations between individuals,^{36, 156} which is currently widely used in evaluation of drug safety and efficacy. Population PK analysis also shows great advantage of analyzing large scale clinical trials where only a few samples are available per subject.¹⁰ Unfortunately, the drug dosing history is often poorly recorded and the extent of noncompliance is usually underestimated, which can cause biased estimation for a population PK analysis and may mislead the decision making in clinical trials and drug pharmacotherapy.¹⁷⁻²³ Vrijens reported that using the detailed records of the subjects' dosing history helps to achieve convergence in model fitting under the sparse sampling measurement situation,¹⁵⁷ explaining 40% of residual variability in the plasma lopinavir concentrations and reduced the overall variability by 55%.¹⁵⁸ Non-adherence is very common among subjects receiving treatment for schizophrenia or depression. Research also demonstrated that poorly adherent schizophrenic subjects had a higher risk of re-hospitalization.¹⁵⁵ Another study demonstrated the relationship of the time to first drug holiday with fluoxetine treatment and the probability of response among subjects with major depressive disorder.³³ Therefore, measuring an individual's specific adherence condition is a very important piece of information in clinical trials, as the non-response or adverse drug effect may be caused by inconsistent drug intake.

Many studies have shown¹⁷⁻²² that inaccurate dosing history information biases estimates of PK and pharmacodynamic (PD) parameters in hierarchical Bayesian analyses. Utilization of a prior established PK/PD model may allow one to utilize these biases by evaluating the deviation between the prior model predicted and the observed drug concentrations (Cpred/Cobs and Cipred/Cobs ratio). This deviation may be used to infer consistency of exposure to drug. Brundage^{32, 159} showed that the Cobs/Cpred ratio correlated with virologic escape in pediatric HIV patients, where the greater the number of Cobs/Cpred ratios outside a specified limit, and thus less consistent the exposure, the shorter time of the first viral rebounds. Based on the work by Brundage,¹⁵⁹ we evaluated²³ whether the Cpred /Cobs ratio could discern erratic versus consistent drug exposure arising from good versus poor adherence to drug therapy by using model-based simulation approach. In the study, the magnitude of the Cpred/Cobs ratio increased with decreasing adherence rates indicating that Cpred/Cobs could discriminate between good and

poor adherence rates. However, when adherence become very low, the ratio unexpectedly decreased although the magnitude remained higher than unity.²³ This raises the question of utility of this ratio under conditions of extremely poor adherence. There are several possible explanations for this observed decrease in the magnitude of the C_{pred}/C_{obs} ratio under conditions of extremely low adherence. As patients become less and less adherence to drug therapy, this may result in a greater number of concentration measurements below the limit of quantitation (BLQ). Censoring of these observations in the analysis may result in a smaller number of ratios contributing to the calculation of the overall C_{pred}/C_{obs} ratio for that adherence group. In addition, the ratios that would have resulted from extremely low concentrations, if they were not BLQ, would likely be very high and expand the overall mean C_{pred}/C_{obs} ratio for that group. Since these values were missing, this may result in a lower overall C_{pred}/C_{obs} ratio. The estimation of individual specific PK parameters for that particular group may become less efficient as information is lost (i.e., fewer usable concentration samples from these individuals) from that group in this way as well as no observations between the BLQ and zero (thus truncating where concentrations are actually declining for the model estimation). The other limitations for the previous study²³ is that 1): the dosing history was simulated based on the study design and the adherence pattern was arbitrarily selected; 2): only one simulation was performed, the reference for the C_{pred}/C_{obs} ratio was unavailable.

In this study, the MEMS based dosing history data from SPECTRUM clinical trial (Depression, the search for treatment-relevant phenotypes) was incorporated in the computer simulations. Adherence, including acceptance, execution and discontinuation phases, generally refers to the percentage of the prescribed doses actually taken correctly as the percentage of days of treatment period when the medication is taken appropriately.¹⁶⁰⁻¹⁶² In this study, adherence defined as the dose taking (number of the prescribe pills taken per day) and the timing of doses taken (pills was taken within a prescribed period). A 100% reliable indirect measure for adherence does not exist to date. The Medication Event Monitoring System (MEMS)³⁴ is a microprocessor-based method for continuous monitoring of adherence, which provides more accurate information than other indirect adherence measurements (e.g., self-report, direct interrogations, tablet estimates or prescription count). Adherence has also be measured by evaluating the stability of plasma level / dose (L/D) ratios, however, these require the precise

timing and scheduling of dosage self administration by the patient and subsequent clinical visit to capture the true trough.^{30,35} Jonsson had suggested that exclusion the data suspected of arising from non-adherence using population PK modeling approach could improve parameter estimates.¹⁶³ However, the information was lost since the excluded data had a high probability to link to the observed clinical event due to their inconsistent drug exposure level. How the excluded data could help to identify the erratic adherence pattern and therefore link to the consequent clinical event has not been reported in the literature.

The primary objective of this study is to assess the stability and robustness of using the ratio of C_{pred}/C_{obs} (i.e., model population predicted to observed concentration ratio) and C_{ipred}/C_{obs} (model individual predicted to observed concentration ratio) in reflecting adherence patterns, by using simulation approaches incorporating design features selected from two clinical trials (SPECTRUM and CATIE). PK models of escitalopram (long half-life drug) and risperidone (short half-life drug) were used for simulation. The trials simulations are 1) the SPECTRUM (depression, the search for treatment – relevant phenotypes) trial that evaluates the use of escitalopram and / or interpersonal therapy (IPT) in depression by use of the SPECTRUM rating scale and 2) the controlled antipsychotic trials of intervention effectiveness (CATIE), which deals with the treatment using atypical anti-psychotics. We hypothesize that the ratios of C_{pred}/C_{obs} and/or C_{ipred}/C_{obs} predicts adherence rate in clinical trial for both short and long-half life drugs. The purposes of this study are a): to evaluate the distribution of the deviation between the model predicted concentrations and observed concentrations across the adherence rate patterns (high to extremely low adherence rates) for both long and short half-life drugs under the situation when the subjects' correct dosing history is known (negative control) and when the correct dosing history is unknown (positive control); b): to evaluate the association between ratios and the adherence rates under the conditions of the positive control; c): to evaluate the bias and precision of parameter estimates under both positive and negative control conditions.

2. Methods

2.1 Study design and subjects

In order to assess the stability and robustness of the C_{pred}/C_{obs} ratio, the SPECTRUM and CATIE clinical trial designs specified below were simulated to generate PK samples under conditions for extremely low, low, intermediate and high adherence rates (see table 2). Adherence rate was defined as the % of tablets taken correctly in a specified period preceding the clinic visit and PK sample. PK models for a representative long (escitalopram) and short (risperidone) half-life drug were used for the simulations.

SPECTRUM clinical trial

The SPECTRUM trial evaluated the use of escitalopram and / or interpersonal therapy (IPT) in depression by use of the SPECTRUM rating scale. Up to five concentrations per patients are proposed in the study. In the simulation study, the plasma samples were assumed taken at each clinical visit. The PK model was adapted from the literature,^{164, 165} which was then used as the basis of the escitalopram PK simulation model. SPECTRUM trial proposed using the MEMS cap as part of pharmacotherapy adherence monitoring. MEMS cap data included number of doses taken (MEMS cap opening record) and the time of dose taken (MEMS cap opening time), which was considered as patients' actual dosing history and was incorporated in the simulation study to generate 'observed' concentrations.

CATIE clinical trial

The CATIE study (NIMH #N01 MH90001) was two separate multi-site trials. It investigated the comparative effectiveness of atypical antipsychotics in up to 2,250 subjects with either Alzheimer disease (AD) or schizophrenia. One to six concentrations per subject are proposed to be provided for each antipsychotics (e.g., risperidone, olanzapine, and quetiapine). The risperidone concentration measurements obtained from CATIE-AD clinical trial were used to build the population PK model, and then used in the simulation study. MEMS data is unavailable in CATIE study.

2.2 Simulation Study

2.2.1. Analysis Platform

Non-linear Mixed Effects Modeling is applied to perform population PK analysis using NONMEM computer program (Version V, GloboMax, Hanover, MD).^{40, 166} The models

consisted of a structural model that describe the disposition of the drug following oral administration, and a pharmaco-statistical model that describes the inter- and intra-individual variability. NONMEM is also utilized for performing the model-based simulations. ‘Virtual subjects’ datasets simulation, graphics and post-processing of NONMEM outputs are performed using S-PLUS (Version 6.2.1, Insightful, Seattle, WA). Perl (version.5.6) is used for scripts of data-extraction and simulation routines.

2.2.2. Simulations and Estimation Step

Simulation - MEMS cap data provided the actual dosing history (dose and time of dose taken) for subjects in SPECTRUM study. This information is unavailable for CATIE trial. The MEMS data from SPECTRUM was adapted to provide the dosing history information for CATIE (see below for detail). Subjects recruited in both clinical trials had chronic psychiatric disorders. Depression is a mood disorder that frequently co-exists with schizophrenia, therefore we assumed that subjects in CATIE had similar adherence pattern as those in the SPECTRUM study. Since subjects received BID risperidone in CATIE trial, while QD escitalopram in SPECTRUM trial, it is also assumed that if subjects took one dose, he should take the other dose 12 hour later with standard deviation of 1 hour.

S-PLUS was applied to simulate datasets, which composed of ‘virtual subjects’ with a unique virtual concentrations time profile under sampling conditions outlined in CATIE and SPECTRUM studies. The simulated dataset included information of the actual PK sampling time at each clinical visit (negative control) and incorrectly-reported dosage history (nominal dose and dose taking time) and recorded PK sampling time (positive control). The simulated datasets provide individual PK parameters and concentration measurements for each virtual subject. The ‘observed’ concentrations for subjects at each clinical visit were generated using the NONMEM simulation option. A PK sample was assumed to be taken at each clinic visit during the clinic opening time. The actual dosing taken time and number of dose taken was provided from MEMS data. The actual PK sampling time was selected between 8:00 am to 6:00 pm within clinical opening period using a random uniform distribution. The selected erroneous nominal time of dose taken (incorrect dosing) was 9:00 pm, with an SD of 1 hour from the selected erroneous nominal time. The reported PK sampling time was erroneously reported with an SD of 15 min

from the actual PK sampling time. 100% of adherence was assumed for the positive control. The detailed description of simulation scenarios for SPECTRUM and CATIE trial were summarized in Table 1, e.g., numbers of subjects, PK sampling per subject, simulation replicates, etc. Subjects with MEMS data in SPECTRUM study were bootstrapped (n=100) to provide reference intervals.

Estimations - The estimated concentrations from the virtual patient's dataset were obtained under two conditions: 1): given correct dosage history (MEMS cap data) and actual sampling time, considered the negative control for this experiment, to confirm that there was enough information to build a model with relatively accurate individual specific predictions if all of the information was known correctly, 2): given incorrect (nominal) dosage history and reported sampling time, the positive control for this experiment, evaluated the nature of the Cpred/Cobs ratio in relation to the dosing history; and 3): The association between ratio and adherence rate under the positive control was assessed and their relationship(s) were applied for rate prediction and rate classification. The estimations were done by using the first-order analysis with POSTHOC option in NONMEM.¹⁶⁶

PK Model - Risperidone was selected as a representative short half-life drug from the CATIE trial and escitalopram was selected as a representative long half-life drug from the SPECTRUM trial. The one-compartment with additive and proportional residual error model was developed using risperidone data from CATIE study and the two-compartment model with additive and proportional residual error models was adapted from the literature report for escitalopram.^{164, 165} The models were then used to generate a unique set of PK parameters for each patient using NONMEM program (one-compartment: ADVAN2 TRANS2 and two-compartment: ADVAN4 TRANS4). In the risperidone model, the population mean (inter-individual variance) of oral clearance (CL), volume of distribution (V), and absorption rate constant (Ka) were 16.6 L/h (123%), 214 L (114%) and 2.5 h⁻¹ respectively. In the escitalopram model, the population mean (inter-individual variance) of CL, volume of distribution of central compartment (V2), volume of distribution of peripheral compartment (V3), inter-compartment clearance (Q) and Ka were 24.4 L/h (50%), 357 L (35%), 35.7 L/h (30%), 575 L (30%) and 0.16 h⁻¹ respectively. The covariance structure was established between clearance and volume, since

they were typically dependent. We proposed to evaluate the use of the “deviation” of a predicted concentration value from the observed, when the PK model is anchored with an established Bayesian prior PK model. The observed concentrations were generated by the simulation of the virtual patients. The concentrations obtained by the NONMEM estimation and PK parameters for each individual at each PK sampling measurement were used to create the model predicted concentration at the sampling time and thus serve as the basis of the derivation of the Cpred/Cobs and Cipred/Cobs ratio. The ratios under the conditions of the negative (known dosing history) and positive controls (unknown dosing history) were calculated for each patient and were tested to evaluate the consistency of the exposure in the positive control.

2.2.3 Evaluation of the overall distribution of the derivation of the ratio measurement across the adherence rates in long and short half-life drugs

2.2.3.1 CATIE and SPECTRUM clinical trial

According to the CATIE protocol, up to 350 patients are expected to enter each arm of the study. According to the SPECTRUM protocol, the 288 subjects are expected to enter into the study, 178 subjects are expected to provide plasma concentrations. Study design and simulation steps have been described in our previous report.²³ The strategy of simulating the virtual subjects for both clinical trials was modified based on the purpose of this study.

Sample size - One of the objectives of this study was to assess the distribution of the derivation of the Cpred/Cobs ratio measurements across all adherence patterns. Data from SPECTRUM trial was bootstrapped to create 100 replicates.

Dosage and PK sampling – In the CATIE study, subjects are assumed to take their medications twice a day. In the SPECTRUM study, 90% of subjects are assumed to take their medication in the evening and 10% in the morning. The MEMS cap data from the SPECTRUM study was applied to the negative control and was considered as the actual dosing history. In the positive control, subjects were assumed to take 2 mg risperidone twice a day in CATIE study and 10 mg escitalopram once a day. Since MEMS data is not available for CATIE study, we assumed that the subjects in CATIE trial (2 mg BID risperidone) had similar adherence pattern as those in SPECTRUM (10 mg QD escitalopram) trial, and it was also assumed that if there was one dose

taken record, there should be a 2nd dose record 12 hours after the 1st dose with a standard deviation of 1 hour. For both studies, the dosing time of 9:00 PM were selected as mean (nominal) administration time with normal distribution and a standard deviation of 1 hour. The plasma samples were taken from 11 to 21 hours in subjects taking the dose. The actual sampling time was modeled as a random uniform distribution with the open times through the full 9 hours from 8AM to 6PM. The reported sampling time was erroneous, with a standard deviation of 15 min from the actual sampling time.

Adherence rate – The adherence rate was calculated based on different patterns, e.g., weekly and 2 days, where rate equal to the total number of MEMS cap opening record (total number of dosing actually taken) divided by total number of doses prescribed. Some literature classified rates into groups as: ‘good’ (75-100% of dosage intake), ‘fair’ (25-75% of dosage intake) and ‘poor’ (<25% of dosage intake). The dosage intake over 100% is defined as ‘hyper-compliance’, often relates to the belief that this may accelerate the onset of action or enhance drug’s efficacy. In this study, the adherence rate was categorized into weekly and 2-day adherence rate patterns, as shown in Table 2 and Table 3. The ratios at each adherence rate pattern were assessed under the conditions of the negative and positive control.

2.2.3.2 Evaluate the overall distribution of the derivation of the ratio measurement

In order to assess the distribution of the C_{pred}/C_{obs} ratio measurement across all adherence patterns, box-whisker plots were generated for all the adherence rates in SPLUS for both short and long half-life drugs. The box itself contains the middle 50% of the ratio values at each adherence rate level. If the median value within the box is not equidistant from the upper edge (75th percentile) and lower edge (25th percentile), then the data value was skewed. From the boxplot, we can examine the consistency of the C_{pred}/C_{obs} ratio in reflecting erratic adherence patterns (extremely low to high adherence rates). The ratio of predicted and observed concentrations should equal to one under the ideal situation (negative control). Under the positive control, concentrations were expected over-predicted if the adherence rate was assumed to be 100% while it was actually less than 100%, and under-predicted if the actual adherence rate over 100% was assumed to be 100%. Thus the systematic deviations between the differences between observed and predicted concentrations could be reflected by the shift of the median ratio

value with adherence rate level change. These plots allowed us to examine whether or not there were systematic deviations in the difference between observed and predicted concentrations, and how these central tendencies of the deviations (ratios) shifted with the erratic drug taking pattern (adherence rate) change for both short and long half-life drugs.

2.2.3.3 Evaluate the BLQ impact on the derivation of the C_{pred}/C_{obs} ratio measure under the extremely low adherence condition

The impact of BLQ on the ratio distribution was assessed, with a focus on the subjects with extremely low adherence rate. As mentioned above, the C_{pred}/C_{obs} ratio was found unexpectedly decreased in our previous study.²³ Several possible explanations / hypothesis have been discussed above. Since for the poorly adherent subjects, they are likely produce concentrations measurements that are BLQ. Thus, fewer ratios are calculable directly from the measured data. This may change the nature of the ratio, perhaps reducing its explanatory power under conditions of extreme non-adherence. In order to test the unexpected reduced ratio under extremely low adherence condition was more related to the unnatural truncation of the distribution caused by censoring concentrations BLQ rather than due to the model performance. Different levels of limit of quantitation (LOQ) were tested under negative control, and the percentage of the censored concentrations BLQ and the corresponding median ratio were calculated under the extremely low adherence rate condition for both long and short half-life drug.

2.2.4 Evaluate the association between ratio and the adherence rate

The central tendency of the ratio (mean) at each adherence rate was calculated. The association between the mean ratio and its corresponded observed adherence rate (weekly and 2 days rate pattern) was assessed using NONMEM program. The relationship was then used to predict adherence rate at a given C_{pred}/C_{obs} or C_{ipred}/C_{obs} ratio. The predicted adherence rate was classified based on minimum Euclidean distance classification criteria,¹⁶⁷ where the differences between the predicted rate and each observed adherence rate was calculated. The rate was assigned to be one of the observed adherence rate if the minimal difference between the predicted rate and the observed adherence rate was achieved. The percentage of the correct assigned rate was calculated for both weekly and 2 days adherence rate pattern.

2.2.5 Evaluate the bias and precision of parameter estimates under positive and negative control

The true parameter values were obtained from the simulation step, where all the correct dosing history was known. The parameter estimates under negative control (correct dosage history and actual sampling time) and positive control (incorrect dosage history and reported sampling time) were obtained from the estimation step. The bias and precision of the parameter estimates under each condition were evaluated using percentage prediction error (% PE) as shown below:

$$\%PE = \frac{\theta_{est} - \theta_{true}}{\theta_{true}} \times 100\%$$

Where θ_{est} is the estimated parameter values under negative or positive conditions obtained from the estimation step, and θ_{true} is the true parameter values obtained from the simulation step. The %PE was calculated from the 100 simulation replicates under each condition. The mean and standard deviation (SD) of %PE was calculated at each adherence rate, which was used as bias and precision measurement. The cutoff value for bias and precision was set to be 15% and 35%,¹⁶⁸ respectively, which was considered a threshold for good prediction..

3. Results

3.1 Subjects

A total of 65 patients' MEMS data were available from the ongoing SPECTRUM clinical trial during the first 6 month, which had 863 clinical visit records. The adherence rate was calculated for each clinical visit event (PK sampling), which was then grouped into different patterns, e.g., weekly, and 2 days adherence rate. The adherence rate was found to be varying within subject during the treatment. In the weekly adherence rate pattern, there were 9.7 % of the events with more than 7 doses taken record (rate >100%) before the clinical visit, 52.5 % of events with 6 to 7 doses taken record (rate: 85 to 100 %), 19.0 % of events with 3 to 5 doses record (rate: 30 to 85%), 4.3 % of events with 1 to 2 doses record (rate: 0 to 30%), and 14.5 % of events without any dose taken record before the visit.

3.2 Overall distribution of the derivation of the ratio across the adherence rates

The boxplots were generated for both long and short half-life drug under both positive and negative control. In the negative control, where the estimation was based on the subject with correct dosing history, the log median of C_{pred}/C_{obs} and C_{ipred}/C_{obs} ratios was approximately to zero under each adherence rate condition, as shown in Figure 1a and Figure 1b for the long half-life drug and Figure 2a and Figure 2b for the short half-life drug.

As suggested by plots under negative conditions that the concentrations were underestimated under the extremely low adherence rate condition (0%), causing the C_{pred}/C_{obs} ratios less than one. As discussed above, there're several possible reasons contributing to the reduced magnitude of the C_{pred}/C_{obs} ratio under the extremely low adherence condition. The impact of the different levels of LOQ on the magnitude of the C_{pred}/C_{obs} ratio was tested for escitalopram. In 0% adherence rate condition, the median value of the C_{pred}/C_{obs} ratio decreased with LOQ increase. The median (SD) ratio was 0.79 (1.14e+29) if LOQ is 0 ng/ml (without censoring), decreasing to 0.35 (20.3) if LOQ is 0.001ng/ml, and 0.16 (0.44) if LOQ is 1ng/ml. Censoring of the observed concentrations BLQ significantly reduced the number of ratios contributing to the overall C_{pred}/C_{obs} ratio calculation. If the LOQ was set to be 1ng/ml, 90.6% of the observed concentrations under the 0% weekly adherence rate condition were censored, and 57.8% was censored if LOQ was set to be 0.001ng/ml. For the results above, it suggested that the unexpected under-predicted concentrations under extremely low adherence condition were more caused by the high percentage of the censored concentrations BLQ than due to the model performance for long half-life drug.

For the short half-life drug, without censoring BLQ, the median C_{pred}/C_{obs} ratios under the extremely low adherence rate condition were 0.005 (weekly rate pattern) and 0.2 (2 days adherence rate pattern). In the 2 days adherence rate pattern, 73.8% of the individual ratios were censored if LOQ was set to be 0.05ng/ml and 65.2% was censored if LOQ was set to be 0.005ng/ml. Since the ratio under very low adherence rate conditions was significantly lower than 1, even without censoring any concentrations BLQ. The other possible explanations for this observation could be the model artifact. One compartment model was developed using highly sparse data from CATIE-AD study, while 2-compartment model had been reported for risperidone.¹⁶⁹ Higher inter-individual variability (IIV) was evaluated using the highly sparse

data from CATIE-AD trial. Trying to evaluate the impact of model structure, PK parameters and IIV on the ratio under extremely low adherence conditions, The additional study was conducted using the 2-compartment PK model with reported PK parameters and IIV from our previous study.²³ Similar BLQ effect on the ratio was found for the short half-life drug based on the previous model, where the C_{pred}/C_{obs} obtained from the extremely low adherence rate condition (2 days adherence rate pattern) become 0.7 without censoring (LOQ=0) BLQ and reduced to 0.5 if LOQ was set to be 0.005ng/ml and 0.2 if LOQ was set to be 0.2ng/ml. Under the weekly adherence rate patter, 100% of the concentrations were censored when LOQ was 0.0005ng/ml. This was due to the nature of elimination processes for the short half-life, where the concentrations should be extremely low if the sample measuring time after dose is greater than 5 times half-life.

For the results above, it suggested that if the model developed under highly sparse sampling data was used in simulations, the unexpected under-predicted concentrations under extremely low adherence condition were related to both the model performance and the censored concentrations BLQ for short half-life drug. Due to these observations for short half-life drug, C_{ipred}/C_{obs} ratio was considered for assessing its relationship with rate for the short half-life drug.

In the positive control, the estimation was based on the subjects with unknown dosing history. The median of C_{pred}/C_{obs} and C_{ipred}/C_{obs} ratios increased with adherence rate decreasing as shown in Figure 1c and Figure 1d for the long half-life drug and Figure 2c and Figure 2d for the short half-life drug. The differences of the C_{ipred}/C_{obs} ratio tended to be more differentiable among adherence rate groups than that of C_{pred}/C_{obs} ratio.

3.3 Evaluation of the association between ratio and the adherence rate pattern

The mean value of C_{ipred}/C_{obs} ratio was obtained and its relationship with the observed weekly adherence rate was modeled. Bi-exponential and tri-exponential functions adequately described the relationship between C_{ipred}/C_{obs} ratio and the weekly adherence rate for long and short half-life drug, respectively. The population predicted rate and the observed rate versus C_{ipred}/C_{obs} ratio were shown in Figure 3a (long half-life drug) and Figure 3b (short half-life drug). The exponential relationship between C_{ipred}/C_{obs} ratio and rate were shown below:

Long half-life drug: $Rate = 396e^{-3.76 \times Ratio} + 194e^{-0.6 \times Ratio}$

Short half-life drug: $Rate = 89.9e^{-0.0827 \times Ratio} + 175e^{-0.521 \times Ratio} + 17.5e^{-0.6 \times Ratio}$

The exponential relationship developed above was then applied for rate prediction at each ratio obtained under positive control, and then classified into weekly and 2 days adherent rate pattern. The predicted rate classification was based on the minimum Euclidean distance classification criteria.¹⁶⁷ At a given Cipred/Cobs ratio, the distance between the predicted rate and the observed rate was calculated using equation: $d = |Rate_{pred} - Rate_{obs}|$ and the predicted adherence rate was assigned to the class (observed rate) for which the distance "d" was minimum. The assigned rates were then grouped based on weekly adherence pattern as described in the methods section. The result of the correct rate classification at each rate groups was shown in Table 2 (weekly adherence rate classification) and Table 3 (2 days adherence rate classification). The result of weekly adherence rate condition showed that the correct assigned rate in PK samples measured under very high adherence rate condition (i.e., hypercompliant) for long and short half-life drug were 73.8% and 89.1%, respectively. In PK samples measured under extremely low adherence rates (0% in the last week) the correct classification was 64.0% for long half-life drug and 39.9% for short half-life drug. The rates were better classified in PK samples measured under extremely low (0%) and extremely high adherence rate condition (>100%) than that under other adherence rate conditions. Two days adherence rate patterns were also evaluated. The relationship between 2 days adherence rate and Cipred/Cobs ratio was adequately described using a mono-exponential and bi-exponential function as shown below:

Long half-life drug: $Rate = 834e^{-2.05 \times Ratio}$

Short half-life drug: $Rate = 83.7e^{-0.069 \times Ratio} + 482e^{-0.713 \times Ratio}$

Similar as the results obtained from weekly adherence pattern, the rates were well classified for the event under extremely high (rate >100%) and extremely low (rate=0%) rate condition. The correct classified rates in the 2 days adherence rate pattern (Table 2 and 3) for long and short half-life drug were 80.8% and 91.8% under extremely high and 87.6% and 35.81% under extremely low rate condition, respectively.

For the long half-life drug, the overall rates of correct adherence classification based on Cpred/Cobs ratios were: 42.3% for weekly adherence rate pattern and 50.2% for the 2 days adherence rate pattern. For short half-life drug, the total correct assigned rate based on Cpred/Cobs ratio was 15.8% in weekly adherence rate pattern and 19.3% in 2 days adherence rate pattern.

The association of Cpred/Cobs ratio with adherence rate was also evaluate for long half-life drug, following the same procedure as above. The total correct assigned rate based on Cpred/Cobs ratio were 26.4% in weekly adherence rate pattern and 29.9% in 2 days adherence rate pattern, which was lower than the correct assignment based on the Cpred/Cobs ratio. The correct assigned rate in PK samples measured under very high and very low adherence rate condition for long half-life drug were 75.4% and 54.6% under weekly rate pattern, and 79.8% and 69.8% under 2 days rate pattern.

3.4 Evaluation of the bias and precision of parameter estimates

The bias and precision of parameter estimates under negative and positive control was shown in Table 4/Figure 4a and Figure 4b for long half-life drug and Table 5/Figure 5a and Figure 5b for short half-life drug. Generally, all individual PK parameters for long half-life drug were well estimated under both positive and negative conditions, with mean %PE less than 15% and standard deviation (SD) of %PE less than 35% (except V2 and Q estimate under positive control). The parameter estimates tend to be more biased and less precise under positive control conditions where the subjects' correct dosing history was assumed. The precision (SD of %PE) of clearance estimate was approximately 4 fold higher under negative control than that under the positive control. For the short half-life drug, estimates of individual oral clearance and Ka were unbiased, while volume of distribution estimates was biased. Most of the parameter estimates had SD of %PE over 35%, and the parameter estimates tend to be less precise under positive control where the subjects' incorrect dosing history was used than that in negative control. The biased and less precise parameter estimates results could due to the high IIV of PK parameters estimated from CATIE-AD study, and the substantial variability was then contributed to the parameter estimates in simulation and estimation steps. The estimates of variability for clearance and volume of distribution were 123% and 114%, respectively. An additional study were

performed to assess the impact of the variability on the parameter estimates, using the 2-compartment PK model, reported PK parameters and IIV from our previous study.²³ The parameters were well estimated under both negative control and positive control with bias (%PE) less than 15% and precision (SD of %PE) less than 35%, except the less precise KA estimate (%PE SD: 49.3% in negative control and 119.9% in positive control). Thus the bias and precise parameter estimates for short half-life drug was related to the model structure and the lower IIV.

4. Discussion

Many studies have demonstrated that non-adherence is very common in subjects with schizophrenia and depression.^{33, 126, 155} In the clinical trials, it was reported that the average adherence rate is only 43-78% among subjects during chronic treatment.^{24, 25} There are many other similar terminologies used in the literature to describe adherence such as compliance, concordance, alliance.^{26, 27} In this article, adherence is defined in two ways: the percentage of prescribed doses taken; and the percentage of days of therapy when the medication was taken appropriately. Thus, we focus on the continuous middle “execution” phase of drug taking (these patients have all initiated therapy-acceptance phase) and we are looking at patterns that occurred prior to discontinuation, the dichotomous end.¹⁷⁰ The inconsistency of drug exposure caused by variable adherence to the prescribed therapy was suggested to be a single largest source of variance to the drug response.¹⁵⁸ Therefore, adherence plays an important role in the pharmacotherapy efficacy assessment, since the dosage adjustments may not be relevant if the subject is inconsistently receiving the prescribed medicine. Population PK analysis showed many advantages over traditional PK analysis, especially for the larger clinical trial where only a few sample were available per subject.¹⁰ The aim of this study was to identify erratic adherence pattern using modeling and simulation approach. This is the first study to evaluate the ability of using the deviation between the predicted versus observed concentrations in reflecting the erratic adherence rate, by using population PK modeling combined with MEMS data from a target population. We also assessed the relationship between adherence rate and the ratio of C_{pred}/C_{obs} and C_{pred}/C_{obs} and assigned the adherence rate based on their relationship.

As demonstrated in many studies, adherence is related to the clinical outcomes.²⁹⁻³³ Our simulation study suggested that the population PK model with incorporation MEMS data could

be used to detect erratic exposure and thus reflect the subject specific adherence pattern (extremely high and extremely low adherence patterns) for both long and short half-life drugs. The predicted weekly and 2 days adherence rate pattern was well classified under the extremely high adherence condition and extremely low adherence conditions. Two days adherence rate pattern had a higher percentage of correct assignment than that of weekly adherence pattern for the extreme high and extremely low adherence conditions. Since the Cipred/Cobs was more differentiable than Cpred/Cobs for long half-life drug, the percentage of the correct weekly adherence rate assignment was approximately 1.5 fold higher if using Cipred/Cobs as the rate indicator than that if using Cpred/Cobs as the rate indicator. Diaz¹⁵⁵ demonstrated that the adherence rates in subjects with schizophrenia decreased from 63% in the 1st month to 45% over the following 5 month. Subjects with adherence rate lower than 50% were experienced a higher probability of re-hospitalization. This was also true in the depression study, where an index representing adherence was associated with the poor response or non-response clinical event.³³ Therefore, identifying the subjects with extremely low or high adherence conditions, is important for any dosage adjustment during treatment, since the non-response could due to the poor adherence and adverse side effect could due to the extremely high adherence condition, especially when the clinical event is concentration dependent. There were only about 10% correctly assigned high, intermediate, and low adherence rates for short half-life drug and about 20% for long half-life drug, which suggested that the drug monitoring may be necessary under these conditions, since these types of inconsistency of drug taken could lead to moderate adverse side effect which may be less severe than those under extreme adherence conditions.

In this study, we didn't find the reduced magnitude of Cpred/Cobs ratio under the extremely low adherence rate condition for positive control (using incorrect dosing history) as reported in our previous study.²³ However, the concentrations were unexpectedly under-predicted in the extreme condition for negative control, where the correct dosing history was known for the population PK analysis. The results suggested that the unexpectedly decreased ratio was caused by the greater number of the censored concentrations BLQ as well as a disproportion number of measurement which is close for but above BLQ, for long half-life drug. This may bias the ratio distribution under extremely low adherence pattern. The higher the BLQ, the more concentration measurements was censored and then more likely the concentrations

were under-predicted. However, for the short half-life drug, even without censoring any concentrations BLQ, the concentrations were still under-predicted, although less severely than that with concentrations censored BLQ. The other possible explanation for the reduced ratio could be the PK model structure and IIV. The risperidone PK model used in the simulation and estimation steps was developed using sparse data from CATIE-AD study. One compartment was found to be adequately described the data, however some studies suggested that two-compartment model best fitted the risperidone data.¹⁷¹ The results from the 2-compartment study for short half-life drug suggested that the reduced C_{pred}/C_{obs} under extremely low adherence condition was not only related to the censored concentrations BLQ, but also related to the model structure, IIV and the method for adherence rate pattern calculation (e.g., weekly versus 2 days). In general, since the C_{pred}/C_{obs} and C_{ipred}/C_{obs} ratios for both long and short half-life drugs was estimated to be approximate to one (Figure 1 and Figure 2), except in the most extreme situation, suggesting that there was enough information to build the model with relative accurate individual specific predictions.

Correct subjects dosing history is very important for a PK model not only for the parameter estimates^{22, 163} but also for model convergence.¹⁵⁷ It also can explain much of the residual variability.¹⁵⁸ In our study, the bias and precision of parameter estimates under both positive and negative conditions were evaluated. For long half-life drug, all the parameters were well estimated with %PE (bias) less than 15%. The parameter estimates were more precise under negative control than that in positive control, especially for clearance. For the short half-life drug, the clearance and K_a were unbiased estimated. The %PE for V under positive condition was approximately 5 fold higher than that in the negative condition; however the %PE was over 15% under both conditions. It was also found that %PE SD were higher than 35% for all parameters under both conditions, except K_a under negative control. Since the PK model was developed using the sparse data from the CATIE-AD trial, high IIV was obtained with IIV on CL and V were 151% and 130% respectively. The high IIV was suspected to be contributing to the less precise parameter estimates. Additional studies (data not shown) were performed using the PK model and parameter values including population mean value and IIV, from our previous study.²³ The result showed that all the parameters were estimated precisely and accurately, with %PE SD less than 35% and %PE less than 15% under both negative and positive control, except

Ka estimate. Thus the IIV on PK parameters had a higher impact on the parameter estimates than the incorrect dosing history. The other interesting finding was that using the model developed using hyper-sparse data resulted in biased and imprecise parameter estimates, but did not reduce the ability for the rate assignment based on ratio under the extreme adherence conditions (Table 2 and Table 3).

5. Conclusion

The simulation study demonstrated that the combination of the population PK model with MEMS information could be used to detect erratic exposure and thus reflect the subject with extremely low or high adherence conditions for both long and short half-life drugs. Since both of the extremely high and extremely low adherence rate conditions can be well reflected by the C_{pred}/C_{obs} and C_{pred}/C_{obs} ratio, which provides a basis where the magnitude and consistency of exposure can be examined in conjunction with the maintenance response of subjects in a future study as response data become available.

Table 1: The detailed description of simulation scenarios for long half-life drug and short half-life drug

Simulation Profile	simulation scenarios
Sample size for each simulation replicate	65
Dose (mg)	Escitalopram: 10 Risperidone: 2
N of Clinical visit record per subject	18 (2 to 43 record)
Time for dose administration	Actual: MEMS cap opening time Nominal: 21:00 (normal distribution, SD=1h)
PK sampling time	Actual: 8:00 AM to 6:00 PM (uniform distribution) Nominal: Actual sampling time + reported time error (normal distribution, SD=15min)
Adherence rate (%)	1: Weekly and 2 days actual rate 2: Adherence rate groups (very high, high, inter-mediate, low and extremely low) based on weekly and 2 days pattern
Simulation replicates	100
Simulation conditions	Time: actual dosage time and actual PK sampling time
Estimation conditions for negative control	Time: actual dosage time and actual sampling time Number of dose taking was reflected by adherence rate as shown above
Estimation conditions for positive control	Time: nominal dosage time and reported sampling time Adherence rate assumed in the estimation step: 100% for all of the simulation sets

* SD: standard deviation

Table 2 The Correct classified rate at weekly adherence rate condition for long half-life drug and short half-life drug

Adherence rate	n of dose taken	Long half-life drug		Short half-life drug	
		n of event	% correct classification	n of event	% correct classification
Group 1	>7	8014	73.82	3593	89.06
Group 2	6,7	45319	39.19	21939	5.98
Group 3	3,4,5	15972	36.65	7035	9.05
Group 4	1,2	2733	25.72	1252	9.03
Group 5	0	1128	64.01	353	39.94

* Group 1: very high adherence rate condition (>100%); group 2: high adherence rate condition (85-100%); group 3: intermediate adherence rate condition (30-85%); group 4: low adherence rate condition (0-30%) and group 5: extremely low adherence rate condition (0%).

Table 3 The Correct classified rate at 2 days adherence rate condition for or long half-life drug and short half-life drug

Adherence rate	n of dose taken	Long half-life drug		Short half-life drug	
		n of event	% correct classification	n of event	% correct classification
Group 1	>2	8437	80.75	3935	91.82
Group 2	2	43653	44.69	21677	6.64
Group 3	1	17396	41.25	7496	15.62
Group 4	0	3680	87.58	1064	35.81

* Group 1: very high adherence rate condition (>100%); group 2: high adherence rate condition (100%); group 3: intermediate adherence rate condition (50%); group 4: low adherence rate condition (0%) and group.

Table 4 The overall bias and precision of parameter estimates under positive and negative control for long half-life drug

PE (%)	Negative control		Positive control	
	MEAN	SD	MEAN	SD
CL/F	-1.9	5.7	3.4	24
V2	3.0	29.1	10.5	39.3
V3	3.9	26.7	6.0	32.8
Q	5.4	31.8	8.4	35.8
KA	0.6	6.4	-3.3	7.1

Table 5 The overall bias and precision of parameter estimates under positive and negative control for short half-life drug

PE (%)	Negative control		Positive control	
	MEAN	SD	MEAN	SD
CL/F	-3.7	53.3	-0.38	83.2
V	37.9	327.6	206.1	893.5
KA	-1.86	23.4	-0.69	53.5

Figure 1 Boxplot of the overall all ratio distribution at each adherence rate condition for long half-life drug (escitalopram). Dots in each group were median values.

Figure 1a Boxplot of the log Cpred/Cobs ratio under negative control

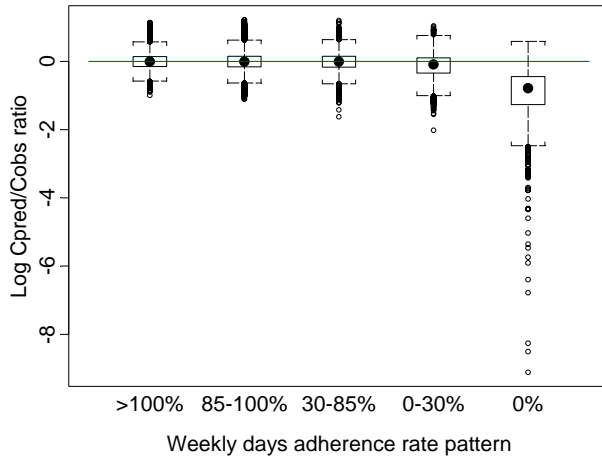


Figure 1b Figure1b: Boxplot of the log Cipred/Cobs ratio under negative control

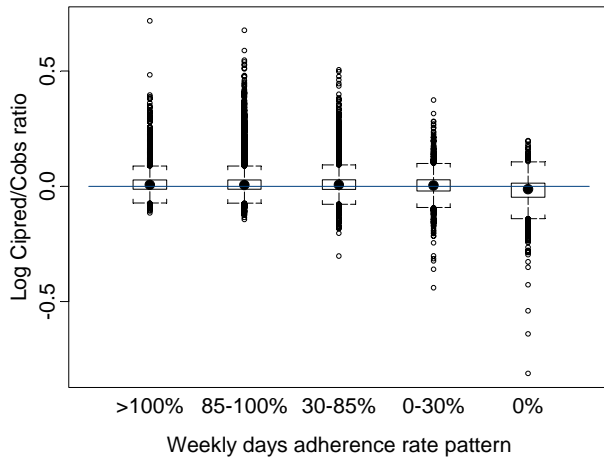


Figure1c: Boxplot of the log Cpred/Cobs ratio under positive control

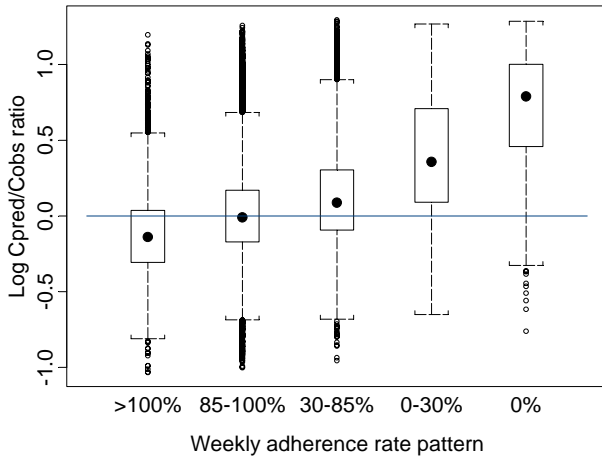


Figure1d: Boxplot of the log Cipred/Cobs ratio under positive control.

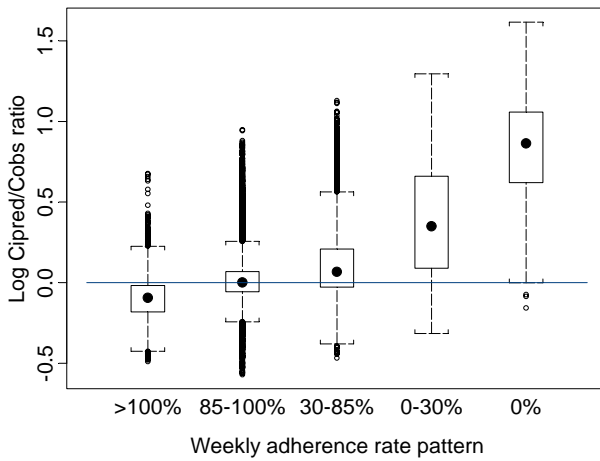


Figure 2c Boxplot of the log Cpred/Cobs ratio under positive control

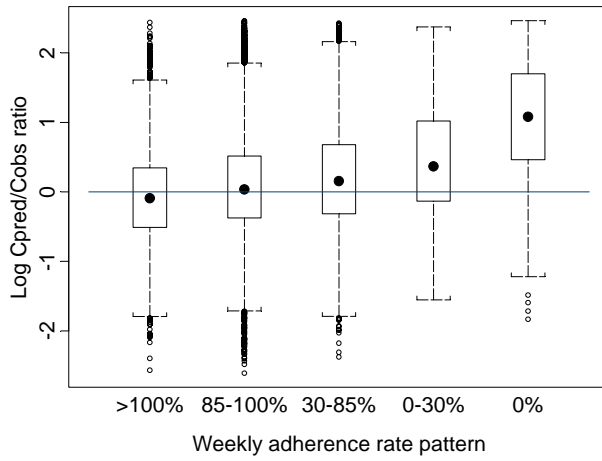


Figure 2d Boxplot of the log Cipred/Cobs ratio under positive control.

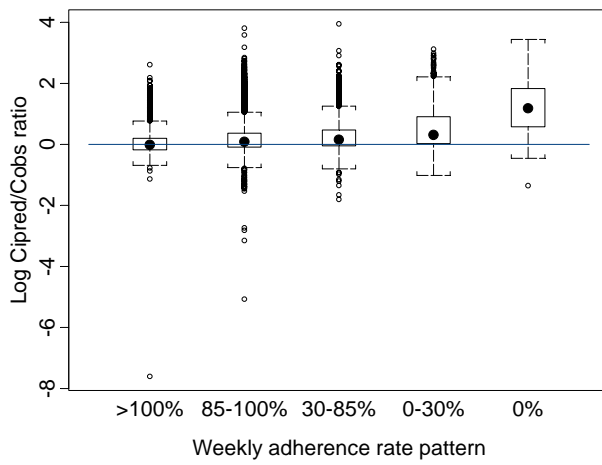


Figure 3 The association between Cipred/Cobs ratio and adherence rate in long half-life drug (Figure 3a) and in short half-life drug (Figure 3b). Dots represented the median values of Cipre/Cobs ratio at each observed adherence rate conditions. The line represented the model predicted rate at given Cipred/Cobs ratios.

Figure 3a

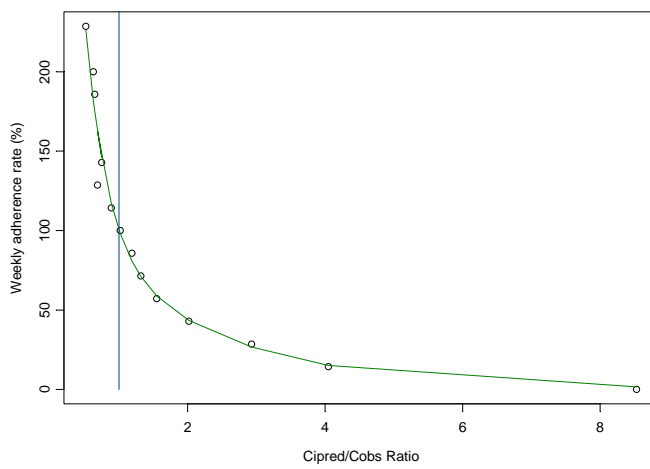


Figure 3b

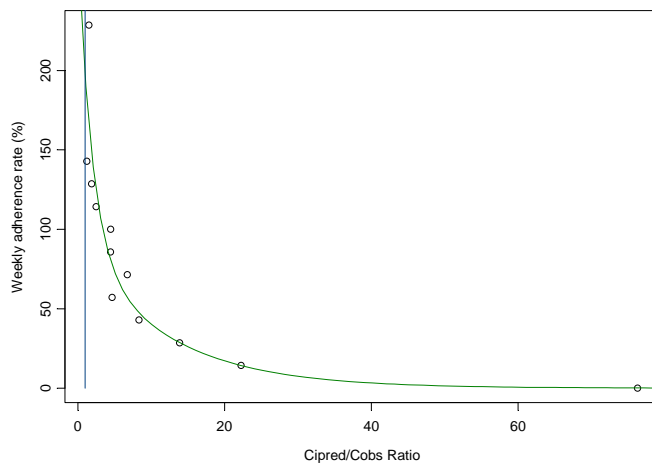


Figure 4: Bias and precision of parameter estimates under negative and positive control.

Figure 4a: Bias of parameter estimates for long half-life drug; Figure 4b: Precision of parameter estimates for long half-life drug

Figure 4a

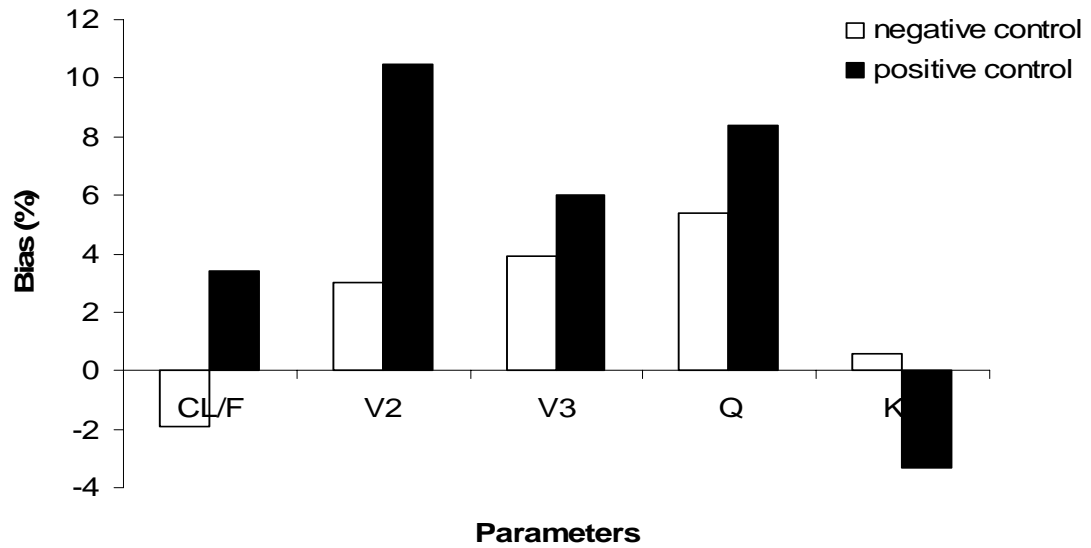


Figure 4b

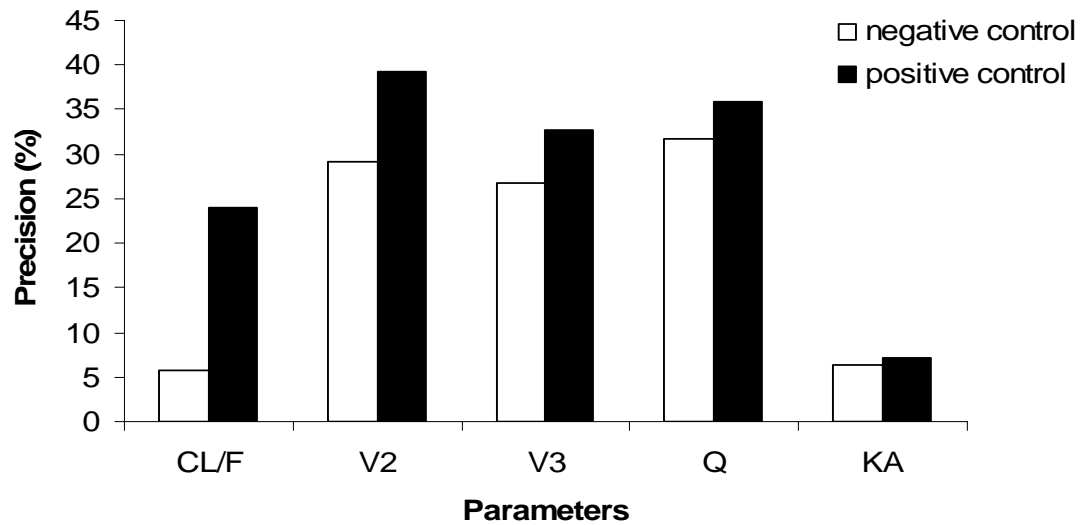


Figure 4c: Bias of parameter estimates for short half-life drug; Figure 4d: Precision of parameter estimates for short half-life drug.

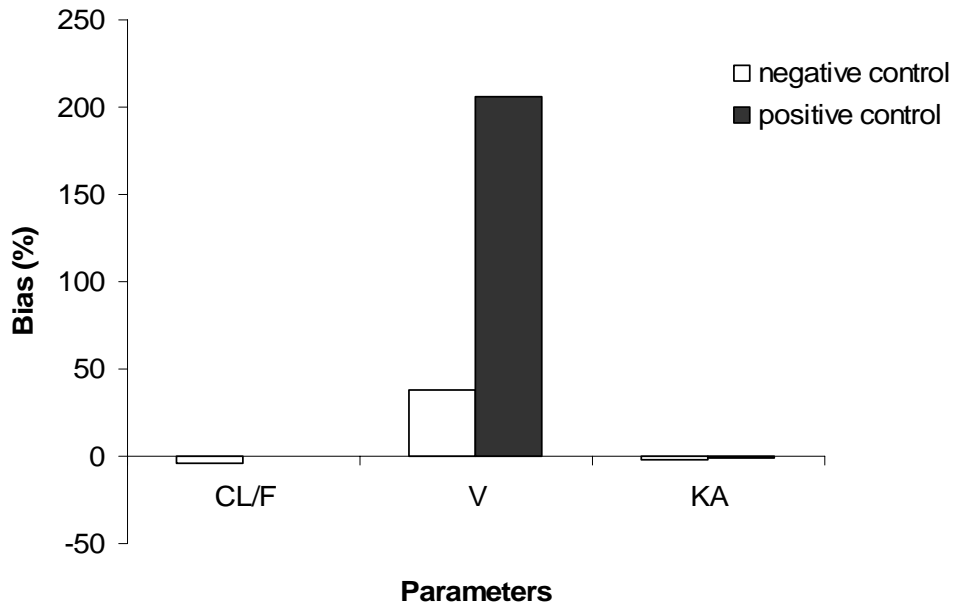
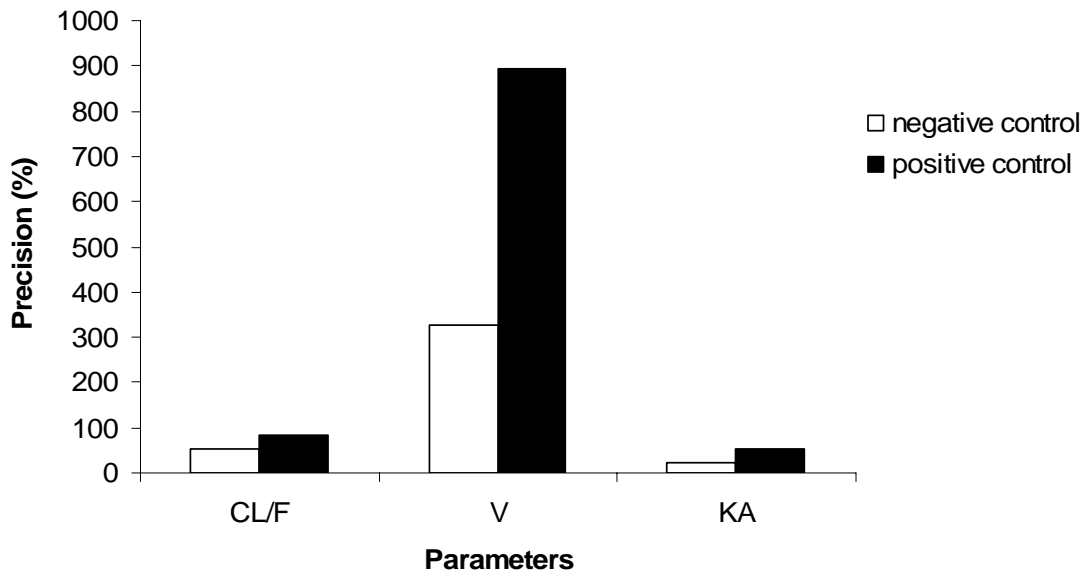


Figure 4d



CHAPTER 6 OVERALL SUMMARY AND FUTURE DIRECTIONS

6.1 Overall summary

Population PK analysis is an important technique used to explore and define sources of variation in drug exposure in a target population. The purpose of the thesis work was to explore the usefulness of the mixed effect modeling approach in analysis sparse sampling measurements in large-scale clinical settings, including understanding variability among outpatients/inpatients with mental disorder, dose optimization and evaluation the consistency of drug exposure.

To meet these goals, the following were carried out: 1): the study performed to evaluate age effect in subjects with major depressive disorder receiving citalopram using highly sparse data measurements; 2): the first study conducted to evaluate CYP2D6 genotypes impact on paroxetine disposition in late-life depression; 3): the first study to optimize dosage strategy for intensive care and general medical unit patients receiving enoxaparin by continuous intravenous infusion; and 4): the first study to evaluate the usefulness of population PK modeling with MEMS in evaluating the consistency of exposure. The conclusions from each study were shown as below:

Elderly patients are not easily studied using the traditional PK analysis approaches, where intensive sampling measurements are needed for analysis. In the study, the data from two clinical trials were combined and analyzed. Age and weight were found to be significant covariates on clearance and volume of distribution. After the corrections include weight effect, age was a significant covariate across the entire age range (22-93 years). The study was able to extend these findings by demonstrating a continuous relationship between age and clearance of citalopram, as well as simultaneously accounting for the contribution of weight to citalopram pharmacokinetics. Clearance declined by 0.23 L/h per year of age and increased by 0.14 L/h per kg of body weight. The results also are important in understanding the magnitude and variability of drug exposure, as well as the specific factors that contributed to the inter-individual differences in the exposure.

Late-life depression is a prevalent disorder that causes significant suffering and disability. Paroxetine, mainly metabolized by CYP2D6, is widely used in the treatment of depression. The

association between CYP2D6 genetics and paroxetine PKs in geriatric subjects after chronic paroxetine treatment is still unknown. In our study, it was found that the order of magnitude for V_m by CYP2D6 phenotype was: UMs>EMs>IMs>PMs. The other interesting finding in the study was that race was a significant covariate when CYP2D6 was not included in the model. One possible explanation for this observation is related to the correlation between race and CYP2D6 genotypes. When the CYP2D6 genotypes were incorporated, the race effect was no longer significant.

Modeling and simulation can facilitate dosage strategies for the target populations. The target populations in our study were the general medical unit and intensive care unit subjects who received CII enoxaparin. Enoxaparin is mainly metabolized by the kidney. CrCL and weight were the significant covariates on clearance and central volume of distribution. The study showed that the dose of CII enoxaparin should be individualized based on the subjects' renal function and weight. It is also suggested that subjects in the ICU appears to have higher exposure than those in general medical unit, even though the ICU patients are likely to receive slightly lower doses.

Inconsistency of drug exposure caused by non-adherence is very common among subjects with schizophrenia or depression. Our studies examined the usefulness of population PK modeling combined with MEMS data in reflecting the consistency of exposure. Simulations showed that the deviation of model-predicted and observed concentrations adequately reflected subjects under the extremely high and extremely low adherence rate conditions. This methodology developed was very important in evaluation of individual specific adherence characteristics, and thus for understanding the clinical outcomes in the clinical trial, since the non-response or adverse drug effect may be caused by the inconsistency drug intake and it may be possible to get a sparse concentration sample for an individual rather than provide electronic monitoring to every individual assessed.

6.2 Future directions

Evaluate the impact of adherence on Escitalopram response in SPECTRUM study

The non-adherence is very common among schizophrenic and depressed patients during chronic treatment. The future study will be focused on examining the impact of the inconsistent escitalopram exposure driven by the erratic adherence rate during the treatment on the clinical response, including both safety and efficacy clinical outcomes from SPECTRUM study. Moreover, we will examine the ability of rate classification based on the relationship between ratio and adherence rate, when the actual concentrations are available.

Paroxetine Pharmacodynamic study

Evaluate the relationship between paroxetine response and serotonin genetics

Reducing or at least capturing the immense variability in drug concentration is the first step towards optimizing power in pharmacodynamic studies. In the MTL2 study, we have demonstrated the impact of CYP2D6 genotypes on paroxetine pharmacokinetic parameters. In addition, the ability of capturing the magnitude of individual specific drug exposure over time provides a basis where the magnitude of exposure can be evaluated in conjunction with the maintenance response. Future work in MTL2 clinical study is focusing on understanding the variability of disease recurrence for similarly exposed subjects in the maintenance phase. There are two descriptors for the return of depressive symptoms. The first is a relapse of the disease which is defined as a new episode of major depression occurring within 16 weeks of the initial treatment response. The second is recurrence, and this is defined as the new episode of major depression at least 16 weeks after initial resolution of depression. A new episode of major depressive disorder is defined by SCID/DSM-IV criteria in addition to HAMD score equal or greater than 15.

The causes of depression are complex. One of the hypotheses is related to serotonergic activity, which suggests that decreased levels of serotonin at the synapse are factor causing depression. The initial site of action for SSRI (e.g., paroxetine) is the 5-HT transporter (SLC6A4); accordingly, the majority of studies to date have examined polymorphisms in or near the gene coding for the transporter. The association of the serotonin transporter promoter polymorphism with the speed or degree of a response or side effects of SSRI treatment is showing considerable promise.^{172, 173} Therefore, the differences in the level or function of serotonin receptors, enzymes involved in synthesis (THP1) or metabolism (MAOA) of 5-HT

may also influence response. Genes correlated with antidepressant response are also believed to contribute to the high level of response variability. After the determination of the paroxetine exposure, the relationship between these 5-HT related genes and the probability of having recurrence will be examined. The results will help to understand the sources of variability related to depression recurrence, thus potentially providing for the individualization of dosage in the target populations.

APPENDIX A

LIST OF ABBREVIATION& NOMENCLATURE

ABW	Adjusted body weight
AIC	Akaike information criterion
AUC _{ss}	Area under the curve at steady state
CII	Continuous intravenous infusion
CL	Clearance
BMI	Body mass index
BSA	Body surface area
CrCL	Creatinine clearance
C _{ss}	Steady state concentration
DV	Observed concentrations
DVT	Deep vein thrombosis
EDTA	Ethylene diamine tetraacetic acid
EMs	Extensive metabolizers
F1	Bioavailability
FO	First order
FOCE	First order conditional estimate
FOCEI	First order conditional estimate with interaction
HAMD-17	Hamilton rating scale for depression
K _a	Absorption rate constant
IBW	Ideal body weight
ICU	Intensive care unit
IMs	Intermediate metabolizers
IIV	Inter-individual variability
IPRED	Individual predicted concentration
LBW	Lean body weight
LMWHs	Low molecular weight heparins

MI	Multiple imputation
MMSE	Mini-mental state exam
MTLD-2	Maintenance therapies in late-life depression
OBJ	Objective function
OFV	Objective function value
PCR	Polymerase chain reaction
PE	Pulmonary embolus
PD	Pharmacodynamics
PI	Predicted interval
PK	Pharmacokinetics
PMs	Poor metabolizers
PRED	Population predicted concentrations
SC	Subcutaneous
SSRIs	Selective serotonin reuptake inhibitors
TS	Two-stage approach
UFH	Unfractionated heparin
UMs	Ultra-rapid metabolizers
V	Volume of distribution
V_2 & V_c	Volume of distribution of central compartment
V_3 & V_p	Volume of distribution of peripheral compartment
V_m	Maximal velocity
WRES	Weighted residual error
WT	Weight

APPENDIX B

**APPENDIX B.1 PREDICTION OF CREATININE CLEARANCE FROM SERUM
CREATININE**

1: Cockcroft & Gault equation to predict creatinine clearance from stable serum creatinine

In male

$$CL_{Cr}(mL/min) = \frac{(140 - age) \times IBW}{72 \times Scr(mg/dL)}$$

In female

$$CL_{Cr}(mL/min) = \frac{(140 - age) \times IBW}{72 \times Scr(mg/dL)} \times 0.85$$

Ideal Body Weight (IBW)

Male: IBW (kg) = 50 + (2.3 × Height in inches over 5 feet)

Female: IBW (kg) = 45.5 + (2.3 × Height in inches over 5 feet)

2: Brater equation to predict creatinine clearance from unstable serum creatinine

In male

$$CL_{Cr}(mL/min) = \frac{[293 - 2.03 \times age][1.035 - 0.0168 \times (Scr_1 + Scr_2)] + \frac{49 \times (Scr_1 - Scr_2)}{time(day)}}{70 \times (Scr_1 + Scr_2)} \times wt$$

In female

$$CL_{Cr}(mL/min) = \frac{[293 - 2.03 \times age][1.035 - 0.0168 \times (Scr_1 + Scr_2)] + \frac{49 \times (Scr_1 - Scr_2)}{time(day)}}{70 \times (Scr_1 + Scr_2)} \times wt \times 0.86$$

Scr_1 and Scr_2 are the 1st and 2nd measured values of serum creatinine (mg/dL) respectively; time is the interval between Scr_1 and Scr_2 measurements in days, wt is the weight in kilogram unit.

* Unstable Scr defined as the two separate determinations of serum creatinine obtained at least 12 hours apart have values within 0.2 mg/dL.

**APPENDIX B.2 RELEVANT PART OF THE NONMEM CODE FOR ENOXAPARIN
COVARIATE MODEL**

\$SUBROUTINES ADVAN4 TRANS4

\$PK

BMI=WT/(HT*HT/10000) ;Body mass index
BSA=SQRT(HT*WT/3600) ;Body surface area
IBW=45.5+0.89*(HT-152.4)+4.5*SEX ;Ideal body weight

IF (SEX.EQ.1) THEN

LBW=1.1*WT-0.0128*BMI*WT ;Lean body weight

ELSE

LBW=1.07*WT-0.0148*BMI*WT

END IF

ABW=IBW+0.4*(WT-IBW) ;Adjusted body weight

PIBW=WT*100/IBW ;Percentage IBW

IF (SEX.EQ.1) THEN

PNWT=1.57*WT-0.0183*BMI*WT-10.5 ;Predicted normal weight

ELSE

PNWT=1.75*WT-0.0242*BMI*WT-12.6

END IF

IF (GFR.EQ.0) THEN

TVCL=THETA(7)

ELSE

TVCL=THETA(1)+(GFR/4.8)*THETA(6)

END IF

```
CL=TVCL*EXP(ETA(1))
TVV2=THETA(2)*(WT/70)
V2=TVV2*EXP(ETA(2))
TVV3=THETA(3)
V3=TVV3
TVQ=THETA(4)
Q=TVQ
KA=THETA(5)
K = CL/V2
F1=THETA(8)
S2=V2
```

\$ERROR

```
IPRED=F
IRES =F-DV
IF (LO.EQ.0) THEN
  Y = F*(1+ERR(1))+ERR(2)
ELSE
  Y = F*(1+ERR(3))
END IF
```

\$THETA

(0.229, FIXED)	; Non-renal clearance component
(0, 30)	; Volume of central compartment distribution
(0.1, 1.5)	; Volume of peripheral compartment distribution
(0.1, 1.5, 200)	; Inter-compartmental clearance
(0, 0.5)	; KA
(0, 0.5)	; Renal clearance component

(0,1,5) ;CL for missing situation
(0,0.8,1) ;F1

\$OMEGA

0.2 ; between subject variability of CL

0.2 ; between subject variability of V2

\$SIGMA

0.1 ; initial estimate of proportional residual error for ward patients

130 ; initial estimate of additive residual error for ward patients

0.1 ; initial estimate of proportional residual error for ICU patients

\$ESTIMATION MAXEVAL=5000 PRINT=10 METHOD=1 INTERACTION
SIGDIG=3 POSTHOC

\$COV

**APPENDIX B.3 RELEVANT PART OF THE NONMEM CODE FOR CITALOPRAM
COVARIATE MODEL (1-COMPARTMENT MODEL USING FOCEI METHOD)**

\$SUB ADVAN2 TRANS2

\$PK

$$TVCL1 = THETA(1)*(WT/80)**THETA(5)$$

$$TVCL = TVCL1*(AGE/60)**THETA(4)$$

$$CL = TVCL*EXP(ETA(1))$$

$$TVV = THETA(2)$$

$$V = TVV*EXP(ETA(2))$$

$$TVKA = THETA(3)$$

$$KA = TVKA*EXP(ETA(3))$$

$$S2 = V$$

$$K = CL/V$$

\$THETA

(0,10) ;CL

(0,2000);V

(0,0.5);KA

(,-0.5,) ;AGE

(,2,) ;WT

\$ERROR

IPRED=F

IRES =F-DV

Y = F*(1+ERR(1))+ERR(2)

\$OMEGA

0.1

0.1

1 FIXED

\$SIGMA

0.1

3

\$EST METH=1 INTERACTION MAX=9999 PRINT=5 NOABORT POSTHOC SLOW
MSFO=c1aw4.msf

\$COV

APPENDIX B.4 CYP2D6 GENOTYPING PROTOCOL

The CYP2D6 genotyping study has been briefly presented in the submitted manuscript in chapter 4, including specific primers, restriction enzyme, restriction pattern and agarose gel. The other detail method information and related results in the CYP2D6 genotyping study, which wasn't included in the manuscript, are shown below:

1: DNA Extraction

After separating lymphocytes from whole blood using BD Vacutainer CPT™ tubes, DNA is extracted using the standard procedure.^{138, 139} In brief, thawed lymphocyte pellets are resuspended in cell lysis buffer (0.01 M Tris-HCl pH 7.4, 0.32 M sucrose, 5 mM MgCl₂, 1% Triton X100). The tubes are centrifuged at 3300 g for 20 min at 4°C. The supernatant is discarded and each pellet of cell nuclei is resuspended in nuclei lysis buffer (0.4 M Tris-HCl pH 8.0, 0.06 M EDTA, 400 mM NaCl). Next, the cell lysates are digested overnight at 37°C by adding 200 µl of 10% sodium dodecyl sulfate (SDS) and 500 µl of proteinase-K solution (2 mg protease K in 1 % SDS and 2 mM EDTA). Then 1 ml of 6 M NaCl is added and sample is centrifuged at 2500 g for 15 min. Supernatant containing DNA is transferred to a polypropylene tube. DNA is ethanol precipitated and resuspended in 200 – 1000 µl Tris-EDTA buffer (pH 8.0). Genomic DNA fractions are stored at -20°C.

2: CYP2D6 alleles' Amplification

A polymerase chain reaction (PCR)-based allele-specific analysis described before,¹⁴⁰ will be used. To determine whether individuals are carrying duplicated *CYP2D6* genes, long PCR will be used to amplify a fragment spanning the potential crossing-over sites.^{140, 141}

Amplification reactions are performed on a MJ PCR System in 0.2 ml thin-walled tubes. The 25 µl PCR mix for CYP2D6 allele's amplification (CYP2D6 *4, *5, *10, *17, and CYP2D6*XN) is shown in Table 4.1.a. The PCR conditions for each allele's amplification are provided below:

Table B4.1: PCR mix (25µl) for CYP2D6 allele amplifications

Long PCR	2D6 (5kb)	Nest PCR	*2, *4, *10	*17	Long PCR	*5 and *XN
	1 x (µl)		1 x (µl)			1 x (µl)
dNTP	4	dNTP	4	4	dNTP	4
5XBuffer	5	10XBuffer	2.5	2.5	5XBuffer	5
50 mM Mg ²⁺	-	50 mM Mg ²⁺	0.5	0.375	50 mM Mg ²⁺	-
5M GC	2.5	5M GC	-	-	5M GC	2.5
H ₂ O	6	H ₂ O	13.8	13.9	H ₂ O	5.5
DNA	4	DNA template (long PCR product)	1	1	1 DNA template (MTLD-2 sample)	4
GC rich Taq	0.5	Invitro Taq	0.2	0.2	GC rich Taq	1
Primer F	1.5	Primer F	1.5	1.5	Primer F	1.5
Primer R	1.5	Primer R	1.5	1.5	Primer R	1.5

CYP2D6 (5kb), CYP2D6*XN (gene duplication) and CYP2D6*5 (deletion) allele

Amplification reactions are performed on a MJ PCR System. The PCR conditions include initial denaturation at 95 °C for 4 min, followed by 39 PCR cycles of denaturation at 94.8 °C for 30 s, annealing at 54.5 °C for 30 s, synthesis at 72 °C for 4.5 min. The program ends with a final extension at 72°C for 5 min.

CYP2D6*2 (C2938T), *4 (G1934A), *10 (G4268C) and *10 (C188T) allele

***2 and *4:** Amplification reactions are performed on a MJ PCR System. The PCR conditions include initial denaturation at 95 °C for 3 min, followed by 39 PCR cycles of denaturation at 94.8 °C for 30 s, annealing at 56 °C for 30 s, synthesis at 72 °C for 30 s. The program ends with a final extension at 72°C for 1 min.

***10 (G4268C):** Amplification reactions are performed on a MJ PCR System. The PCR conditions include initial denaturation at 95 °C for 3 min, followed by 38 PCR cycles of denaturation at 94.8 °C for 30 s, annealing at 58 °C for 30 s, synthesis at 72 °C for 30 s. The program ends with a final extension at 72°C for 1 min.

***10 (C188T):** Amplification reactions are performed on a MJ PCR System. The PCR conditions include initial denaturation at 95 °C for 3 min, followed by 38 PCR cycles of denaturation at 94.8 °C for 30 s, annealing at 58.5 °C for 30 s, synthesis at 72 °C for 30 s. The program ends with a final extension at 72°C for 1 min.

CYP2D6*17 allele specific PCR

***17:** Amplification reactions are performed on a MJ PCR System. The PCR conditions include initial denaturation at 95 °C for 3 min, followed by 27 PCR cycles of denaturation at 94.8 °C for 30 s, annealing at 57.5 °C (wt) or 58 °C (mut) for 30 s, synthesis at 72 °C for 30 s. The program ends with a final extension at 72°C for 1 min.

3: Nest PCR product digestion

The digestion buffer for each CYP2D6 allele is presented in Table 4.1.b. Mixing 7 µl Digestion buffer with 15 µl DNA products and followed by overnight digestion. Then load on gel after mixing with 4 µl orange dye.

Table B4.2. Digestion Buffers for CYP2D6 alleles

CYP2D6 Allele (Mutation)	*2 (C2938T)	*4 (G1934A)	*10 (C188T)	*10 (G4268C)
Restriction enzyme Name	<i>cfo I</i> or <i>Hha I</i>	<i>Bst NI</i>	<i>HphI</i>	<i>BstEII</i>
Volume (µl)	0.225	0.23	0.6	0.23
Activity (KU/ml)	20	10	5	10
Temperature (°C)	37	60	37	60
Buffer	2.25 (Buf4)	2.25 (Buf2)	2.25 (NEB4)	2.25
BSA	0.23	0.23	-	-
H ₂ O	5.02	4.8	4.62	5.02

**APPENDIX B.5 RELEVANT PART OF THE NONMEM CODE FOR PAROXETINE
COVARIATE MODEL**

```

$SUBROUTINES ADVAN9 TOL=5
$MODEL COMP=(GUT, DEFDOS), COMP=(CENTRAL, DEFOBS),
COMP=(PERIPH)

$PK
IF (GENO.EQ.0) TVVM=THETA(1)      ;Vm for subjects with missing 2D6 genotype
information
IF (GENO.EQ.1) TVVM=THETA(7)      ;Vm for PMs
IF (GENO.EQ.2) TVVM=THETA(8)      ;Vm for IMs
IF (GENO.EQ.3) TVVM=THETA(9)      ;Vm for EMs
IF (GENO.EQ.4) TVVM=THETA(10)     ;Vm for UMs

TVVM1=TVVM*(WT/75)**THETA(11)
VM=TVVM1*EXP(ETA(1))
KM=THETA(2)*EXP(ETA(2))
TVV21=THETA(3)
TVV2=TVV21+(1-SEX)*THETA(12)
V2=TVV2*EXP(ETA(3))
V3=THETA(4)
Q=THETA(5)
S2=V2
KA=THETA(6)

$DES
CON=A(2)/V2
CL=VM/(KM+CON)
DADT(1)=-KA*A(1)
DADT(2)=KA*A(1)-A(2)*CL/V2-A(2)*Q/V2+A(3)*Q/V3

```

$$DADT(3)=-A(3)*Q/V3+A(2)*Q/V2$$

\$ERROR

$$IPRED=F$$

$$IRES=DV-IPRED$$

$$Y=F*(1+ERR(1)) + ERR(2)$$

\$THETA

$$(0,200,3000);VM$$

$$(0,20);KM$$

$$(20,200);V2$$

$$(20,200);V3$$

$$(0,20);Q$$

$$(0,10);KA$$

$$(0,10);PM$$

$$(0,10);IM$$

$$(0,10);EM$$

$$(0,10);UM$$

$$(0,0.5);WT$$

$$(.10,);SEX$$

\$OMEGA

0.1 ; between subject variability of Vm

0.1 ; between subject variability of Km

0.6 ; between subject variability of V2

\$SIGMA

0.1 ; initial estimate of proportional residual error

10 ; initial estimate of additive residual error

\$COV

\$EST SIG=3 MAX=9999 PRINT=10 NOABORT METHOD=0 POSTHOC

APPENDIX B.6 RELEVANT S SCRIPT FOR ADHERENCE RATE CALCULATION

Below is the S code for weekly adherence rate pattern calculation

```
# Total subjects
subj.vec <- unique(df11$ID)
nsubj <- length(subj.vec)

# Calculate weekly adherence rate pattern (7 days)
rate <- 7
for (isubj in 1:nsubj){
# isubj <- 1
  ###Extract data for isubj##
  TF.subj<-df11$ID==subj.vec[isubj]
  tmp.df<-df11[TF.subj,]
  # Total rows for the isubj
  nEV <-nrow(tmp.df)

# Temp variables
j <- x <- 1
for (iEV in j:nEV){
  # Record for each PK sample (MDV=0)
  if(any(tmp.df$MDV[iEV]==0)){
    # Calculate total rows within one week before PK sample (Clinical visit)
    nDV.tmp <- iEV-x
    # T.dose is used to calculate total dose within each time frame
    T.dose <- 0
    # Select the time frame before each PK sample (one week)
    Time.df <- tmp.df$Time1.tmp[iEV]-rate
    for (iDV.tmp in 1:nDV.tmp){
      TF.ad1 <- tmp.df$Time1.tmp[iEV-iDV.tmp]>Time.df
      if(any(TF.ad1)){
        # Total MEMS opening: could be more than 7
        T.dose <- tmp.df$MDV[iEV-iDV.tmp]+T.dose
      }
    }
    # Calculate weekly adherence rate pattern
    tmp.df$ADH7[iEV] <- T.dose/rate #
    # Change to the next searching point (next PK sampling)
    j <- x <- iEV+1
  }
}
df11[TF.subj, ]<- tmp.df
}
```

BIBLIOGRAPHY

1. Wagner JG: **History of pharmacokinetics.** *Pharmacol Ther* 1981, **12**(3):537-562.
2. Gibaldi M, Levy G: **Pharmacokinetics in clinical practice. 2. Applications.** *Jama* 1976, **235**(18):1987-1992.
3. Gibaldi M, Levy G: **Pharmacokinetics in clinical practice. I. Concepts.** *Jama* 1976, **235**(17):1864-1867.
4. Ross E, HKenakin T: **Goodman & Gilman's The Pharmacological Basis Of Therapeutics: Pharmacodynamics: Mechanisms of drug action and relationship between drug concentrations and effect**, 10th edn. New York: McGraw-Hill; 2001.
5. Bruno R, Baille P, Retout S, Vivier N, Veyrat-Follet C, Sanderink GJ, Becker R, Antman EM: **Population pharmacokinetics and pharmacodynamics of enoxaparin in unstable angina and non-ST-segment elevation myocardial infarction.** *Br J Clin Pharmacol* 2003, **56**(4):407-414.
6. Green B, Duffull SB: **Development of a dosing strategy for enoxaparin in obese patients.** *Br J Clin Pharmacol* 2003, **56**(1):96-103.
7. Green B, Greenwood M, Saltissi D, Westhuyzen J, Kluver L, Rowell J, Atherton J: **Dosing strategy for enoxaparin in patients with renal impairment presenting with acute coronary syndromes.** *Br J Clin Pharmacol* 2005, **59**(3):281-290.
8. Cullberg M, Eriksson UG, Larsson M, Karlsson MO: **Population modelling of the effect of inogatran, at thrombin inhibitor, on ex vivo coagulation time (APTT) in healthy subjects and patients with coronary artery disease.** *Br J Clin Pharmacol* 2001, **51**(1):71-79.
9. Callies S, de Alwis DP, Harris A, Vasey P, Beijnen JH, Schellens JH, Burgess M, Aarons L: **A population pharmacokinetic model for paclitaxel in the presence of a novel P-gp modulator, Zosuquidar Trihydrochloride (LY335979).** *Br J Clin Pharmacol* 2003, **56**(1):46-56.
10. Bies RR, Feng Y, Lotrich FE, Kirshner MA, Roose S, Kupfer DJ, Pollock BG: **Utility of sparse concentration sampling for citalopram in elderly clinical trial subjects.** *J Clin Pharmacol* 2004, **44**(12):1352-1359.
11. Troconiz IF, Naukkarinen TH, Ruottinen HM, Rinne UK, Gordin A, Karlsson MO: **Population pharmacodynamic modeling of levodopa in patients with Parkinson's disease receiving entacapone.** *Clin Pharmacol Ther* 1998, **64**(1):106-116.
12. Shi J, Pfister M, Jenkins SG, Chapel S, Barrett JS, Port RE, Howard D: **Pharmacodynamic analysis of the microbiological efficacy of telithromycin in patients with community-acquired pneumonia.** *Clin Pharmacokinet* 2005, **44**(3):317-329.

13. Sheiner LB, Beal SL: **Evaluation of methods for estimating population pharmacokinetics parameters. I. Michaelis-Menten model: routine clinical pharmacokinetic data.** *J Pharmacokinet Biopharm* 1980, **8**(6):553-571.
14. Sheiner BL, Beal SL: **Evaluation of methods for estimating population pharmacokinetic parameters. II. Biexponential model and experimental pharmacokinetic data.** *J Pharmacokinet Biopharm* 1981, **9**(5):635-651.
15. Sheiner LB, Beal SL: **Evaluation of methods for estimating population pharmacokinetic parameters. III. Monoexponential model: routine clinical pharmacokinetic data.** *J Pharmacokinet Biopharm* 1983, **11**(3):303-319.
16. Gisleskog PO, Karlsson MO, Beal SL: **Use of prior information to stabilize a population data analysis.** *J Pharmacokinet Pharmacodyn* 2002, **29**(5-6):473-505.
17. Lu J, Gries JM, Verotta D, Sheiner LB: **Selecting reliable pharmacokinetic data for explanatory analyses of clinical trials in the presence of possible noncompliance.** *J Pharmacokinet Pharmacodyn* 2001, **28**(4):343-362.
18. Vrijens B, Goetghebeur E: **The impact of compliance in pharmacokinetic studies.** *Stat Methods Med Res* 1999, **8**(3):247-262.
19. Vrijens B, Goetghebeur E: **Comparing compliance patterns between randomized treatments.** *Control Clin Trials* 1997, **18**(3):187-203.
20. Girard P, Sheiner LB, Kastrissios H, Blaschke TF: **Do we need full compliance data for population pharmacokinetic analysis?** *J Pharmacokinet Biopharm* 1996, **24**(3):265-282.
21. Girard P, Blaschke TF, Kastrissios H, Sheiner LB: **A Markov mixed effect regression model for drug compliance.** *Stat Med* 1998, **17**(20):2313-2333.
22. Mu S, Ludden TM: **Estimation of population pharmacokinetic parameters in the presence of non-compliance.** *J Pharmacokinet Pharmacodyn* 2003, **30**(1):53-81.
23. Bies RR, Gastonguay MR, Coley KC, Kroboth PD, Pollock BG: **Evaluating the consistency of pharmacotherapy exposure by use of state-of-the-art techniques.** *Am J Geriatr Psychiatry* 2002, **10**(6):696-705.
24. Cramer JA: **A systematic review of adherence with medications for diabetes.** *Diabetes Care* 2004, **27**(5):1218-1224.
25. Waeber B, Leonetti G, Kolloch R, McInnes GT: **Compliance with aspirin or placebo in the Hypertension Optimal Treatment (HOT) study.** *J Hypertens* 1999, **17**(7):1041-1045.
26. Wahl C, Gregoire JP, Teo K, Beaulieu M, Labelle S, Leduc B, Cochrane B, Lapointe L, Montague T: **Concordance, compliance and adherence in healthcare: closing gaps and improving outcomes.** *Healthc Q* 2005, **8**(1):65-70.
27. Cleemput I, Kesteloot K, DeGeest S: **A review of the literature on the economics of noncompliance. Room for methodological improvement.** *Health Policy* 2002, **59**(1):65-94.
28. Urquhart J, Bernard V: **New findings about patient adherence to prescribed drug dosing regimens: an introduction to pharmionics.** *The European Journal of Hospital Pharmacy Science* 2005, **11**(5):103-106.
29. Paterson DL, Swindells S, Mohr J, Brester M, Vergis EN, Squier C, Wagener MM, Singh N: **Adherence to protease inhibitor therapy and outcomes in patients with HIV infection.** *Ann Intern Med* 2000, **133**(1):21-30.

30. Frank E, Perel JM, Mallinger AG, Thase ME, Kupfer DJ: **Relationship of pharmacologic compliance to long-term prophylaxis in recurrent depression.** *Psychopharmacol Bull* 1992, **28**(3):231-235.
31. Cramer JA, Glassman M, Rienzi V: **The relationship between poor medication compliance and seizures.** *Epilepsy Behav* 2002, **3**(4):338-342.
32. Brundage RC, Yong FH, Fenton T, Spector SA, Starr SE, Fletcher CV: **Intrapatient variability of efavirenz concentrations as a predictor of virologic response to antiretroviral therapy.** *Antimicrob Agents Chemother* 2004, **48**(3):979-984.
33. Thompson C, Peveler RC, Stephenson D, McKendrick J: **Compliance with antidepressant medication in the treatment of major depressive disorder in primary care: a randomized comparison of fluoxetine and a tricyclic antidepressant.** *Am J Psychiatry* 2000, **157**(3):338-343.
34. Kruse W, Weber E: **Dynamics of drug regimen compliance--its assessment by microprocessor-based monitoring.** *Eur J Clin Pharmacol* 1990, **38**(6):561-565.
35. Altamura AC, Mauri M: **Plasma concentrations, information and therapy adherence during long-term treatment with antidepressants.** *Br J Clin Pharmacol* 1985, **20**(6):714-716.
36. Aarons L: **Population pharmacokinetics: theory and practice.** *Br J Clin Pharmacol* 1991, **32**(6):669-670.
37. FDA: **Center for Drug Evaluation and Research: Guidance for industry: Population pharmacokinetics.** In. Rockville, MD: Food and Drug Administration; 1999.
38. Beal SL, Sheiner LB: **Estimating population kinetics.** *Crit Rev Biomed Eng* 1982, **8**(3):195-222.
39. Grasela TH, Jr., Antal EJ, Ereshefsky L, Wells BG, Evans RL, Smith RB: **An evaluation of population pharmacokinetics in therapeutic trials. Part II. Detection of a drug-drug interaction.** *Clin Pharmacol Ther* 1987, **42**(4):433-441.
40. Sheiner LB, Rosenberg B, Marathe VV: **Estimation of population characteristics of pharmacokinetic parameters from routine clinical data.** *J Pharmacokinet Biopharm* 1977, **5**(5):445-479.
41. King G, Honaker J, Joseph A, Scheve. K: **Analyzing Incomplete Political Science Data.** *American Political Science Review* 2001, **95**(1):49-69.
42. Rubin D: **Multiple Imputation After 18+ Years.** *Journal of the American Statistical Association* 1996, **91**: 473-489.
43. Rubin D: **Multiple Imputation for Nonresponse in Surveys.** Wiley, NY 1987.
44. Bonate PL: **Recommended reading in population pharmacokinetic pharmacodynamics.** *Aaps J* 2005, **7**(2):E363-373.
45. Beal S, B.Sheiner L: **NONMEM User's guide version IV, part vii. Conditional estimation methods.** San Francisco, CA: University of California 1992.
46. Racine-Poon A, Wakefield J: **Statistical methods for population pharmacokinetic modelling.** *Stat Methods Med Res* 1998, **7**(1):63-84.
47. Akaike H: **A new look at the statistical model identification.** *IEEE Trans Automat Control* 1974, **AC-19**:716-723.
48. Parke J, Holford NH, Charles BG: **A procedure for generating bootstrap samples for the validation of nonlinear mixed-effects population models.** *Comput Methods Programs Biomed* 1999, **59**(1):19-29.

49. Gelman A, Meng X-L, Stern H: **POSTERIOR PREDICTIVE ASSESSMENT OF MODEL FITNESS VIA REALIZED DISCREPANCIES**. *Statistica Sinica* 1996, **6**:733-807.
50. Pfister M, Martin NE, Haskell LP, Barrett JS: **Optimizing dose selection with modeling and simulation: application to the vasopeptidase inhibitor M100240**. *J Clin Pharmacol* 2004, **44**(6):621-631.
51. Holford NH, Kimko HC, Monteleone JP, Peck CC: **Simulation of clinical trials**. *Annu Rev Pharmacol Toxicol* 2000, **40**:209-234.
52. Kimko HC, Duffull SB: **Simulation for Designing Clinical Trials: A Pharmacokinetic-pharmacodynamic Modeling Perspective (Drugs & the Pharmaceutical Sciences S.)**. 2002.
53. Kimko HC, Reece SS, Holford NH, Peck CC: **Prediction of the outcome of a phase 3 clinical trial of an antischizophrenic agent (quetiapine fumarate) by simulation with a population pharmacokinetic and pharmacodynamic model**. *Clin Pharmacol Ther* 2000, **68**(5):568-577.
54. Hull RD, Raskob GE, Brant RF, Pineo GF, Elliott G, Stein PD, Gottschalk A, Valentine KA, Mah AF: **Low-molecular-weight heparin vs heparin in the treatment of patients with pulmonary embolism**. American-Canadian Thrombosis Study Group. *Arch Intern Med* 2000, **160**(2):229-236.
55. Mismetti P, Laporte-Simitsidis S, Tardy B, Cucherat M, Buchmuller A, Juillard-Delsart D, Decousus H: **Prevention of venous thromboembolism in internal medicine with unfractionated or low-molecular-weight heparins: a meta-analysis of randomised clinical trials**. *Thromb Haemost* 2000, **83**(1):14-19.
56. Hull RD, Raskob GE, Pineo GF, Green D, Trowbridge AA, Elliott CG, Lerner RG, Hall J, Sparling T, Brettell HR *et al*: **Subcutaneous low-molecular-weight heparin compared with continuous intravenous heparin in the treatment of proximal-vein thrombosis**. *N Engl J Med* 1992, **326**(15):975-982.
57. Gould MK, Dembitzer AD, Sanders GD, Garber AM: **Low-molecular-weight heparins compared with unfractionated heparin for treatment of acute deep venous thrombosis. A cost-effectiveness analysis**. *Ann Intern Med* 1999, **130**(10):789-799.
58. Antman EM, McCabe CH, Gurfinkel EP, Turpie AG, Bernink PJ, Salein D, Bayes De Luna A, Fox K, Lablanche JM, Radley D *et al*: **Enoxaparin prevents death and cardiac ischemic events in unstable angina/non-Q-wave myocardial infarction. Results of the thrombolysis in myocardial infarction (TIMI) 11B trial**. *Circulation* 1999, **100**(15):1593-1601.
59. Cohen M, Demers C, Gurfinkel EP, Turpie AG, Fromell GJ, Goodman S, Langer A, Califf RM, Fox KA, Premmureur J *et al*: **A comparison of low-molecular-weight heparin with unfractionated heparin for unstable coronary artery disease. Efficacy and Safety of Subcutaneous Enoxaparin in Non-Q-Wave Coronary Events Study Group**. *N Engl J Med* 1997, **337**(7):447-452.
60. Kaul S, Shah PK: **Low molecular weight heparin in acute coronary syndrome: evidence for superior or equivalent efficacy compared with unfractionated heparin?** *J Am Coll Cardiol* 2000, **35**(7):1699-1712.
61. Bendetowicz AV, Beguin S, Caplain H, Hemker HC: **Pharmacokinetics and pharmacodynamics of a low molecular weight heparin (enoxaparin) after**

- subcutaneous injection, comparison with unfractionated heparin--a three way cross over study in human volunteers. *Thromb Haemost* 1994, **71**(3):305-313.
62. Greer IA: **Prevention of venous thromboembolism in pregnancy.** *Best Pract Res Clin Haematol* 2003, **16**(2):261-278.
 63. Wong G, Giugliano R, Antman E: **Use of low-molecular-weight heparins in the management of acute coronary artery syndromes and percutaneous coronary intervention.** *JAMA* 2003, **289**:331-342.
 64. Bergmann JF, Mouly S: **Thromboprophylaxis in medical patients: focus on France.** *Semin Thromb Hemost* 2002, **28 Suppl 3**:51-55.
 65. Sanderink GJ, Le Liboux A, Jariwala N, Harding N, Ozoux ML, Shukla U, Montay G, Boutouyrie B, Miro A: **The pharmacokinetics and pharmacodynamics of enoxaparin in obese volunteers.** *Clin Pharmacol Ther* 2002, **72**(3):308-318.
 66. Frydman A: **Low-molecular-weight heparins: an overview of their pharmacodynamics, pharmacokinetics and metabolism in humans.** *Haemostasis* 1996, **26 Suppl 2**:24-38.
 67. Gerlach AT, Pickworth KK, Seth SK, Tanna SB, Barnes JF: **Enoxaparin and bleeding complications: a review in patients with and without renal insufficiency.** *Pharmacotherapy* 2000, **20**(7):771-775.
 68. Hulot JS, Vantelon C, Urien S, Bouzamondo A, Mahe II, Ankri A, Montalescot G, Lechat P: **Effect of Renal Function on the Pharmacokinetics of Enoxaparin and Consequences on Dose Adjustment.** *Ther Drug Monit* 2004, **26**(3):305-310.
 69. Ma JM, Jackevicius CA, Yeo E: **Anti-Xa Monitoring of Enoxaparin for Acute Coronary Syndromes in Patients with Renal Disease (October).** *Ann Pharmacother* 2004.
 70. Brophy D, Wazny L, Gehr T, Cornstock T, Venitz J: **The pharmacokinetics of subcutaneous enoxaparin in end-stage renal disease.** *Pharmacotherapy* 2001, **21**(2):169-174.
 71. Power B, Forbes A, Heerden P, Ilett K: **Pharmacokinetics of drugs used in critically III adults.** *Clin Pharmacokinet* 1998, **34**:25-56.
 72. Cook D, Attia J, Weaver B, McDonald E, Meade M, Crowther M: **Venous thromboembolic disease: an observational study in medical-surgical intensive care unit patients.** *J Crit Care* 2000, **15**(4):127-132.
 73. Priglinger U, Delle Karth G, Geppert A, Joukhadar C, Graf S, Berger R, Hulsmann M, Spitzauer S, Pabinger I, Heinz G: **Prophylactic anticoagulation with enoxaparin: Is the subcutaneous route appropriate in the critically ill?** *Crit Care Med* 2003, **31**(5):1405-1409.
 74. Haas CE, Nelsen JL, Raghavendran K, Mihalko W, Beres J, Ma Q, Forrest A: **Pharmacokinetics and pharmacodynamics of enoxaparin in multiple trauma patients.** *J Trauma* 2005, **59**(6):1336-1343; discussion 1343-1334.
 75. Kane-Gill SL, Feng Y, Bobek MB, Bies RR, Pruchnicki MC, Dasta JF: **Administration of enoxaparin by continuous infusion in a naturalistic setting: analysis of renal function and safety.** *J Clin Pharm Ther* 2005, **30**(3):207-213.
 76. Laposata M, Green D, Van Cott EM, Barrowcliffe TW, Goodnight SH, Sosolik RC: **College of American Pathologists Conference XXXI on laboratory monitoring of anticoagulant therapy: the clinical use and laboratory monitoring of low-molecular-**

- weight heparin, danaparoid, hirudin and related compounds, and argatroban.** *Arch Pathol Lab Med* 1998, **122**(9):799-807.
77. Brater D, Chennavasin P: **Dosing regimens: determination of creatinine clearance as an index of renal function.** In: **Drug use in renal disease.** Boston: Adis Health Science Press; 1983.
 78. Cockcroft DW, Gault MH: **Prediction of creatinine clearance from serum creatinine.** *Nephron* 1976, **16**(1):31-41.
 79. Beal B, Sheiner L: **NONMEM user's guide, Part I.** San Francisco: University of California at San Francisco. 1992.
 80. Green B, Duffull SB: **What is the best size descriptor to use for pharmacokinetic studies in the obese?** *British Journal of Clinical Pharmacology* 2004, **58**(2):119-133.
 81. Gobburu JV, Lawrence J: **Application of resampling techniques to estimate exact significance levels for covariate selection during nonlinear mixed effects model building: some inferences.** *Pharm Res* 2002, **19**(1):92-98.
 82. **WFN Randomization Test.** <http://wfnsourcesforgenet/wfnrthtm> 2003.
 83. Ette EI, Ludden TM: **Population pharmacokinetic modeling: the importance of informative graphics.** *Pharm Res* 1995, **12**(12):1845-1855.
 84. Collet JP, Montalescot G, Choussat R, Lison L, Ankri A: **Enoxaparin in unstable angina patients with renal failure.** *Int J Cardiol* 2001, **80**(1):81-82.
 85. Montalescot G, Polle V, Collet JP, Leprince P, Bellanger A, Gandjbakhch I, Thomas D: **Low molecular weight heparin after mechanical heart valve replacement.** *Circulation* 2000, **101**(10):1083-1086.
 86. Collet JP, Montalescot G, Lison L, Choussat R, Ankri A, Drobinski G, Sotirov I, Thomas D: **Percutaneous coronary intervention after subcutaneous enoxaparin pretreatment in patients with unstable angina pectoris.** *Circulation* 2001, **103**(5):658-663.
 87. Boneu B: **Low molecular weight heparin therapy: is monitoring needed?** *Thromb Haemost* 1994, **72**(3):330-334.
 88. Abbate R, Gori AM, Farsi A, Attanasio M, Pepe G: **Monitoring of low-molecular-weight heparins in cardiovascular disease.** *Am J Cardiol* 1998, **82**(5B):33L-36L.
 89. FDA: **Center for Drug Evaluation and Research: Pharmacokinetics in Patients with Impaired Renal Function - Study Design, Data Analysis, and Impact on Dosing and Labeling.** In. Rockville, MD: Food and Drug Administration; 1998.
 90. K/DOQI: **Clinical practice guidelines for chronic kidney disease. evaluation, classification, and stratification.** **Kindney Disease Outcome Quality Initiative.** *Am J Kidney Dis* 2002, **39** (2 Suppl 1):S1-246.
 91. Feng Y, Bies R, Bobek M, Kane S: **Population pharmacokinetics analysis of patients receiving enoxaparin by continuous intravenous infusion.** *Clinical Pharmacology & Therapeutics* 2004, **75**(2):30.
 92. Bodenham A, Shelly MP, Park GR: **The altered pharmacokinetics and pharmacodynamics of drugs commonly used in critically ill patients.** *Clin Pharmacokinet* 1988, **14**(6):347-373.
 93. Huet Y, Gouault-Heilmann M: **Low molecular weight heparin fraction PK 10169: a new therapeutic means for anticoagulant therapy?** *Haemostasis* 1986, **16**(2):165-172.
 94. Huet Y, Gouault-Heilmann M, Contant G, Brun-Buisson C: **Treatment of acute pulmonary embolism by a low molecular weight heparin fraction. A preliminary study.** *Intensive Care Med* 1987, **13**(2):126-130.

95. Pollock BG: **Citalopram: A comprehensive review.** *Expert Opinion in Pharmacotherapy* 2001, **2**(4):681-698.
96. Sheiner LB, Beal SL: **Evaluation of methods for estimating population pharmacokinetic parameters. III. Monoexponential model: routine clinical pharmacokinetic data.** *J Pharmacokinet Biopharm* 1983, **11**(3):303-319.
97. Mandema J, Verotta D, Sheiner LB: **Building population pharmacokinetic--pharmacodynamic models. I. Models for covariate effects.** *J Pharmacokinet Biopharm* 1992, **20**(5):511-528.
98. Fredericson Overo K, Toft B, Christophersen L, Gylding-Sabroe J: **Kinetics of citalopram in elderly patients.** *Psychopharmacology (Berl)* 1985, **86**:253-257.
99. Gutierrez M, Abramowitz W: **Steady-state pharmacokinetics of citalopram in young and elderly subjects.** *Pharmacotherapy* 2000, **20**(12):1441-1447.
100. Leinonen E, Lepola U, Koponen H, Kinnunen I: **The effect of age and concomitant treatment with other psychoactive drugs on serum concentrations of citalopram measured with a nonenantioselective method.** *Ther Drug Monit* 1996, **18**(2):111-117.
101. Reis M, Lundmark J, Bengtsson F: **Therapeutic drug monitoring of racemic citalopram: A 5-year experience in Sweden.** *Ther Drug Monit* 2003, **25**:183-191.
102. Kupfer DJ, Chengappa KN, Gelenberg AJ, Hirschfeld RM, Goldberg JF, Sachs GS, Grochocinski VJ, Houck PR, Kolar AB: **Citalopram as adjunctive therapy in bipolar depression.** *J Clin Psych* 2001, **62**(12):985-990.
103. Roose SP, Sackeim HA, Krishnan KR, Pollock BG, Alexopoulos G, Lavretsky H, Katz IR, Hakkarainen H: **Antidepressant pharmacotherapy in the treatment of depression in the very old: a randomized, placebo-controlled trial.** *Am J Psychiatry* 2004, **161**(11):2050-2059.
104. Roose S, Alexopoulos G, Burke W, Grossberg G, Hakkarainen H, Hassman H, Jacobsen A, Katz I, Kirby L, Krishnan R: **Treatment of depression in the "old-old": A randomized, double-blind, placebo-controlled trial of citalopram in patients at least 75 years of age.** *Fifteenth Annual Meeting of the American Association for Geriatric Psychiatry* 2002.
105. Pollock BG, Mulsant BH, Sweet RA, Burgio LD, Kirshner MA, Shuster K: **An open pilot study of citalopram for behavioral disturbances of dementia: Plasma levels and real-time observations.** *Am J Ger Psychiatr* 1997, **5**:70-78.
106. Bies RR, Gastonguay MR, Coley KC, Kroboth PD, Pollock BG: **Evaluating the consistency of pharmacotherapy exposure by use of state-of-the-art techniques.** *Am J Ger Psych* 2002, **10**:696-705.
107. Bies RR, Lotrich FE, Smith G, Muldoon M, Pollock BG: **Pharmacokinetics of citalopram after IV infusion.** *Clin Pharmacol Ther* 2003, **73**(2):P71.
108. Jonsson E, Karlsson M: **Xpose--an S-PLUS based population pharmacokinetic/pharmacodynamic model building aid for NONMEM.** *Computer Methods & Programs in Biomedicine* 1999, **58**(1):51-64.
109. West G, Brown J, Enquist B: **The fourth dimension of life: fractal geometry and allometric scaling of organisms.** *Science* 1999, **284**(5420):1677-1679.
110. West G, Brown J, Enquist B: **A general model for the origin of allometric scaling laws in biology.** *Science* 1997, **276**(5309):122-126.
111. Efron B, Tibshirani R: **An introduction to the bootstrap.** In., vol. 57. New York: Chapman and Hall; 1993: 436.

112. Fredericson Overo K, Toft B, Christophersen L, Gylding-Sabroe JP: **Kinetics of citalopram in elderly patients.** *Psychopharmacology (Berl)* 1985, **86**(3):253-257.
113. Krecic-Shepard M-E, Park K, Barnas C, Slimko J, Kerwin DR, Schwartz JB: **Race and sex influence clearance of nifedipine: Results of a population study.** *Clin Pharmacol Ther* 2000, **68**(2):130-142.
114. Kang D, Verotta D, Krecic-Shepard M-E, Modi NB, Gupta SK, Schwartz JB: **Population analysis of sustained-release verapamil in patients: Effects of sex, race and smoking.** *Clin Pharmacol Ther* 2003, **73**(1):31-40.
115. Fredericson Overo K: **Kinetics of citalopram in man: plasma levels in patients.** *Prog Neuropsychopharmacol & Biol Psychiat* 1982, **6**:311-318.
116. Milne RJ, Goa KL: **Citalopram: A review of its pharmacodynamic and pharmacokinetic properties, and therapeutic potential in depressive illness.** *Drugs* 1991, **41**(3):450-477.
117. Gillooly J, Brown JH, West GB, Savage VM, EL C: **Effects of size and temperature on metabolic rate.** *Science* 2001, **293**(5538):2248-2251.
118. Overo KF: **Preliminary studies of the kinetics of citalopram in man.** *Eur J Clin Pharmacol* 1978, **14**(1):69-73.
119. Gutierrez M, Abramowitz W: **Steady-state pharmacokinetics of citalopram in young and elderly subjects.** *Pharmacotherapy* 2000, **20**(12):1441-1447.
120. Wagstaff AJ, Cheer SM, Matheson AJ, Ormrod D, Goa KL: **Paroxetine: an update of its use in psychiatric disorders in adults.** *Drugs* 2002, **62**(4):655-703.
121. Pollock BG, Ferrell RE, Mulsant BH, Mazumdar S, Miller M, Sweet RA, Davis S, Kirshner MA, Houck PR, Stack JA *et al*: **Allelic variation in the serotonin transporter promoter affects onset of paroxetine treatment response in late-life depression.** *Neuropsychopharmacology* 2000, **23**(5):587-590.
122. Reis M, Lundmark J, Bengtsson F: **Therapeutic drug monitoring of racemic citalopram: a 5-year experience in Sweden, 1992-1997.** *Ther Drug Monit* 2003, **25**(2):183-191.
123. Feng Y, Pollock B, Roose S, Kirshner M, Lotrich F, Kupfer D, Bies R: **Mixed effects pharmacokinetic modeling of an age effect on citalopram disposition.** *AAPS PharmSci* 2003, **5**(4):Abstract M1063.
124. Kaye CM, Haddock RE, Langley PF, Mellows G, Tasker TC, Zussman BD, Greb WH: **A review of the metabolism and pharmacokinetics of paroxetine in man.** *Acta Psychiatr Scand Suppl* 1989, **350**:60-75.
125. Walters G, Reynolds CF, 3rd, Mulsant BH, Pollock BG: **Continuation and maintenance pharmacotherapy in geriatric depression: an open-trial comparison of paroxetine and nortriptyline in patients older than 70 years.** *J Clin Psychiatry* 1999, **60 Suppl 20**:21-25.
126. Meijer WE, Bouvy ML, Heerdink ER, Urquhart J, Leufkens HG: **Spontaneous lapses in dosing during chronic treatment with selective serotonin reuptake inhibitors.** *Br J Psychiatry* 2001, **179**:519-522.
127. Henry ME, Moore CM, Kaufman MJ, Michelson D, Schmidt ME, Stoddard E, Vuckevic AJ, Berreira PJ, Cohen BM, Renshaw PF: **Brain kinetics of paroxetine and fluoxetine on the third day of placebo substitution: a fluorine MRS study.** *Am J Psychiatry* 2000, **157**(9):1506-1508.

128. Findling RL, Reed MD, Myers C, O'Riordan MA, Fiala S, Branicky L, Waldorf B, Blumer JL: **Paroxetine pharmacokinetics in depressed children and adolescents.** *J Am Acad Child Adolesc Psychiatry* 1999, **38**(8):952-959.
129. Sindrup SH, Brosen K, Gram LF, Hallas J, Skjelbo E, Allen A, Allen GD, Cooper SM, Mellows G, Tasker TC *et al*: **The relationship between paroxetine and the sparteine oxidation polymorphism.** *Clin Pharmacol Ther* 1992, **51**(3):278-287.
130. Sindrup SH, Brosen K, Gram LF: **Pharmacokinetics of the selective serotonin reuptake inhibitor paroxetine: nonlinearity and relation to the sparteine oxidation polymorphism.** *Clin Pharmacol Ther* 1992, **51**(3):288-295.
131. Sawamura K, Suzuki Y, Someya T: **Effects of dosage and CYP2D6-mutated allele on plasma concentration of paroxetine.** *Eur J Clin Pharmacol* 2004, **60**(8):553-557.
132. **Human Cytochrome P450 (CYP) Allele Nomenclature Committee.**
<http://www.imm.ki.se/CYPalleles/>.
133. Kagimoto M, Heim M, Kagimoto K, Zeugin T, Meyer UA: **Multiple mutations of the human cytochrome P450IID6 gene (CYP2D6) in poor metabolizers of debrisoquine. Study of the functional significance of individual mutations by expression of chimeric genes.** *J Biol Chem* 1990, **265**(28):17209-17214.
134. Bradford LD: **CYP2D6 allele frequency in European Caucasians, Asians, Africans and their descendants.** *Pharmacogenomics* 2002, **3**(2):229-243.
135. Ozdemir V, Tyndale RF, Reed K, Herrmann N, Sellers EM, Kalow W, Naranjo CA: **Paroxetine steady-state plasma concentration in relation to CYP2D6 genotype in extensive metabolizers.** *J Clin Psychopharmacol* 1999, **19**(5):472-475.
136. Thomas L, Mulsant BH, Solano FX, Black AM, Bensasi S, Flynn T, Harman JS, Rollman BL, Post EP, Pollock BG *et al*: **Response speed and rate of remission in primary and specialty care of elderly patients with depression.** *Am J Geriatr Psychiatry* 2002, **10**(5):583-591.
137. Foglia JP, Sorisio D, Kirshner M, Pollock BG: **Quantitative determination of paroxetine in plasma by high-performance liquid chromatography and ultraviolet detection.** *J Chromatogr B Biomed Sci Appl* 1997, **693**(1):147-151.
138. Bartlett J, White A: **PCR Protocols**, 2 edn: Humana Press; 2003.
139. Higuchi R: **PCR Technology: Principles and Applications for DNA Amplification.**, 2 edn. New York: Oxford University Press; 1992.
140. Lundqvist E, Johansson I, Ingelman-Sundberg M: **Genetic mechanisms for duplication and multiduplication of the human CYP2D6 gene and methods for detection of duplicated CYP2D6 genes.** *Gene* 1999, **226**(2):327-338.
141. Cheng S, Fockler C, Barnes WM, Higuchi R: **Effective amplification of long targets from cloned inserts and human genomic DNA.** *Proc Natl Acad Sci U S A* 1994, **91**(12):5695-5699.
142. Steen VM, Andreassen OA, Daly AK, Tefre T, Borresen AL, Idle JR, Gulbrandsen AK: **Detection of the poor metabolizer-associated CYP2D6(D) gene deletion allele by long-PCR technology.** *Pharmacogenetics* 1995, **5**(4):215-223.
143. Wan YJ, Poland RE, Han G, Konishi T, Zheng YP, Berman N, Lin KM: **Analysis of the CYP2D6 gene polymorphism and enzyme activity in African-Americans in southern California.** *Pharmacogenetics* 2001, **11**(6):489-499.

144. Mendoza R, Wan YJ, Poland RE, Smith M, Zheng Y, Berman N, Lin KM: **CYP2D6 polymorphism in a Mexican American population.** *Clin Pharmacol Ther* 2001, **70**(6):552-560.
145. Masimirembwa C, Persson I, Bertilsson L, Hasler J, Ingelman-Sundberg M: **A novel mutant variant of the CYP2D6 gene (CYP2D6*17) common in a black African population: association with diminished debrisoquine hydroxylase activity.** *Br J Clin Pharmacol* 1996, **42**(6):713-719.
146. Raimundo S, Toscano C, Klein K, Fischer J, Griese EU, Eichelbaum M, Schwab M, Zanger UM: **A novel intronic mutation, 2988G>A, with high predictivity for impaired function of cytochrome P450 2D6 in white subjects.** *Clin Pharmacol Ther* 2004, **76**(2):128-138.
147. Rau T, Heide R, Bergmann K, Wuttke H, Werner U, Feifel N, Eschenhagen T: **Effect of the CYP2D6 genotype on metoprolol metabolism persists during long-term treatment.** *Pharmacogenetics* 2002, **12**(6):465-472.
148. Wennerholm A, Johansson I, Masseur AY, Lande M, Alm C, Aden-Abdi Y, Dahl ML, Ingelman-Sundberg M, Bertilsson L, Gustafsson LL: **Decreased capacity for debrisoquine metabolism among black Tanzanians: analyses of the CYP2D6 genotype and phenotype.** *Pharmacogenetics* 1999, **9**(6):707-714.
149. Preskorn S: **Targeted pharmacotherapy in depression management: comparative pharmacokinetics of fluoxetine, paroxetine and sertraline.** *Int Clin Psychopharmacol* 1994, **Suppl 3**:13-19.
150. Bertilsson L, Dahl M: **Polymorphic drug oxidation. Relevance to the treatment of psychiatric disorders.** *CNS Drugs* 1996, **5**(200-223).
151. Cornish-Bowden A: **Fundamentals of Enzyme Kinetics.** *Portland Press, London* 1995.
152. Cornish-Bowden A: **Analysis of Enzyme Kinetic Data.** *Oxford University Press, Oxford and New York* 1995.
153. Feng Y, Pollock B, Reynolds C, Bies R: **Paroxetine pharmacokinetics in geriatric patients.** *AAPS PharmSci* 2004, **Abstract M1116.**
154. Wennerholm A, Dandara C, Sayi J, Svensson JO, Abdi YA, Ingelman-Sundberg M, Bertilsson L, Hasler J, Gustafsson LL: **The African-specific CYP2D6*17 allele encodes an enzyme with changed substrate specificity.** *Clin Pharmacol Ther* 2002, **71**(1):77-88.
155. Diaz E, Levine HB, Sullivan MC, Sernyak MJ, Hawkins KA, Cramer JA, Woods SW: **Use of the Medication Event Monitoring System to estimate medication compliance in patients with schizophrenia.** *J Psychiatry Neurosci* 2001, **26**(4):325-329.
156. Anon: **FDA: Guidance for industry: Population pharmacokinetics.** In. Rockville, MD: Food and Drug Administration; 1999.
157. Vrijens B, Tousset E, Rode R, Bertz R, Mayer S, Urquhart J: **Successful projection of the time course of drug concentration in plasma during a 1-year period from electronically compiled dosing-time data used as input to individually parameterized pharmacokinetic models.** *J Clin Pharmacol* 2005, **45**(4):461-467.
158. Vrijens B, Gross R, Urquhart J: **The odds that clinically unrecognized poor or partial adherence confuses population pharmacokinetic/pharmacodynamic analyses.** *Basic Clin Pharmacol Toxicol* 2005, **96**(3):225-227.
159. Brundage RC: **An intergrated pharmacokinetic-adherence measure for virologic outcome. Presented at the University of Southern California.** *Biomedical Simulation resource, Workshop on Advanced PK/PD Systems Analysis* 2001, **June.**

160. Urquhart J: **Role of patient compliance in clinical pharmacokinetics. A review of recent research.** *Clin Pharmacokinet* 1994, **27**(3):202-215.
161. Urquhart J: **Compliance and clinical trials.** *Lancet* 1991, **337**(8751):1224-1225.
162. Urquhart J: **The impact of compliance on drug development.** *Transplant Proc* 1999, **31**(4A):39S.
163. Jonsson EN, Wade JR, Almqvist G, Karlsson MO: **Discrimination between rival dosing histories.** *Pharm Res* 1997, **14**(8):984-991.
164. Sogaard B, Mengel H, Rao N, Larsen F: **The pharmacokinetics of escitalopram after oral and intravenous administration of single and multiple doses to healthy subjects.** *J Clin Pharmacol* 2005, **45**(12):1400-1406.
165. Gutierrez MM, Rosenberg J, Abramowitz W: **An evaluation of the potential for pharmacokinetic interaction between escitalopram and the cytochrome P450 3A4 inhibitor ritonavir.** *Clin Ther* 2003, **25**(4):1200-1210.
166. Beal B, Sheiner L: **NONMEM user's guide, Part I. San Francisco: University of California at San Francisco.** 1992.
167. Weisstein EW: **"Distance." From MathWorld--A Wolfram Web Resource.** <http://mathworld.wolfram.com/Distance.html>.
168. Sun H, Ette EI, Ludden TM: **On the recording of sample times and parameter estimation from repeated measures pharmacokinetic data.** *J Pharmacokinet Biopharm* 1996, **24**(6):637-650.
169. Huang ML, Van Peer A, Woestenborghs R, De Coster R, Heykants J, Jansen AA, Zyllicz Z, Visscher HW, Jonkman JH: **Pharmacokinetics of the novel antipsychotic agent risperidone and the prolactin response in healthy subjects.** *Clin Pharmacol Ther* 1993, **54**(3):257-268.
170. Urquhart J, Bernard V: **Taxonomy of patient compliance-related events in drug trials.** *Snowbird Conference, Snowbird, UT, 2001, August 9-13.*
171. Byerly MJ, DeVane CL: **Pharmacokinetics of clozapine and risperidone: a review of recent literature.** *J Clin Psychopharmacol* 1996, **16**(2):177-187.
172. Lotrich FE, Pollock BG, Ferrell RE: **Polymorphism of the serotonin transporter: implications for the use of selective serotonin reuptake inhibitors.** *Am J Pharmacogenomics* 2001, **1**(3):153-164.
173. Perlis RH, Mischoulon D, Smoller JW, Wan YJ, Lamon-Fava S, Lin KM, Rosenbaum JF, Fava M: **Serotonin transporter polymorphisms and adverse effects with fluoxetine treatment.** *Biol Psychiatry* 2003, **54**(9):879-883.